IDENTIFICATION OF A NOVEL SOURCE OF TASTE BUD PROGENITORS UNDER LINGUAL EPITHELIUM

by

WENXIN YU

(Under the Direction of Hong-Xiang Liu)

ABSTRACT

Taste buds are taste sensory organs that require continuous cell renewal to maintain their homeostasis. Thus, properly functioning progenitors in the surrounding tissue compartments are necessary throughout the developmental course of taste buds. Lingual taste bud resides in taste papillae in oral tongue, in which taste buds are surrounded by lingual epithelium, underlying connective tissue core, and minor salivary gland, i.e., von Ebner's gland. In the past decades, taste bud-surrounding basal epithelium has been considered as the sole progenitor source for taste buds. However, our recent findings revealed that Sox10-expressing cells, i.e., neural crest, and/or cells in tissue compartments under lingual epithelium, i.e., connective tissue core of taste papillae and/or von Ebner's gland, serve as taste bud cell progenitors that differentiate to mainly type III taste cells during taste bud maturation and maintenance in postnatal mice. Follow-up studies mapping the lineage of Sox10-expressing neural crest cells in three model species indicated that neural crest cells and their derivatives in the tongue connective tissue do not give rise to taste buds, leaving non-neural crest-derived cells in connective

tissue and von Ebner's glands to be determined. To investigate the potential contribution of those progenitor candidates to taste buds, multiple inducible Cre mouse models were used to map the lineage of cells in connective tissue (including stromal cells and Schwann cells) and cells in von Ebner's glands. The observations from those studies indicated that von Ebner's glands, but not connective tissue cores of taste papillae, most likely host the progenitors for taste buds during postanal maturation and maintenance. Future studies will focus on collecting solid evidence to verify von Ebner's glands' contribution to taste buds. At last, a protocol for cell dissociation from tongue epithelium and mesenchyme/connective tissue was developed for cell preparation for single cell RNA-Sequencing and 3D organoid cultures that will facilitate our studies to better understand the origin of taste bud cells.

INDEX WORDS: Taste bud, progenitor, neural crest, connective tissue core, von Ebner's gland, Sox10, Lineage, cell dissociation.

IDENTIFICATION OF A NOVEL SOURCE OF TASTE BUD PROGENITORS UNDER LINGUAL EPITHELIUM

by

WENXIN YU

B.S., South China Agricultural University, China, 余文欣, 2014

A Dissertation Submitted to the Graduate Faculty of the University of Georgia in Partial Fulfillment of the Requirements for the Degree

DOCTOR OF PHILOSOPHY

ATHENS, GEORGIA

2021

IDENTIFICATION OF A NOVEL SOURCE OF TASTE BUD PROGENITORS UNDER LINGUAL EPITHELIUM

by

WENXIN YU

Major Professor:	Hong-Xiang Liu
Committee:	Luke J. Mortensen
	Franklin D. West
	Steven L. Stice

Electronic Version Approved:

Ron Walcott
Dean of the Graduate School
The University of Georgia
May 2021

ACKNOWLEDGEMENTS

Throughout my PhD study at the University of Georgia in Dr. Hong-Xiang Liu's Lab, I have received a great deal of support and assistance.

I would like to express my deep sense of thanks and gratitude to my mentor, Dr. Hong-Xiang Liu, who encourages and leads me to pursue the scientific success. It is my honor to have a mentor with genuine passion in science and always preparing to help. I really enjoyed the time when we worked together as a team to resolve the difficulties in research. Your immense knowledge and insistence on scientific rigor helped me all the time of my research and thesis writing.

Beside my mentor, I would like to profusely thank the rest of my advisory committee members, Dr. Franklin D. West, Luke J. Mortensen, and Steven L. Stice, for their prompt inspirations and timely suggestions at every stage of my research. It is your time and effort that kept me on the right track. In addition, I would like to thank Dr. Yao Yao, who gave me invaluable advice about my experimental design and future career.

For my labmates in Dr. Liu's lab, I had a wonderful time with you all during my PhD study. Special thanks to Mohamed Ishan, you are so responsive and helpful whenever I need you. Zhonghou Wang, you are a smart person who can always come up with good ideas for our projects. Naomi Kramer, I learn a lot from you for my English editing and oral English. Importantly, your friendship is most precious and irreplaceable. In addition, I would like to thank all the students and professors in the Regenerative Bioscience Center for their generous help and feedbacks.

Last but not the least, I would like to thank my father Guobin Yu and mother Yanping Lai, who supported me and gave me the courage to study abroad. Luhan Yang, my lovely wife, it is your companionship and love that made me get this far. My son Areo and his fluffy brother Matz, you brought us so much fun during the special time since 2020.

TABLE OF CONTENTS

LIST OF TABLES

Page

LIST OF FIGURES

Page

CHAPTER 1

INTRODUCTION AND LITERATURE REVIEW: DISTRIBUTION OF PROGENNITOR CELLS FOR TASTE BUDS

1.1 Introduction

Taste buds are the sensory end organs for taste that transduce chemical stimuli into neural signals conveyed to the central nervous system. Each taste bud is an aggregate of 50~100 heterogenous epithelial cells that have a short life span and undergo continuous turnover [1-5]. Thus, properly functioning progenitors are required throughout the developmental course of taste buds. The known progenitor cell populations for taste buds have been categorized based on their expression of specific molecular markers, e.g., keratin (Krt) 14 [6] , Krt5 [6], transformation related protein 63 (TRP63) [6], SRY-Box transcription factor 2 (Sox2) [6, 7], and leucine rich repeat containing G protein-coupled receptor 5/6 (LGR5/6) [8-10]. These defined progenitor cell populations have been mainly found in lingual epithelium surrounding taste buds at postnatal stages [3, 4, 6-14]. In addition to lingual epithelium, underlying connective tissue and von Ebner's gland have been indicated to be potential progenitor sources for taste buds [15-17]. However, further studies are needed to collect solid evidence in support of the specific progenitor cell population for taste buds in tissue compartments under lingual epithelium.

Taste bud development pass through three phases, including (1) the emergence of early taste buds that are structurally recognizable in late embryos; (2) maturation after birth during which taste buds increase in size and differentiated taste bud cells populate

proportionately; and (3) maintenance when cells of mature taste buds undergo continuous turnover for taste bud homeostasis. The expression of molecular markers in taste cell progenitor is distinct at different phases, e.g., Sonic Hedgehog (Shh) labels epithelial progenitors for early taste buds at embryonic stages [18] while Krt14 marks the progenitor cells in the taste bud-surrounding epithelium at postnatal stage [6]. To get a better idea for future translational and clinical studies for taste cell regeneration, it is important to understand the distribution of progenitor sources of taste buds. In this review article, we will summarize and discuss the distribution of progenitor sources for taste buds at different phases of taste bud development focusing on the lingual taste buds that are hosted by specialized organs called taste papillae.

1.2 Progenitors for early taste buds

1.2.1 Embryonic development of taste papilla placodes, taste papillae, and taste buds

In mice at embryonic day (E) 10.5, branchial arch 1 is evident, on which lateral lingual swellings develop at E11.5 and later fuse to form the anterior 2/3 of the tongue at E12.5 [19]. At around the same time, the posterior 1/3 of tongue forms from branchial arches 3 and 4 [19]. Taste papilla placodes emerge as epithelial thickenings at E12.5. These papilla placodes are known as progenitors for taste buds hosted by taste papillae, which are classified into three types - fungiform, foliate, and circumvallate. Among them, fungiform papilla placodes are specified at E12.5 as single layer of columnar epithelia and widely distributed in anterior 2/3 of oral tongue [20-26]. A single circumvallate papilla placode initiates at E12.5 immediately in front of the sulcus terminalis as a slight invagination of the epithelium in the midline of the border between oral and pharyngeal

tongue [27, 28]. Foliate papilla placodes develop later at E14.5 on both lateral sides in posterior oral tongue.

At E14.5, all three types of taste papillae are well formed and their underlying mesenchymal cores of taste papillae are evident. Two invaginated trenches are clear in circumvallate papillae [20-26, 29, 30]. At E18.5, early taste buds are histologically distinguishable but mostly immature, in which taste bud cells are not fully differentiated and a taste pore is rarely found [20-26, 31].

1.2.2 Progenitors in the epithelium

In mice at E12.5, taste papilla placodes emerge as protrusions on the surface of the tongue [20] and epithelial cells in taste papillae are distinguished from the surrounding non-placodal cells by expressing Sonic Hedgehog (Shh) [32], one of the vertebrate Hedgehogs involved in numerous patterning processes during embryogenesis [33]. These Shh-expressing (Shh^+) taste papilla placodal cells have been found to give rise specifically to type I and II, but not type III, taste bud cells in postnatal mice at ages younger than 4 months [34]. These findings suggest that type III taste bud cells have distinct embryonic progenitors from those for type I and II taste cells. Given that differentiated type III taste bud cells have been observed in ~20% of fungiform taste buds at birth [35], we speculate that progenitors for type III taste bud cells are specified at embryonic stages. More studies are needed to identify the tissue compartment(s) and cell type(s) of type III taste cell progenitors.

Back to E11.0, the homogenous Shh^+ epithelium covering the tongue primordium has been reported to be the progenitors for fungiform taste buds and surrounding epithelium at E18.5 [18]. Thus, future studies are necessary to determine whether the

existence of Shh$^+$ progenitor cells applies to early taste buds in other types of taste papillae. At E14.5 when fungiform and circumvallate papillae are well formed, Shh expression is retained in taste papilla cells [29, 30], while surrounding epithelium switches its expression from Shh to keratin 14 (Krt14) [18, 29, 30], an intermediate filament protein expressed in basal cells of stratified squamous epithelium [36] and known as taste cell progenitor marker in postnatal mice [6]. However, these Krt14$^+$ epithelial cells do not give rise to cells in taste papillae and early taste buds in embryos, unlike what they do to taste buds at postnatal stages [18].

In addition to the expression of Shh, taste papilla placodal cells express several other markers that label taste cell progenitors in postnatal mice, including leucine rich repeat containing G protein-coupled receptor 5 (LGR5), and SRY-Box transcription factor 2 (Sox2) [7-9, 37-40]. LGR5 is a component of the Wnt signaling pathway and known as a perigemmal progenitor marker for circumvallate taste buds in postnatal mice. It is expressed in both fungiform and circumvallate taste papilla placodes not later than E13.5 [9, 37]. Sox2 is a transcription factor involved in cell fate determination. Sox2 expression has been found in both taste buds and surrounding epithelium at postnatal stages [7, 38], as well as in taste papilla placodes at E12.5 [39, 40]. Although lineage tracing studies have not been done using these progenitor markers, we have evidence to support the idea that LGR5$^+$ and Sox2$^+$ cells within taste papilla placodes share the similar cell fate with Shh$^+$ taste papilla placodal cells. For examples, the expression pattern of these makers within taste papilla placodes is similar to that of Shh, i.e., taste papilla placodes were almost fully labeled by immunohistochemistry against LGR5, Sox2, and Shh at

E13.5 [9, 32, 34, 37, 39-42]. Thus, there is a possibility that these markers may be co-expressed with Shh in the same taste papilla placodal cell population.

1.2.3 Taste bud progenitors in the tongue mesenchyme

The potential contribution of underlying connective tissue, largely derived from neural crest, to taste buds has been indicated in postnatal mice by mapping the lineage of cells expressing Myelin Protein Zero (P0) [16], Dermis-Expressed Protein 1 (Dermo1) [16], and SRY-Box Transcription Factor 10 (Sox10) [15] using the Cre/loxP site-specific DNA recombination system. Among those potential progenitor cell population, $P0^+$ cells have been found to give rise to taste papillae and immature taste buds at embryonic stages [17]. However, P0-Cre also labels the lingual epithelium [17], which raises concerns about the specificity of P0-Cre in labeling neural crest cell lineage. Of note, Sox10-Cre labeled taste buds cells emerge as early as newborn in fungiform taste buds [15], indicating the fate specification of $Sox10^+$ cell population towards taste cell progenitors at embryonic stages. In addition, our recent studies show that $Sox10^+$ progenitors contribute primarily to type III taste bud cells [15], which complements with the previous finding that Shh^+ taste papilla placodal cells only give rise to type I and II taste bud cells [34]. However, broad distribution and heterogeneity of neural crest-derived cells in tongue mesenchyme [15, 17, 43, 44] necessitate future studies to determine the existence of embryonic stem cell niche under lingual epithelium and the specific cell types that serve as taste cell progenitors.

1.2.4 Summary

Early taste buds are derived from the homogeneous Shh^+ lingual epithelial cells in the tongue swellings at E11.0 [18]. Given that little is known about the heterogeneity of

lingual epithelium at E11.0, it is too early to point out the specific epithelial cell types serving as progenitor sources. Later at E12.5, Shh^+ taste papilla placodal cells give rise specifically to type I and type II cells of taste buds in postnatal mice [34], which complements with our finding that $Sox10^+$ progenitors under lingual epithelium contributed mainly to type III taste bud cells [15]. However, whether progenitor-residing tissue compartment(s) under lingual epithelium participate in the development of early taste buds remains unknown.

1.3 Taste bud progenitors during maturation and maintenance

1.3.1 Maturation of taste buds and differentiation of specific types of taste bud cells

1.3.1.1 Time course of taste bud maturation

In rodents, early immature taste buds emerge perinatally and maturation is essentially a postnatal process, during which taste bud number, size and cell number per bud increase and stabilize, and a taste pore appears as a sign of maturity of an individual taste bud. The time course of maturation of taste buds in different types of taste papillae varies.

Fungiform taste buds (including mature and immature), distributed on the anterior 2/3 of the oral tongue, increase in number with the growth of tongue until 3 weeks of age and a dramatic increase occurs during the first week after birth [31, 45]. Meanwhile, the overall size of fungiform taste buds increases dramatically during this time, about 4- and 5-folds in mice and rats respectively from postnatal day 1 (P1) to 3 weeks [31, 45]. Afterwards taste buds may undergo further growth as an 4-fold increase in taste cell number has been found in rat fungiform taste buds from P10 to P40 [46]. In rats, the

increasing rate of the taste bud number in total is similar to that of the number with a taste pore, and almost all taste buds possess a taste pore at 8 weeks [31].

Circumvallate tastes buds, resided in the single circumvallate papilla in the midline of the border between oral and pharyngeal tongue in rodents, increase in their total number (including mature and immature) with the growing size of circumvallate papilla. In rats, unlike the fungiform taste bud, the number of circumvallate taste buds continuingly increases until ~P90 [47]. The sizes of circumvallate taste buds rapidly increase during the first 4 weeks after birth, almost tripled from postnatal 1 to 4 weeks [31]. Meanwhile, the cell number in individual taste buds is also tripled from P10 to P45 [47]. The increasing rate of number of circumvallate taste buds with a taste pore is similar to that of the total taste bud number [31]. However, in contrast to ~100% in fungiform taste buds, only ~80% of circumvallate taste buds possess a taste pore at 8 weeks [31].

Foliate taste buds reside in the foliate papillae in the lateral sides of the tongue in mammals. It has been reported that the time course of maturation of foliate taste buds is similar to that of circumvallate taste buds [31]. However, the number of foliate taste buds continue to increase after 9 weeks [31]. Little is known about the increasing rate of the foliate taste bud cell number.

1.3.1.2 Taste cell differentiation during taste bud maturation

The onset of taste bud cell differentiation is another key event during taste bud maturation, which is in vital importance for taste buds to fulfill their function in transducing gustatory signals. Taste buds are composed of three differentiated cell types (I, II, and III) [26, 48, 49] and an undifferentiated type IV [50] as precursors giving rise to the other cell types [25]. Fully differentiated taste bud cells emerge perinatally, when specific types of

taste bud cells are detected with molecular markers [35, 45, 51, 52]. After P5, the ratios of these differentiated cell types become consistent [53, 54].

Type I cells are glial-like in molecular marker and [24, 55] they comprise a large proportion (~65%) of taste bud cells [21-26, 53, 54]. They extend lamellate processes to enwrap other cell types [21, 22, 26] and degrade neurotransmitter (ATP) by producing a specific enzyme, nucleoside triphosphate diphosphohydrolase-2 (NTPDase2) [24, 55]. NTPDase2 is detected in one-third of mouse fungiform taste buds as early as E18.5 [56].

Type II cells are taste receptor cells comprise a subset (14~22%) of taste bud cells [53, 54]. They transduce sweet, umami, and bitter signals from tastants [57-62]. Type II taste cells express a molecular marker phospholipase Cβ2 (PLCβ2) [63], which is detected in mouse circumvallate taste buds as early as E17 [64]. In addition, alpha-gustducin (α-gustducin) [65, 66] and transient receptor potential M5 (Trmp5) [67, 68] are also used as molecular markers for type II taste cells. By P10, almost all mouse fungiform taste buds contain at least one type II taste bud cell [35].

Type III cells are neuronal-like [23, 48, 69-72] and represent a small subset (6~15%) of taste bud cells [53, 54]. These taste cells participate in transducing sour [73-76] and salt [77, 78] sensation. They form identifiable synapses with gustatory nerve endings [79] and express pre-synaptic membrane proteins synaptosomal-associated protein 25 (SNAP25) [80-82], which is found in 20% of mouse fungiform taste bud at P1 and 80% at P10 [35]. In addition, carbonic anhydrase 4 (CAR4) [83], glutamate decarboxylase 67 (GAD67) [84], neural cell adhesion molecule 1 (NCAM1) [85], polycystic kidney disease 2-like 1 (PKD2L1) [86] , and serotonin (5-HT) [87, 88] are also expressed in and commonly used markers to label type III taste cells.

Type IV cells are post-mitotic precursors residing in the basal area of taste buds [25, 50, 89, 90]. They express Shh [91], prospero homeobox protein 1 (Prox1) [92], and mammalian achaete-scute complex homolog 1 (MASH1) [90, 93, 94], and give rise to all types of differentiated taste bud cells [25].

1.3.2 Taste bud maintenance

In mature taste buds, cells undergo continuous turnover to maintain taste bud homeostasis. Previous studies using rats have suggested an average lifespan of 8~12 days in overall taste bud cells [1, 95]. In 5-ethynil-29-deoxyuridine (EdU) label-retention assay in mice, most of the type I and II cells had an estimated half-life of 8 days, and some long-lasting cells could survive till 24 days [5]. Type III cells have a relatively longer half-life of 22 days, and a subset of them could last beyond 40 days [5].

1.3.3 Progenitors for taste buds during maturation and maintenance

1.3.3.1 Precursors within taste buds

In mature taste buds, cell differentiation was observed in ovoid cells in basal compartments [49, 96]. Ovoid basal taste bud cells are characterized as type VI cells as post-mitotic precursors [25, 50, 89, 90]. However, mitotic activities have been also found in taste buds as they are in surrounding lingual epithelium.

BrdU⁺ cells: Analyses of 5-bromo-2′-deoxy uridine (BrdU) labeling in a short term revealed that a few rapid cycling taste cells are distributed in the basal and central regions of taste buds [13]. Moreover, BrdU-labeling retained in a small population of basal cells one month after BrdU administration [13], indicating the existence of slow cycling cells in this population.

Shh⁺ cells: At postnatal stages, Shh expression retained in a population of basal cells in taste buds [91]. BrdU labeling assay showed that Shh⁺ basal taste bud cells are post-mitotic and undergo rapid turnover [89, 90]. Lineage tracing with inducible Cre/loxP model for Shh⁺ basal cells indicated Shh⁺ cells are post-mitotic precursors and give rise to all three types of differentiated taste bud cells [25]. Whether an individual Shh⁺ post-mitotic basal cell in taste buds has the multipotency for distinct types of differentiated taste bud cells remains inconclusive and needs detailed studies.

MASH1⁺ cells: MASH1 is a transcription factor that is involved in neuronal differentiation [97-99]. In adult mice, MASH1 is expressed in a population of basal taste bud cells and most of the type III taste bud cells [100]. In genetic mouse models depleting Mash1⁺ cells, inducible expression of diphtheria toxin A (DTA) in MASH1-expressing cells for consecutive ten days resulted in significant loss of type III but not type II taste bud cells, suggesting that MASH1⁺ precursor cells are specific for type III taste bud cells [101]. However, given the expression of MASH1 in the majority of type III taste bud cells, the significant decrease of type III taste bud cells may result from toxic effect of DTA in type III taste bud cells but not the loss of precursor cells since ten-day time window may not be long enough for regeneration of a large population of type III taste bud cells. A long-term observation will be helpful to provide insights into their fate determination to type III taste bud cells.

LGR5/6⁺ cells: LGR5-GFP labeled cells have been found in both intragemmal and perigemmal cells of fungiform and circumvallate taste buds in neonatal mice [9]. Although they disappeared by postnatal day 50 (P50) in fungiform papillae, the progeny of LGR5⁺ cells at P1 is found at P166 in a small population of fungiform taste buds and their

surrounding epithelial cells [9], suggesting that a population of LGR5$^+$ descendant cells may lose LGR5 expression but remain the stemness dedicated to taste bud cells. Transcriptomic analysis on organoids cultured from dissociated LGR5-GFP labeled cells from the bottom of the trenches of circumvallate papillae revealed the expression of LGR6, which was later demonstrated as a progenitor marker for both fungiform and circumvallate taste buds [10]. LGR6-GFP labeled cells have been found in the basal compartments of both fungiform and circumvallate taste buds in adult mice [10], which is different from Krt14$^+$ and LGR5$^+$ taste cell progenitors.

In summary, progenitors are present within taste buds for their cell renewal, i.e., the type IV basal taste bud cells. These progenitors differentiate to the three types (I-III) of differentiated taste bud cells. The expression of particular molecular signaling components or transcription factors warrants further studies on the potential regulatory roles of these faction in cell differentiation of progenitors to taste bud cells.

1.3.3.2 Progenitors in taste bud-surrounding lingual epithelium

The migration of surrounding lingual epithelial cells and/or their daughter cells to fungiform taste buds has been observed in postnatal rats through radioautography using tritiated thymidine to label proliferating cells [1]. Tritiated thymidine labeled nuclei were initially emerged in surrounding lingual epithelium at 24 hours post treatment and later found in taste buds at 100 hours post treatment. Importantly, tritiated thymidine labeled nuclei were are also sparsely distributed in underlying connective tissue at those examined time points [1], leaving the idea that surrounding lingual epithelium is the sole progenitor source for taste buds remains unconclusive.

The concept that taste buds arise solely from local epithelium, not neurogenic ectoderm, was proposed based on studies using the X chromosome-inactivation mosaic mouse model, in which fungiform and circumvallate taste bud cells and their surrounding epithelium matched each other in terms of mosaic marker [12]. However, such data were obtained in strictly selected tissue pieces that could not represent the general condition; and in their representative figures, cells in underlying connective tissue also shared the same labeling pattern with overlying taste buds and epithelium [12], which raises a question of whether local epithelium is the sole progenitor source for taste buds. Nevertheless, evidence that local epithelium host progenitor cells that give rise to taste bud cells is solid. There are multiple groups of progenitors that are distributed in different locations surrounding taste buds and express distinct markers.

Krt14$^+$ cells: With the advantage of inducible Cre/loxP model for lineage tracing in adult mice, the identity of epithelial progenitors surrounding taste buds was first characterized as Krt14$^+$ basal keratinocytes in lingual epithelium [6] that also express Krt5 and TRP63 [6]. Krt14-CreER labeled ~67% of examined fungiform taste buds and only ~25% taste buds were fully labeled at 30 days post multiple doses tamoxifen treatment in adult mice [6]. The incomplete labeling may attribute to (1) existence of progenitor source(s) other than lingual epithelium, and (2) low Cre recombination efficiency, which is supported by a seemingly full labeling of cells in taste buds after a long term of treatment of tamoxifen.

LGR5$^+$ cells: In contrast to the wide distribution of Krt14$^+$ cells in lingual epithelium, LGR5$^+$ cells represent a subpopulation of long-term taste cell progenitors for circumvallate taste buds in adult mice [8, 9]. LGR5-GFP labeled cells are detected at the

bottom of the trenches of the circumvallate papillae but not within taste buds [8]. Lineage tracing indicated that LGR5$^+$ cells are capable to give rise to all three types of differentiated taste cells of circumvallate taste buds [8, 9]. Of note, LGR5-GFP is detected in the duct of von Ebner's gland that is connected with its opening to the bottom of the trenches of circumvallate papilla [8]. Thus, the potential that von Ebner's gland contain progenitors for taste buds cannot be excluded.

GLI1$^+$ cells: GLI family zinc finger 1 (GLI1) encoded protein is an indicator of hedgehog signaling pathway [102] and serves as a transcription factor by binding to GLI1 responsive genes. Recent studies identify GLI1 expression in osteogenic progenitors for bone formation and fracture repair [103]. In the tongue, previous study has suggested the potency of GLI1$^+$ cells as progenitors for fungiform taste buds [104]. In lingual epithelium, GLI1 expression is restricted to surrounding epithelial cells of fungiform taste buds and the basal cells in the epithelial wall of fungiform papillae, which overlaps with the distribution of Krt14 in taste papillae [104]. In addition, GLI1 expression has been also detected in connective tissue core of taste buds [104], raising a question whether GLI1$^+$ connective tissue cells give rise to taste bud cells.

Sox2$^+$ cells: In adult mice, Sox2 is expressed in both perigemmal and intragemmal cells of fungiform and circumvallate taste buds [6, 7, 38]. However, Sox2$^+$ proliferating cells are only detected at the basal layer of lingual epithelium outside taste buds [7], suggesting that Sox2$^+$ progenitor cells may represent a similar population of Krt14$^+$ progenitor cells in surrounding lingual epithelium of taste buds and Sox2$^+$ cells within taste buds represent a population of differentiated taste bud cells.

In summary, the concept that taste buds arise from surrounding lingual epithelium has well established after decades of studies. However, the question remains whether surrounding epithelium is the “sole” source of taste bud progenitors. Different epithelial progenitor markers labels all or a subset of taste bud-surrounding epithelium. Future studies may focus on those molecular markers in governing the cells migrating and differentiation toward taste bud cells.

1.3.3.3 Progenitors in the underlying connective tissue

Our recent findings have identified Sox10-expressing cells in connective tissue core of taste buds and distribution of Sox10-Cre-labeled cells in taste buds suggest a potential contribution of $Sox10^+$ connective tissue cells to taste buds. The findings lead to a novel idea that taste cell progenitors may reside in the underlying connective tissue of taste buds in addition to lingual epithelium.

The speculation that underlying connective tissue may serve as a potential progenitor source for taste buds is first indicated by the study of Shh-responding, GLI1-expressing cells in fungiform papillae [104]. $GLI1^+$ cells are distributed in taste bud-surrounding tissue compartments in fungiform papillae, but not within taste buds. As aforementioned, GLI1 is expressed in the perigemmal cells of taste buds and at the basal cells of fungiform papilla epithelium [104], as well as connective tissue. In the study on tracing the lineage of $GLI1^+$ cells in adult mice, GLI1-CreER labeled cells are found within taste buds, suggesting the progeny of $GLI1^+$ cells within taste buds [104]. Further studies are necessary to define the specific type(s) of $GLI1^+$ cells in the surrounding tissues that give rise to taste bud cells.

In the mouse tongue at P10, the mesenchymal/connective tissue cells have been found to have a neural crest origin [17]. Meanwhile, in the study tracing the lineage of neural crest using P0-Cre mouse model, taste buds were labeled concurrently with the underlying connective tissue [17], suggesting a potential contribution of neural crest-derived connective tissues to taste buds. However, labeled taste bud cells were rarely [17] or never [34] found in Wnt1-Cre, a widely used mouse model for neural crest cell lineage mapping [105-112]. The discrepant observations between these models may be ascribed to incomplete labeling of all neural crest cell lineage in Wnt1-Cre [113] and/or nonspecific labeling beyond neural crest cell lineage in P0-Cre [114, 115].

At postnatal stages during taste bud maturation and maintenance, a potential contribution of underlying connective tissue to taste buds is supported by the data obtained from tracing the lineage of neural crest-derived connective tissue cells using, Dermo1-Cre, P0-Cre, and Sox10-Cre mouse models [15, 16]. In these mouse models, labeled cells were found concurrently in both taste buds and underlying connective tissue [15, 16]. However, concerns remain in these models regarding the specificity or recapitulation in tracing lineage of connective tissue cells.

Dermo1-Cre has been frequently used to map mesenchymal cell lineage [116-120]. However, in addition to specifically labeling neural crest-derived cells, Dermo1-Cre also labels mesoderm-derived mesenchymal cells, e.g., osteoblasts, chondrocytes [121], perichondrial, and periosteal cells in the trunk and part of the head region [122].

P0-Cre mainly labels rhombencephalic stream of neural crest [113], which is a major contributor to mesenchyme of pharyngeal arches [123]. However, the expression of P0-Cre is not neural crest cell lineage-restricted, e.g., P0-Cre labeled cells are also

found in notochord [113] and ectoderm-derived non-gustatory lingual epithelium at embryonic stages [17, 115].

Wnt1-Cre mainly labels mesencephalic stream of neural crest [113, 124], which only partially contributes to mesenchyme of pharyngeal arch 1 [123], the primordium of the anterior tongue. In addition, ectopic Wnt1 expression from Wnt1-Cre transgene impairs the midbrain development [125] and subsequently overall development of the mouse.

Vimentin is the major intermediate filament found in the mesenchymal cell lineage including fibroblast, melanocytes, Schwann cells, endothelial cells, lymphocytes, and macrophages [126]. Vimentin-CreER is a useful tool for tracing the lineage of stromal cells in the connective tissue [127]. However, the use of a membrane-bound reporter mGFP in our previous study make it difficult to determine whether the labeled structures within taste buds were truly taste cells or simply fibroblast lamellipodia or nerve fibers [16].

Sox10 is expressed specifically in neural crest cells during early embryonic stages [128, 129]. Sustained Sox10 expression at late embryonic stages and in postnatal mice is evident not only in neural crest cell lineage such as glial cells [129, 130] and melanocytes [131], but also in epithelial cell types of lacrimal [132] and salivary gland cells [133, 134]. Indeed, Sox10-Cre has been found to specifically label migrating neural crest cells in early embryos at E8.5 [15]. In postnatal mouse tongue, Sox10-Cre-labeled cells are abundantly distributed in taste buds as well as underlying connective tissue suggesting a potential origin of taste bud cells from the underlying connective tissue that is largely derived from neural crest. However, in addition to migrating neural crest streams,

Sox10 expression was also found in connective tissue core of taste papillae and von Ebner's glands in postnatal mice [15], which makes this concept remain inconclusive.

In a recent study, neural crest cell lineage is labeled specifically by Sox10-iCreER^{T2} through induced Cre recombination in Sox10^{+} neural crest cells at early embryonic stages [44]. Sox10-iCreER^{T2}-labeled cells are widely distributed in connective tissue but not in lingual epithelium including taste buds [44], which demonstrates that neural crest cells and their derivatives in underlying connective tissue do not give rise to taste buds.

1.3.3.4 Progenitors in von Ebner's gland

Von Ebner's gland is a minor salivary gland underneath circumvallate and foliate papillae [135, 136]. It is a group of tubuloacinar serous glands secreting lingual lipase through the opening to the vallum around the trenches of circumvallate and foliate papillae [135, 136]. In contrast to the ectodermal origin of major salivary glands, e.g., parotid, submandibular, and sublingual, von Ebner's gland is derived from endoderm, which also has a contribution to circumvallate and foliate papilla epithelium [137, 138]. The structural connection, functional reciprocal interaction, and common origin between circumvallate papillae and von Ebner's gland have led to an idea of taking circumvallate papillae and von Ebner's gland as a single functional unit [139].

Indeed, taste buds has been observed in the circular structure supposed to be derived from von Ebner's gland in transplanted circumvallate papillae into mouse eyes [140]. Our recent studies suggest a potential contribution of von Ebner's gland to circumvallate taste buds in Sox10-Cre [15] and Sox10-iCreER^{T2} (unpublished data) mouse models, in which circumvallate taste buds are concurrently labeled with von

Ebner's gland. This idea is further supported by the concurrent absence of labeled cells in circumvallate taste buds and von Ebner's gland in Sox10-iCreER^{T2} (unpublished data) mice for neural crest, and Plp1-CreER^{T} for Schwann cells (unpublished data), and Vimentin-CreER (unpublished data) mice for stromal cell lineage mapping. In these aforementioned mouse models, presence and absence of labeled cells in taste buds are not relevant to that in connective tissue, which excludes the connective tissue cells from the progenitor pool of taste buds and leaves von Ebner's gland as the Sox10-expressing progenitor candidate for circumvallate taste buds. However, to draw a conclusion, direct and solid evidences are needed to demonstrate the differentiation of Sox10^{+} progenitor cells in von Ebner's gland to circumvallate taste bud cells, which is an ongoing study.

1.3.4 Summary

Overall, new findings have advanced our understanding regarding the distribution and cell types of taste bud progenitors. Early taste buds are from Shh^{+} epithelial cells of tongue primordium [18] in distinction from mature taste bud cells that arise from surrounding tissue compartments [3, 6, 11, 12, 14, 141]. Shh^{+} epithelial cells of the tongue primordium give rise to both early taste buds and the surrounding lingual epithelium including Krt14^{+} basal epithelial cells [18] which will eventually contribute to the cell renewal of mature taste buds [6].

Taste bud-surrounding lingual epithelium have been considered as the sole progenitor source for taste buds [3, 6, 11, 12, 14, 141]. These progenitors migrate into the basal area of taste buds and differentiate to three types (I-III) of differentiated taste bud cells [25, 46, 90, 91]. However, our recent findings have revealed that Sox10-expressing tissue compartments under lingual epithelium, i.e., connective tissue core of

taste papillae and/or von Ebner's gland, host progenitor cells that differentiate to mainly type III taste cells during taste bud maturation and maintenance in postnatal mice. Our unpublished data in Chapter 4 support a contribution of von Ebner's gland to circumvallate taste buds. Future studies are ongoing to collect direct evidences to verify connective tissue and Ebner's gland's contribution to taste buds.

CHAPTER 2

SOX10-CRE-LABELED CELLS UNDER THE TONGUE EPITHELIUM SERVE AS PROGENITORS FOR TASTE BUD CELLS THAT ARE MAINLY TYPE III AND KERATIN 8-LOW [1]

[1] Wenxin Yu, Mohamed Ishan, Yao Yao, Steven L. Stice, and Hong-Xiang Liu. 2020. *Stem cell and Development*. 29(10):638-647. Reprinted here with permission of publisher.

2.1 Abstract

Taste bud cells are specialized epithelial cells that undergo continuous turnover, and thus require active progenitors for their renewal and an intact taste function. Our previous studies suggested that a population of taste bud cells originates from outside of the surrounding tongue epithelium - previously regarded sole source of taste bud progenitors. In this study, we demonstrated that Sox10-expressing cells, known to be in the migrating neural crest, were also distributed in taste bud-surrounding tissue compartments under the tongue epithelium, i.e., the connective tissue core of taste papillae and von Ebner's glands. By lineage tracing of Sox10-expressing cells using Sox10-Cre, a Cre model driven by the endogenous Sox10 promoter, crossing with a Cre reporter line R26-tdTomato (tdT), we found Sox10-Cre-labeled tdT^+ cells within taste buds in all three types of taste papillae (fungiform, circumvallate, and foliate) as well as in the soft palate in postnatal mice. The tdT^+ taste bud cells were progressively more abundant along the developmental stages, from virtually zero at birth to over 35% in adults. Most of tdT^+ taste bud cells had a low intensity of immunosignals of Keratin 8 (a widely used taste bud cell marker). In circumvallate taste buds, tdT signals were co-localized principally with a type III taste bud cell marker, less so with type I and II cell makers. Together, our data demonstrate a novel progenitor source for taste buds of postnatal mice - Sox10-Cre-labeled cells in the connective tissue core and/or von Ebner's glands.

Key words: Sox10, taste buds, progenitor, taste papilla, soft palate

2.2 Introduction

Taste bud cells are post-mitotic, specialized epithelial cells that undergo continuous turnover [2, 3, 5, 142, 143]. Thus, progenitors in the immediate surrounding

tissue compartments are essential for cell renewal and homeostasis of taste buds. Previous studies have reported that taste bud progenitor cell populations reside in the basal layer of taste bud-surrounding tongue epithelium [3, 6, 12-14, 143, 144] and express Krt14, Krt5, TRP63, Sox2 and LGR5 [6, 8, 9]. Another possible origin of taste bud cells from the underlying connective tissue, largely derived from neural crest, is also indicated [16, 17] but remains inconclusive. Using P0-Cre [16, 17] and Dermo1-Cre [16] for cell lineage tracing, we observed a large dispersal of labeled cells in taste buds in concurrence with those in the underlying connective tissue. However, Wnt1-Cre labeled cells, while extensive in the connective tissue, were rare in taste buds [17, 34]. Lineage tracing of stromal cells in the connective tissue using Vimentin-CreER indicated a Vimentin^{+} cell lineage for taste bud cells [16]. However, the use of a membrane-bound GFP reporter made it difficult to draw concrete conclusions because the membranes of the taste buds cells would be difficult to distinguish from the labeled nerve fibers, which are thin and fibrous and protrude into the taste bud. Thus, the fundamental issue of whether taste bud progenitors exist in tissue compartments beyond the tongue epithelium remains unsettled.

Discrepancies among these mouse models, e.g., P0-Cre, Dermo1-Cre, and Wnt1-Cre, when tracking cell populations may account for the disparity in the observations [113]. The use of a model system with clear information on the expressing cell populations is needed to address this issue. Sox10 (SRY-Related HMG-Box Gene 10) is expressed specifically in neural crest cells during early embryonic stages [145]. Sustained Sox10 expression in later embryonic stages and in postnatal mice is evident in neural crest lineage cell types such as glial cells [129, 130], melanocytes [146], and salivary gland

cells [133]. To advance our understanding as to whether taste bud progenitors exist in tissue compartments other than in tongue epithelium, we located the Sox10-expressing (Sox10$^+$) cells in taste bud-surrounding tissue compartments and mapped the lineage of Sox10-Cre$^+$ cells using a Sox10-Cre mouse line in which Cre expression under the control of the endogenous promoter of Sox10 [147, 148].

In this study we found that Sox10, in addition to the expression in neural crest, was expressed in the taste bud-surrounding tissue compartments under, but not within, the tongue epithelium, (i.e., connective tissue core of taste papillae and von Ebner's glands in postnatal mice). Sox10-Cre/tdTomato (tdT)-labeled cells were progressively distributed in taste buds after birth and plateaued at 4 weeks, when most taste buds are mature. The labeled cells in taste buds were predominantly neuronal-like type III taste cells and not noticeably immunostained with the pan-taste cell marker Keratin (Krt) 8. Our results complement with the findings that taste papilla placodal cells give rise to type I and II, but not type III, taste cells [29, 34, 149] and thus, demonstrate a novel source of stem/progenitor cells for taste buds during their maturation and maintenance - Sox10-Cre$^+$ cells in the connective tissue and/or von Ebner's glands.

2.3 Materials and methods

2.3.1 Animals

Animal use was approved by The University of Georgia Institutional Animal Care and Use Committee and was in accordance with the National Institutes of Health Guidelines for care and use of animals for research.

Mice were maintained and bred in the animal facility of the Animal and Dairy Science department at the University of Georgia. Wild type (C57BL/6J, Stock#000664), Sox10-Cre (B6; CBA-Tg (Sox10-cre) 1Wdr/J, Stock#025807), and R26-tdTomato

(hereafter tdT) Cre reporter mice (B6.Cg-Gt(ROSA)26Sor$^{tm14(CAG-tdTomato)Hze}$/J, Stock#007914) were obtained from The Jackson Laboratory. The hemizygous Sox10-Cre mice and homozygous tdT reporter breeders were crossed to generate Sox10-Cre/tdT mice. Both male and female mice were used at the examined stages. Cre negative littermates served as controls.

PCR genotyping was performed using the following primers: (1) Cre allele forward 5'-ATTGCTGTCACTTGGTCGGC-3' and reverse 5'-GGAAAATGCTTCTGTCCGTTTGC-3' to detect the Cre recombinase allele; and (2) msSRYz_SexDet forward, 5'-TTGTCTAGAGAGCATGGAGGGCCATGTCAA-3' and reverse 5'-CCACTCCTCTGTGACACTTTAGCCCTCCGA-3' to determine the sex of embryos.

2.3.2 Tissue collections

Mouse embryos at embryonic (E) day 8.0 - 8.5 were collected between 10am and 4pm. Noon of the day of vaginal plug detection was designated E0.5. The embryos were also staged by counting somite pairs. Embryos with 7 - 15 somites were used. Dams were euthanized with CO_2 followed by cervical dislocation. The uterus was removed and placed in a petri dish containing 0.1 M phosphate buffered saline (PBS) (Cat No. CP4390-48; Denville Scientific, Inc, Metuchen, NJ). Embryos were dissected from the uterus under a stereomicroscope and processed for in situ hybridization.

Postnatal mice were harvested at various stages corresponding to different phases of taste bud development, i.e., newborn when early taste buds emerge; 2 weeks when more taste buds become mature, 4, 8, and 16 weeks when taste buds are mature and undergo continuous cell renewal for homeostasis. The day on which the pups were born

was designated postnatal day 1. Mice were euthanized with CO_2 for tongue and soft palate tissue collections.

2.3.3 Immunohistochemistry

Postnatal mice were transcardially perfused using 10 mL warm 0.1 M PBS, followed by 10 mL warm and 20 mL cold 2% Paraformaldehyde (PFA) (Cat No. AAJ19943k2, Fisher HealthCare, Houston, TX) in 0.1 M PBS. Postnatal mouse tongues were dissected from mandible and further fixed in 2% PFA at 4℃ for 2 hours. All fixed tissues were cryoprotected in 30% sucrose in 0.1 M PBS for at least 48 hours at 4℃. Tissues were trimmed and dissected, embedded in O.C.T. (Cat No. 23-730-571, Fisher Healthcare, Houston, TX) and rapidly frozen as such for: (1) sagittal sections of the left and right halves of the anterior 2/3 of the oral tongue where fungiform papillae are distributed, sagittal sections of both foliated papillae, left and right halves of soft palate; and (2) sagittal or transverse sections of the single circumvallate papilla.

Frozen sections were cut at 8 μm in thickness and mounted onto charged slides (Fisher brand™ Superfrost™ Plus Microscope Slides, Cat No. 12-550-15, Fisher Scientific, Waltham, MA). Non-specific binding was blocked with 10% normal donkey serum (Cat No. SLBW2097, Sigma-Aldrich, St. Louis, MO) in 0.1 M PBS containing 0.3% Triton X-100 (Cat No. X100-100ML, Sigma-Aldrich, St. Louis, MO) for 30 min, followed by overnight incubation with primary antibody diluted with 0.1 M PBS containing 0.3% Triton X-100 and 1% normal donkey serum. Primary antibodies used in this study are listed in Table 2.1.

Table 2.1. Primary antibodies that were used.

Antibodies	Dilution	Source
goat anti-E-cadherin	1:500	Cat No. AF748, Fish Scientific, Waltham, MA
rat anti-Keratin 8 (Krt8)	1:1000	Cat No. TROMA-1, Developmental Studies Hybridoma Bank, Iowa city, IA
rabbit anti-NTPDase II	1:1000	Centre de recherché du CHUL Rhumatologie-Immunologie, Québec, Canada
rabbit anti-PLCβ2	1:500	Cat No. sc-515912, Santa Cruz Biotechnology, Dallas, TX
rabbit anti-SNAP25	1:5000	Cat No. S9684, Sigma-Aldrich, St. Louis, MO

After rinses in 0.1 M PBS (3 times, 10 min each), sections were incubated in Alexa Fluor® 488 (for E-cadherin), and/or Alexa Fluor® 647 (for all the other markers)-labeled secondary antibody (1:500, Invitrogen, Eugene, OR) for 1 hour at room temperature. Sections were rinsed and then counterstained with DAPI (200 ng/mL, Cat No. D1306, Fisher Scientific, Waltham, MA). After rinses with 0.1 M PBS followed by dipping in Milli-Q water (Direct-Q® 3 UV water purification system, Millipore, MA). Sections were air dried and coverslipped with Prolong® diamond antifade mounting medium (Cat No. P36970, Fisher Scientific, Waltham, MA).

2.3.4 In situ hybridization

Postnatal mice were transcardially perfused using 10 mL warm 0.1 M PBS solution, followed by 10 mL warm and 20 mL cold 4% PFA in 0.1 M PBS, and 20 mL cold 4% PFA. Mouse embryos and postnatal tongues were fixed in 4% PFA in 0.1 M PBS overnight followed by cryoprotection in 30% sucrose in 0.1 M PBS for at least 48 hours at 4℃. Rapidly frozen tissues were sectioned at 15 μm in thickness. In situ hybridization for Sox10 was performed, as previously described [150], using digoxigenin-labled riboprobes.

DCGS-10 Plasmid carrying Sox10 probe template was a gift from William Pavan (Addgene plasmid# 24752) [145]. Digoxigenin-labeled antisense RNA probe was prepared by linearizing with EcoR1 followed by transcription with T7 RNA polymerase. A sense RNA probe was prepared by linearizing with Xho1 followed by transcription with T3 RNA polymerase and used as control.

2.3.5 Photomicroscopy and quantification

Immunostained slides were analyzed under a fluorescent light microscope (EVOS FL, Life Technologies, CA) and images were taken using a laser scanning confocal microscope (Zeiss LSM 710, Zeiss, Germany). In situ hybridized slides were examined and imaged using a Zeiss Axio imager (Zeiss, Germany).

Quantitative analyses (n=3 each group) were performed using confocal images and ImageJ software to: (1) quantify the number of Sox10-Cre/tdT labeled and unlabeled taste bud cells in circumvallate taste buds of Sox10-Cre/tdT mice at 2, 4, 8, and 16 weeks of age; (2) quantify the number of Sox10-Cre/tdT labeled tdT^+ type II ($PLC\beta2^+$) and tdT^+ type III ($SNAP25^+$) taste bud cells, total $PLC\beta2^+$ type II cells, total $SNAP25^+$ type III cells, and total tdT^+ taste bud cells in circumvallate taste buds of Sox10-Cre/tdT mice at 8 weeks; (3) evaluate the intensity of Krt8 immunosignals by measuring AREA, INTEGRATED DENSITY, and MEAN GRAY VALUE of individual taste bud cells in circumvallate taste buds of 8-week-old wild type and Sox10-Cre/tdT mice. The circumvallate taste papilla was cut in a sagittal orientation to produce serial sections that were perpendicular to the longitudinal axis of taste bud cells. A representative section, with the most taste buds from each wall of the circumvallate papilla trench, was selected for analyses. Taste bud cells with a $DAPI^+$ nucleus were included to analyze the proportion of Sox10-Cre/tdT in

labeling taste bud cell types. Taste bud cells with both strong and weak (but apparently above background) tdT labeling were considered as Sox10-Cre labeled tdT^+ cells. Taste bud cells with a clear boundary marked by E-cadherin immunoproducts were included to analyze the proportion of Sox10-Cre/tdT-labeled taste bud cells at different stages and measure the intensity of Krt8 immunosignals in individual taste bud cells.

2.3.6 Statistical data analysis

The percentages of Sox10-Cre/tdT-labeled tdT^+ type II ($PLC\beta2^+$) and tdT^+ type III ($SNAP25^+$) relative to total tdT^+ taste bud cells, or to total $PLC\beta2^+$ type II cells, or to total $SNAP25^+$ type III cells in the circumvallate taste buds were calculated. Due to the difficulty of identifying individual type I cells with NTPDase II immunosignals, the percentage of tdT^+ type I ($NTPDase\ II^+$) relative to total tdT^+ taste bud cells was extrapolated from the quantitative data for type II and III cells. The corrected total cell fluorescence (CTCF) of Krt8 immunosignals in individual taste bud cells was calculated to represent the intensity using the formula [CTCF= Integrated Density - (Area of selected cell x Mean fluorescence of background readings)].

Quantitative data are represented as histograms (mean ± SD, n=3) using JMP 14 software. Males and females were grouped together because no apparent difference was found between male and female mice regarding proportion and distribution of labeled cells in taste buds, and Sox10 expression in embryos and postnatal mice. Student's t test was used for comparisons between the two groups. One-way analysis of variance (ANOVA) was used to evaluate statistical differences across the groups followed by post-hoc Bonferroni tests. A P-value less than 0.05 was taken as statistical significance.

2.4 Results

2.4.1 Sox10-Cre labels taste bud cells in postnatal mice - few in early and abundant in mature taste buds

To map the lineage of Sox10-expressing cell (hereafter $Sox10^+$) cells in taste buds, Sox10-Cre in which Cre expression is under control of the endogenous sox10 promoter was used. The distribution of Sox10-Cre/tdT-labeled cells in taste buds were thoroughly analyzed in the soft palate and all three types of lingual taste papillae, i.e., fungiform, foliate, and circumvallate, in young adult (8 weeks) mice when taste buds are mature. In serial sections of the soft palate and tongue tissues, Sox10-Cre/tdT-labeled cells were observed in most of the taste buds located by the marker Krt8 in the soft palate (Figure 2.1A), and in all three types of lingual taste papillae, i.e., fungiform (Figure 2.1B), foliate (Figure 2.1C), circumvallate (Figure 2.1D). Concurrently, Sox10-Cre driven tdT^+ cells were extensively distributed in the connective tissue (Figure 2.1A-D) and von Ebner's glands (Figure S2.1). Of note, tdT^+ cells were not found in the taste bud-surrounding tongue epithelium, including basal epithelial cells that are known as progenitors of taste buds [3, 6, 12-14, 143, 144].

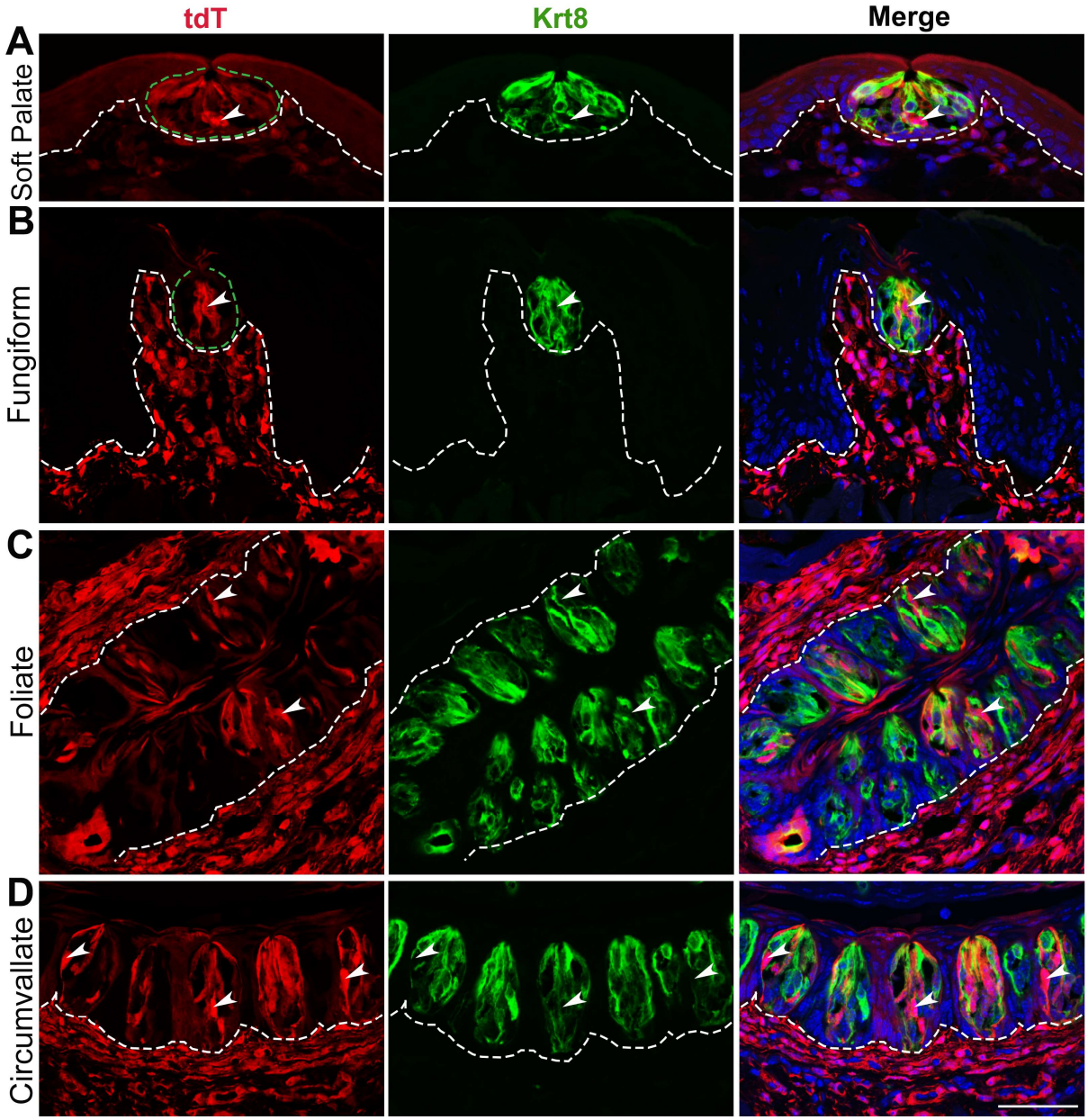

Figure 2.1. Sox10-Cre/tdT (tdTomato) labeled taste bud cells in all examined tissue regions, soft palate (**A**) and taste papillae, i.e., fungiform (**B**), foliate (**C**), and circumvallate (**D**), in young adult (8-week-old) Sox10-Cre/tdT mice. Keratin 8 (Krt8, green) indicates presence of taste buds. White dashed lines demarcate lingual epithelium from the underlying connective tissue. Green dashed lines in A and B bracket a taste bud.

Arrowheads point to tdT^+ taste bud cells. Scale bars: 50 μm for all images (single-plane laser scanning confocal).

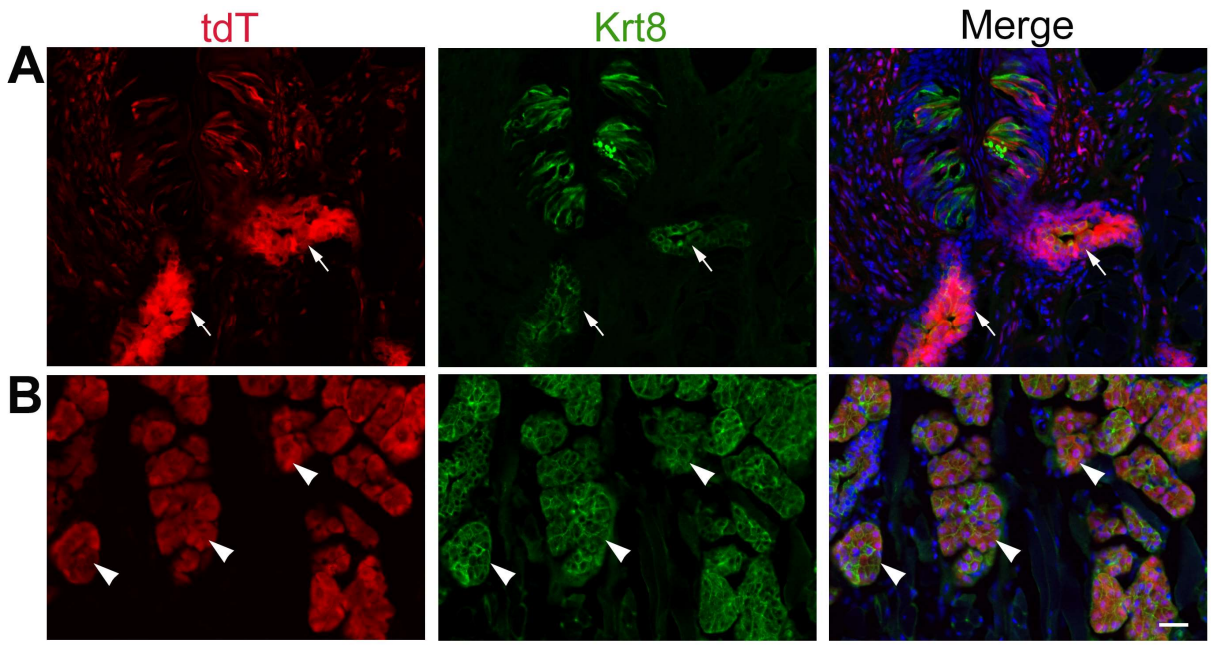

Figure S2.1. Von Ebner's glands were labeled by Sox10-Cre/tdT. In sagittal sections of the circumvallate papilla with von Ebner's glands in an 8-week-old Sox10-Cre/tdT mouse, both the ducts (A, arrows) and acini (B, arrowheads) of the glands were tdT^+ and $Krt8^+$ (green). Scale bars: 50 μm for all images (single-plane laser scanning confocal).

To evaluate at what stages $Sox10\text{-}Cre^+$ cells contribute to taste buds, the distribution of Sox10-Cre/tdT labeled cells in palatal and lingual taste buds was analyzed in newborn and in 2 to 16-week-old mice. At birth when taste buds are structurally recognizable, tdT^+ cells were sporadically seen in $Krt8^+$ taste buds in the soft palate and fungiform papillae (Figure 2.2A); however, no Sox10-Cre/tdT-labeled taste bud cells were observed in the foliate and circumvallate papillae (Figure 2.2A). At 2 weeks and 4 weeks, tdT^+ cells were found in taste buds more frequently in the soft palate and in all three types of lingual papillae (Figure 2.2B, C). At 16 weeks, the distribution of tdT^+ cells within taste buds (Figure 2.2D) was similar to that at 8 weeks in the foliate and circumvallate papillae (Figure 2.1), while a trend of reduced proportion of labeled cells was noticed in the

fungiform papillae and soft palate (Figure 2.2D). In the mice at all examined stages, tdT^+ cells were extensive in the connective tissue of all the tissues (Figure 2.2A-D) and in von Ebner's glands, as shown in Figure S2.1.

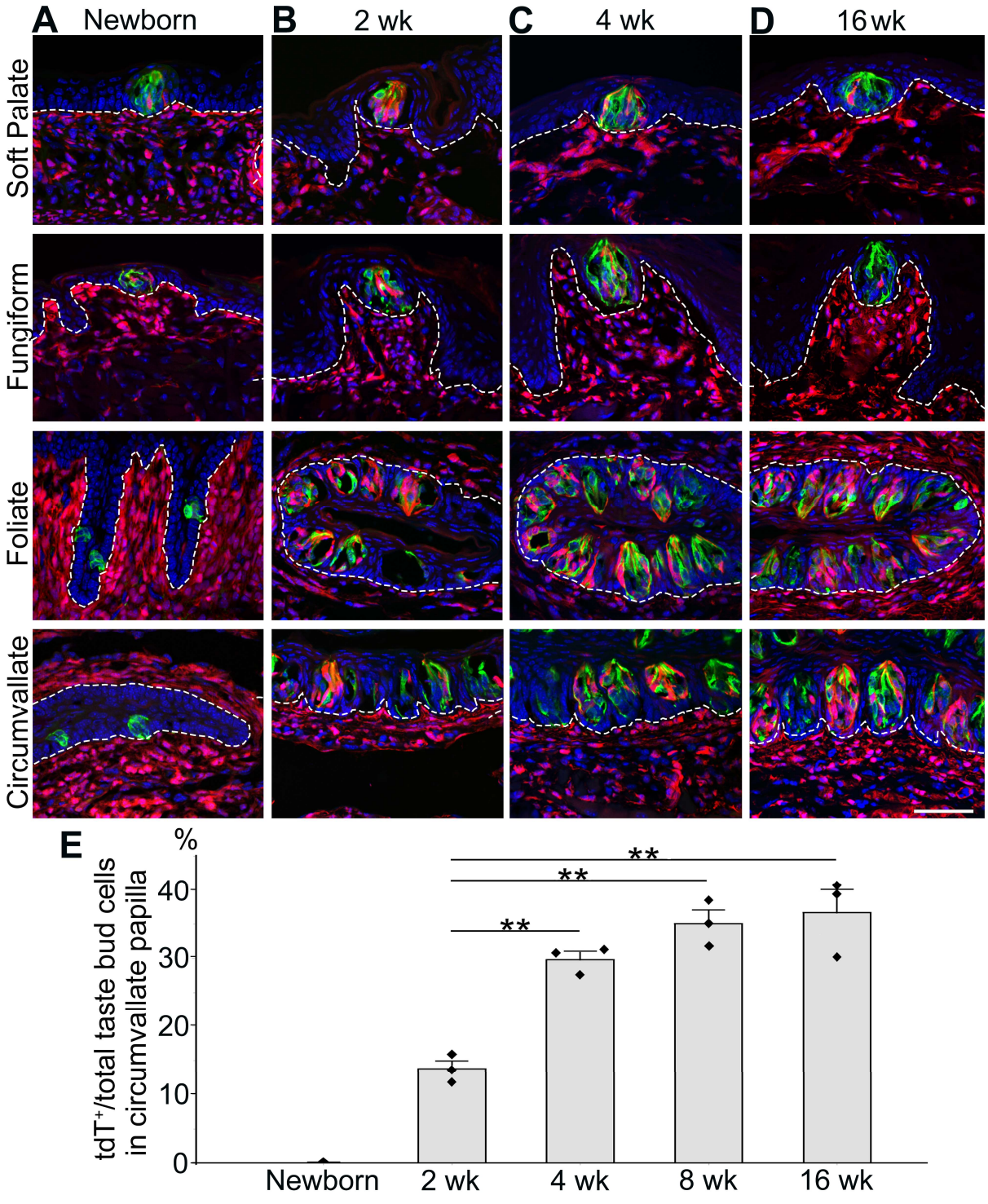

Figure 2.2. Sox10-Cre/tdT-labeled cells in taste buds were rare in newborn and abundant in adult mice. **A-D**: Single-plane laser scanning confocal images of tissue sections of the soft palate and fungiform, foliate, circumvallate papillae in newborn (A), 2-week (B), 4-

week (C), 16-week (D) -old Sox10-Cre/tdT mice. Taste buds were Krt8$^+$ (green). White dashed lines demarcate the lingual epithelium from the underlying connective tissue. Scale bars: 50 μm for all images. **E:** Histograms (X±SD, n=3) to illustrate the percentages of Sox10-Cre/tdT labeled cells relative to total taste bud cells in the circumvallate papilla in newborn, 2-week, 4-week, 8-week, and 16-week-old mice. The diamond dots represent the values of individual samples. **P<0.01 one-way AONVA followed by Bonferroni post-hoc test.

To understand the proportion of taste bud cells that are derived from Sox10-Cre$^+$ cells, sagittal sections of the circumvallate papilla were used to visualize the transverse plane of taste bud cells for quantifications in newborn, 2, 4, 8, and 16-week-old Sox10-Cre/tdT mice (Figure 2.2E). Taste buds were recognized by Krt8 immunosignals and the boundary of each taste bud cell was marked by E-cadherin immunoproducts. The percentage of Sox10-Cre/tdT-labeled tdT$^+$ versus total taste bud cells progressively increased (one-way ANOVA, P<0.01) from zero at birth to 13.8 ± 2.1% at 2 weeks and 30.0 ± 2.0% at 4 weeks (Figure 2.2E). After 4 weeks, when most taste bud cells are mature [151, 152], a slight increase was shown by our quantitative data up to 35.1 ± 3.4% at 8 weeks, and 36.8 ± 5.7% at 16 weeks (Figure 2.2E).

2.4.2 Sox10-Cre labels all three types, but predominanly type III differentiated taste bud cells

Taste buds are comprised of a group of heterogeneous cells, including type I, II, and III differentiated taste bud cells. To better understand which type(s) of taste bud cells are produced by Sox10-Cre$^+$ progenitors, co-localization of tdT with immunosignals of markers for a specific type of differentiated taste bud cells, i.e., NTPDase II for type I,

PLCβ2 for type II, and SNAP25 for type III, was examined in the circumvallate taste buds of young adult (8 weeks) Sox10-Cre/tdT mice. In sections of the circumvallate papilla, with orientations showing both longitudinal and transverse planes of the taste bud cells, we observed that Sox10-Cre driven tdT^+ cells were prevalent throughout the taste buds. Once again, tdT^+ cells were widespread in the connective tissue (Figure 2.3A_1, B_1, C_1) and in von Ebner's glands as shown in Figure S2.1. A subpopulation of taste cells, immunoreacted with a type I, II, or III cell marker, appeared as tdT^+ (Figure 2.3, solid arrowheads) in taste buds. Of interest, tdT^+ taste bud cells were more frequently co-labeled with type III taste cell marker SNAP25 (Figure 2.3C_2) than type II cell marker PLCβ2 (Figure 2.3B_2).

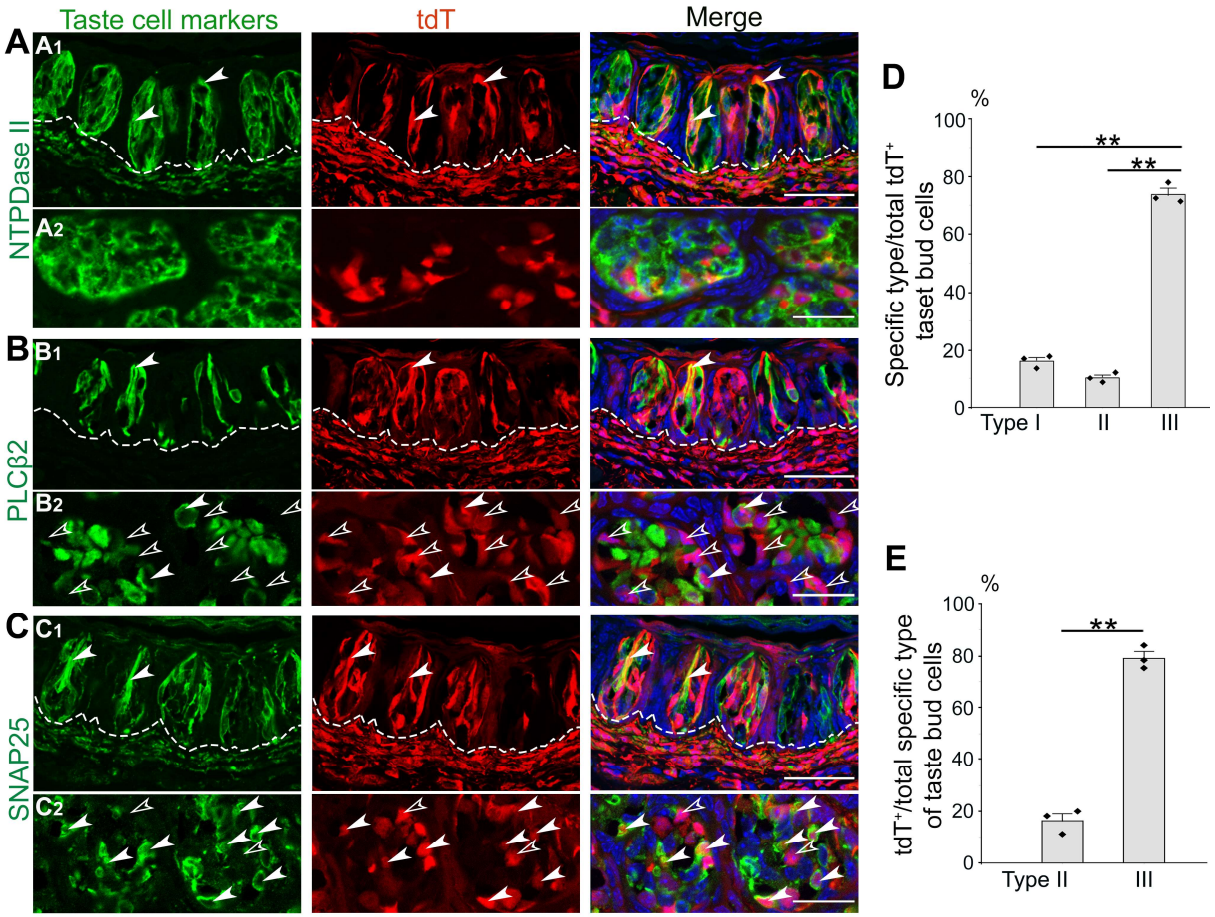

Figure 2.3. Sox10-Cre/tdT labeled distinct proportions of types I, II, and III differentiated taste bud cells. **A-C:** Representative images (single-plane laser scanning confocal) of transverse (A_1, B_1, and C_1) and sagittal (A_2, B_2, and C_2) sections of the circumvallate papilla in 8-week-old Sox10-Cre/tdT mice. Specific types of taste bud cells were labeled by NTPDase II for type I (A_{1-2}), PLCβ2 for type II (B_{1-2}), and SNAP25 for type III (C_{1-2}) cells. Solid arrowheads point to the cells co-labeled by tdT and markers for specific types of taste bud cells. Open arrowheads point to tdT^+ cells in taste buds that were negative for specific taste bud cell type markers. Scale bars: 50 μm in A_1, B_1, and C_1; 20 μm for A_2, B_2, and C_2. **D-E**: Histograms (X±SD, n=3) to illustrate the percentages of tdT^+ specific type (I, II, and III) versus total tdT^+ (D) or versus total type II or III (E) taste bud cells in

circumvallate taste buds. The diamonds represent data points of individual samples. **P<0.01 (D) one-way ANOVA followed by Bonferroni post-hoc test. **P<0.01 (E) Student's t test.

Quantitative analyses were performed in order to understand the proportions of Sox10-Cre driven tdT in labeling each specific type of differentiated taste bud cells (Figure 2.3D). Type II and type III taste bud cells were easily distinguishable and counted. In all of the Sox10-Cre/tdT labeled taste bud cells, tdT labeling was distributed unevenly among the three types (I, II, III) of differentiated taste bud cells (one-way ANOVA, P<0.01). Relative to total tdT^+ taste bud cells, the quantity of tdT^+ type III cells (73.9 ± 3.5%) was significantly higher than tdT^+ type II (10.2 ± 1.6%) (P<0.01) and tdT^+ type I (15.9 ± 2.2%, extrapolated) (P<0.01) cells. No significant difference was found between tdT^+ type I and tdT^+ type II cells (P=0.10) (Figure 2.3D). Relative to the total number of a specific type of taste bud cells, 79.1 ± 4.4% of type III and 16.5 ± 4.7% of type II taste bud cells were tdT^+, and the difference was statistically significant (Student's t test, P<0.01) (Figure 2.3E).

2.4.3 Taste bud cells vary in the intensity of Krt8 immunosignals with Sox10-Cre/tdT-labeled taste bud cells having a low level of Krt8

Krt8 is a widely used marker for taste bud cells. We observed that the intensity of Krt8 immunolabeling in individual taste bud cells varies considerably and that Sox10-Cre/tdT-labeled taste bud cells could not be obviously identified with Krt8 immunostaining. We performed thorough examinations of the co-localization of tdT with Krt8 immunosignals in individual taste bud cells at a perpendicular plane to the elongated taste bud cells of the circumvallate papilla. Within the boundaries of taste bud cells labeled with E-cadherin, tdT^+ taste bud cells did not have significant Krt8 immunoproducts (Figure

2.4A, open arrowheads) (Figure 2.4A, tdT/Krt8/E-cad or tdT/Krt8/DAPI). To illustrate the intensity of Krt8 immunosignals in taste bud cells in a quantitative manner, the corrected total cell fluorescence (CTCF) of individual taste bud cells was calculated to represent Krt8 fluorescence intensity. CTCF values in individual taste bud cells were distributed in a broad range (Figure 2.4B). The average of CTCF values of tdT^+ taste bud cells (15,854±23,950) were significantly lower than that of tdT^- taste bud cells (68,425±54,225) ($P<0.01$) (Figure 2.4C). A small population of tdT^+ taste bud cells were completely absent of Krt8 immunoproducts (Figure 2.4B). Moreover, 52% of tdT^+, in contrast to only 2% of tdT^-, taste bud cells had very low CTCF values, from 0 to 10,000 (Figure 2.4B).

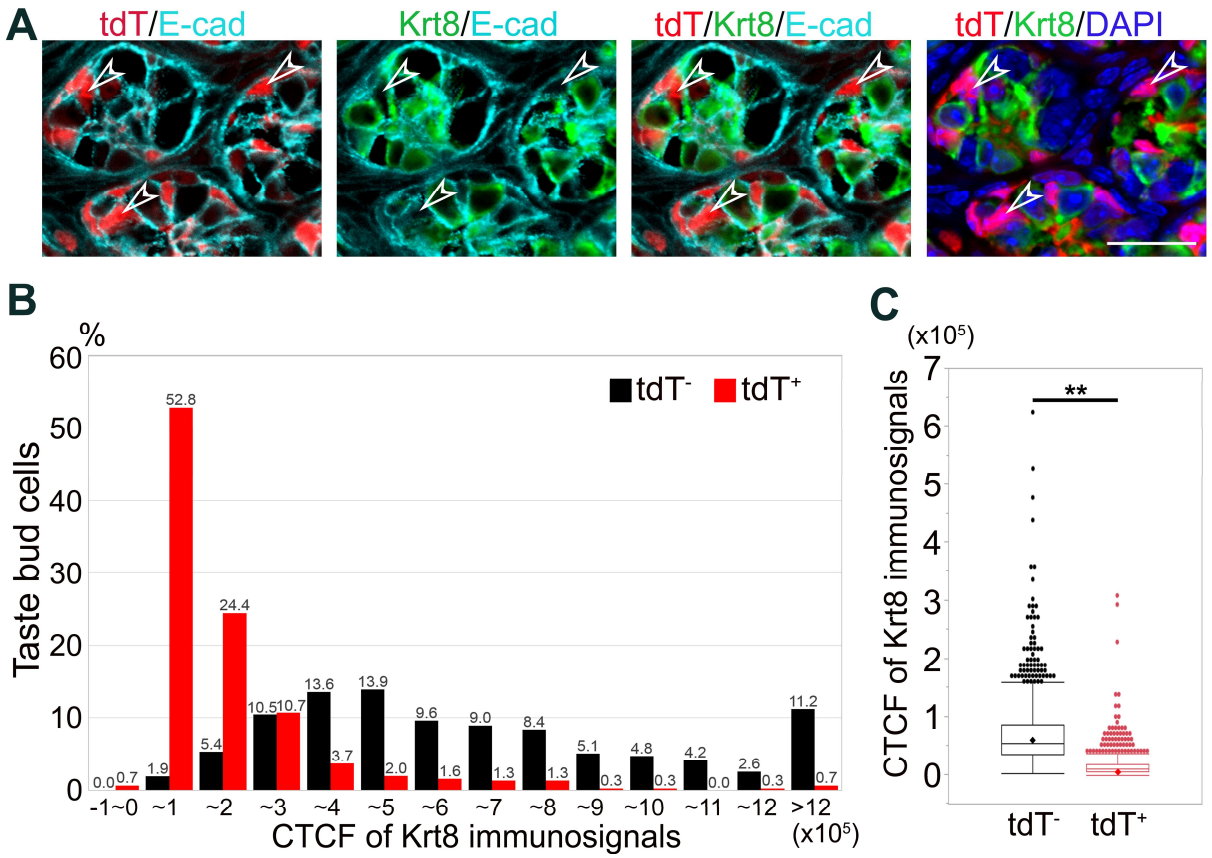

Figure 2.4. Sox10-Cre/tdT-labeled taste bud cells had a low intensity of Krt8 immunosignals (green). **A**: Images of sagital sections of the circumvallate papilla in an 8-week-old Sox10-Cre/tdT mouse. E-Cadherin (E-cad, cyan), Krt8 (green) and counterstained with DAPI (blue). Open arrowheads point to tdT^+ taste bud cells that were not obvious in Krt8 immunolabeling. Scale bars: 20 μm (single-plane laser scanning confocal images). **B-C**: Histograms (B) and box plots (C) to show the CTCF distribution of intensity of Krt8 immunosignals in tdT^+ and tdT^- taste bud cells in Sox10-Cre/tdT mouse circumvallate papilla (n=3). CTCF: The corrected total cell fluorescence. The boxes in (C) represent the interquartile range, the whiskers represent the range of normal distribution, and dots represent the outliners. The line and diamond within each box represent the median and average value respectively. **P<0.01 (C) Student's t test.

To confirm our observation and verify the diversity of Krt8 in labeling taste bud cells, a cocktail of antibodies for type I (NTPDase II), II (PLCβ2), and III (SNAP25) was used to label all differentiated taste bud cells and double-labeled with Krt8 (Figure S2.2A) in young adult (8 weeks) C57BL/6J wild type mice. The heterogeneity of the intensity of Krt8 immunosignals were apparent among the taste bud cells labeled with taste cell markers (type I+II+III). Brightly (Figure S2.2A, solid arrowheads), mildly, and faintly labeled taste bud cells were seen (Figure S2.2A, open arrowheads). Interestingly, $SNAP25^{+}$ type III taste bud cells were always faint in Krt8 labeling (Figure S2.2B).

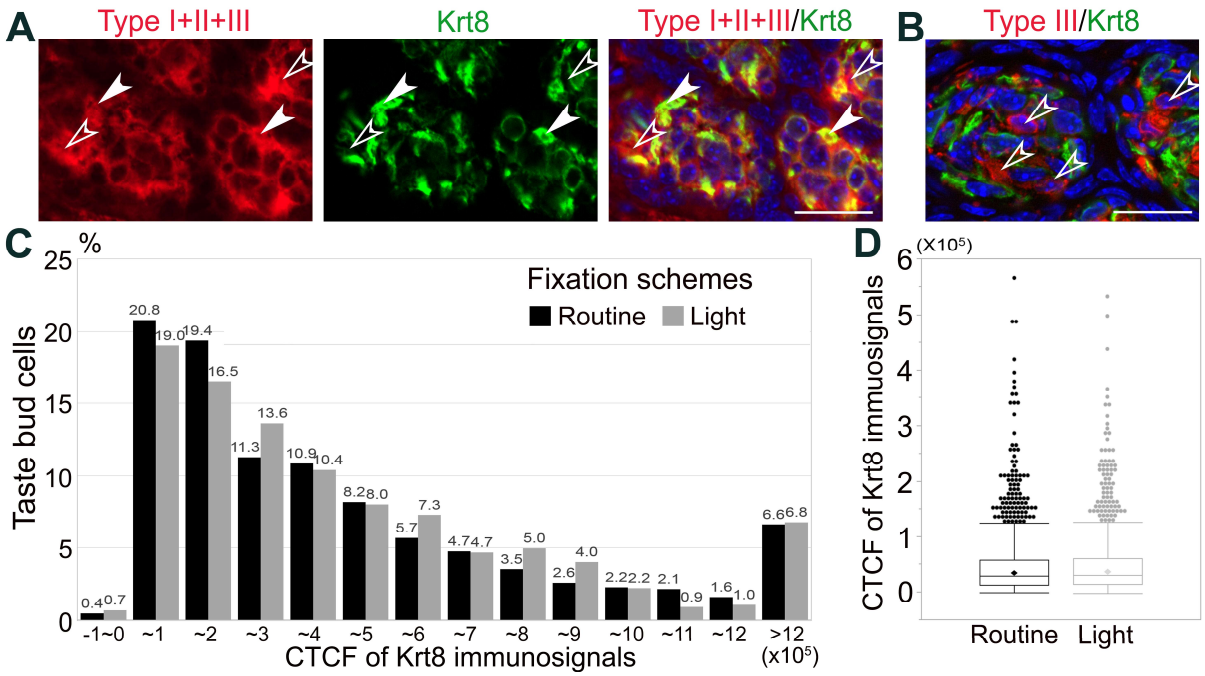

Figure S2.2. Taste bud cells had a broad range of intensity of Krt8 immunosignals. **A**: Taste bud cells were labeled by Krt8 (green) and a mixture of antibodies against NTPDase II for type I, PLCβ2 for type II, and SNAP25 for type III (Type I+II+III, red) in sagital sections of the circumvallate papalla of 8-week-old wild type mice. Solid and open arrowheads point to taste bud cells with high or low intensity of Krt8 immunosignals respectively. **B**: SNAP25^{+} type III (red) taste bud cells had no obvious Krt8^{+} (green) immunoproducts. Open arrowheads point to SNAP25^{+} taste bud cells with low intensity of Krt8 staining. Scale bars: 20 μm in for all images (single-plane laser scanning confocal images). **C-D**: Histograms (C) and box plots (D) to illustrate the diverse intensity of Krt8 immunosignals (CTCF) in individual taste bud cells in the circumvallate papilla of wild type mice (n=3). Tissues were fixed with our routine (transcardially perfused with 2% PFA + 2 hours post-fixation 2% PFA) or light (5-min fixation on fresh tissue sections with 2% PFA) fixation scheme. CTCF: The corrected total cell fluorescence. The boxes in (D) represent the interquartile range, the whiskers represent the range of normal distribution, and dots

represent the outliners. The line and diamond within each box represent the median and average value respectively.

To rule out the possibility that variability in Krt8 staining was due to differences in tissue fixation procedures, CTCF values in taste bud cells were collected from our routinely fixed and more lightly fixed tissues (Figure S2.2C, Fixation scheme, Routine and Light). Our data showed that CTCF ranges and distributions in individual taste bud cells were similar between lightly and routinely fixed taste bud cell population (Figure S2C-D). No significant difference ($P>0.05$) of CTCF was found between routinely and lightly fixed taste bud cell populations (44,341±53,986 vs 45,646±52,921) (Figure S2.2D). The range of CTCF values were broad in both groups, with a distribution from -1971 to 565,427 (routinely fixed) and -3,078 to 532,718 (lightly fixed).

2.4.4 Sox10 expression is detected in multiple tissue compartments, including neural crest, connective tissue core of taste papillae, and von Ebner's glands

To identify tissue compartments where $Sox10^{+}$ progenitors for taste bud cells, the distribution of Sox10 mRNA was examined using in situ hybridization. As with previous reports [145], Sox10 mRNA expression was detected in cranial neural crest cells, including the cells in the trigeminal neural crest (Figure 2.5A, TN), branchial arch 1 (Figure 2.5A, BA1), and optic eminence (Figure 2.5A, OE) of E8.5 embryos. Signals were not seen in the adjacent sections hybridized with sense RNA probe for Sox10 (Figure S2.3A).

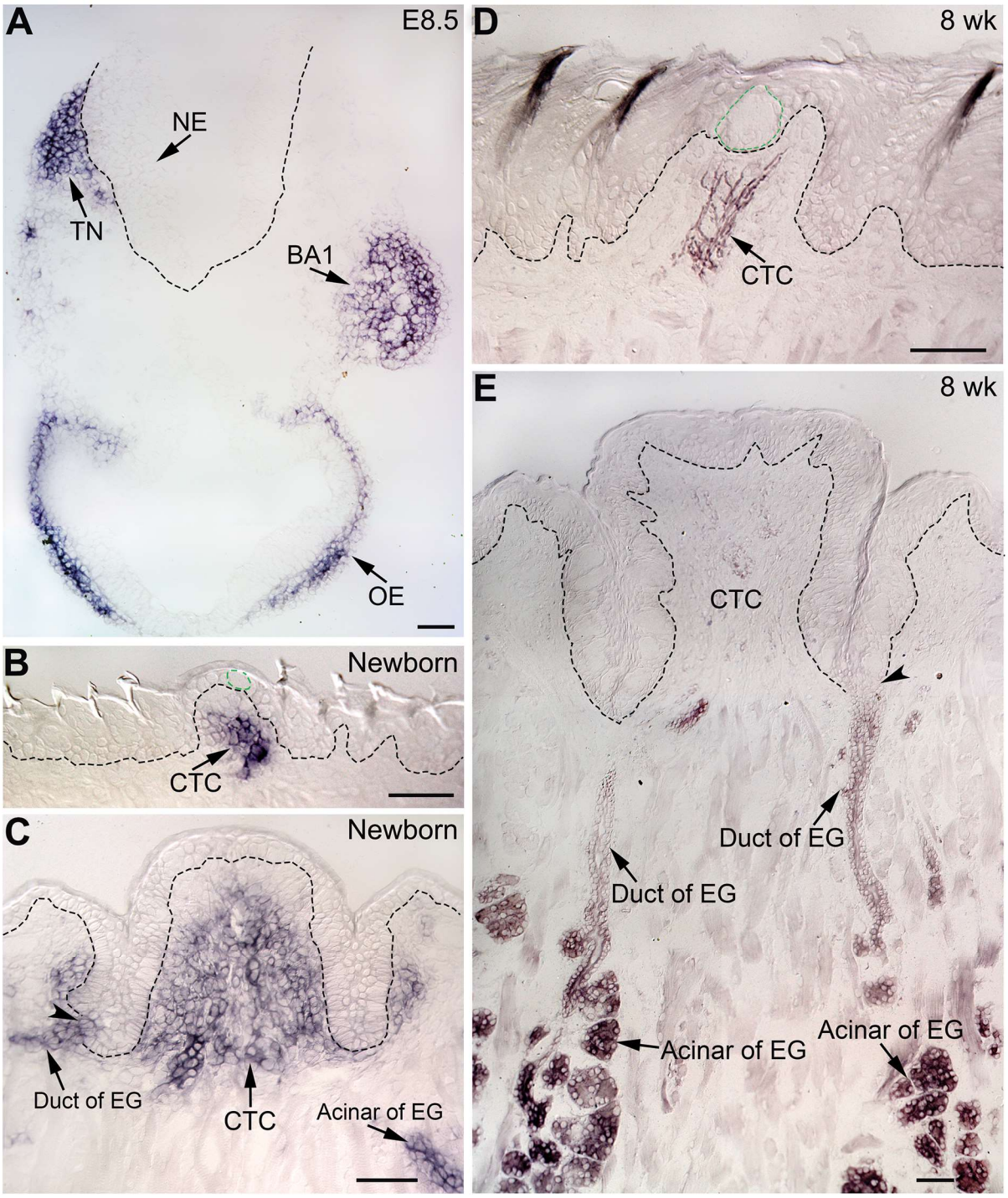

Figure 2.5. Sox10 mRNA was detected with in situ hybridization using the digoxigenin-labeled antisense RNA probe (blue). Sox10 mRNA was detected in: **A**: neural crest cells in trigeminal neural crest stream (TN), branchial arch 1 (BA1), and optic eminence (OE)

in the transverse sections of E8.5 embryo at the hindbrain level. Black dashed lines demarcate the neuroepithelium (NE) from surrounding tissue; **B-C**: the connective tissue core (CTC) of fungiform and circumvallate papillae, acinar of von Ebner's glands (Acinar of EG) and the duct (Duct of EG) opening (arrowhead) to the circumvallate papila in newborn mice; **D-E**: the connective tissue core (CTC) of fungiform and circumvallate papilla, acinar of von Ebner's glands (Acinar of EG) and the duct (Duct of EG) opening (arrowhead) to the circumvallate papila in young adult (8-week-old) mice. Green dashed lines in B and D bracket a taste bud. Black dashed lines mark the borders between the epithelium and underlying tissue. Scale bars: 50 μm for all images.

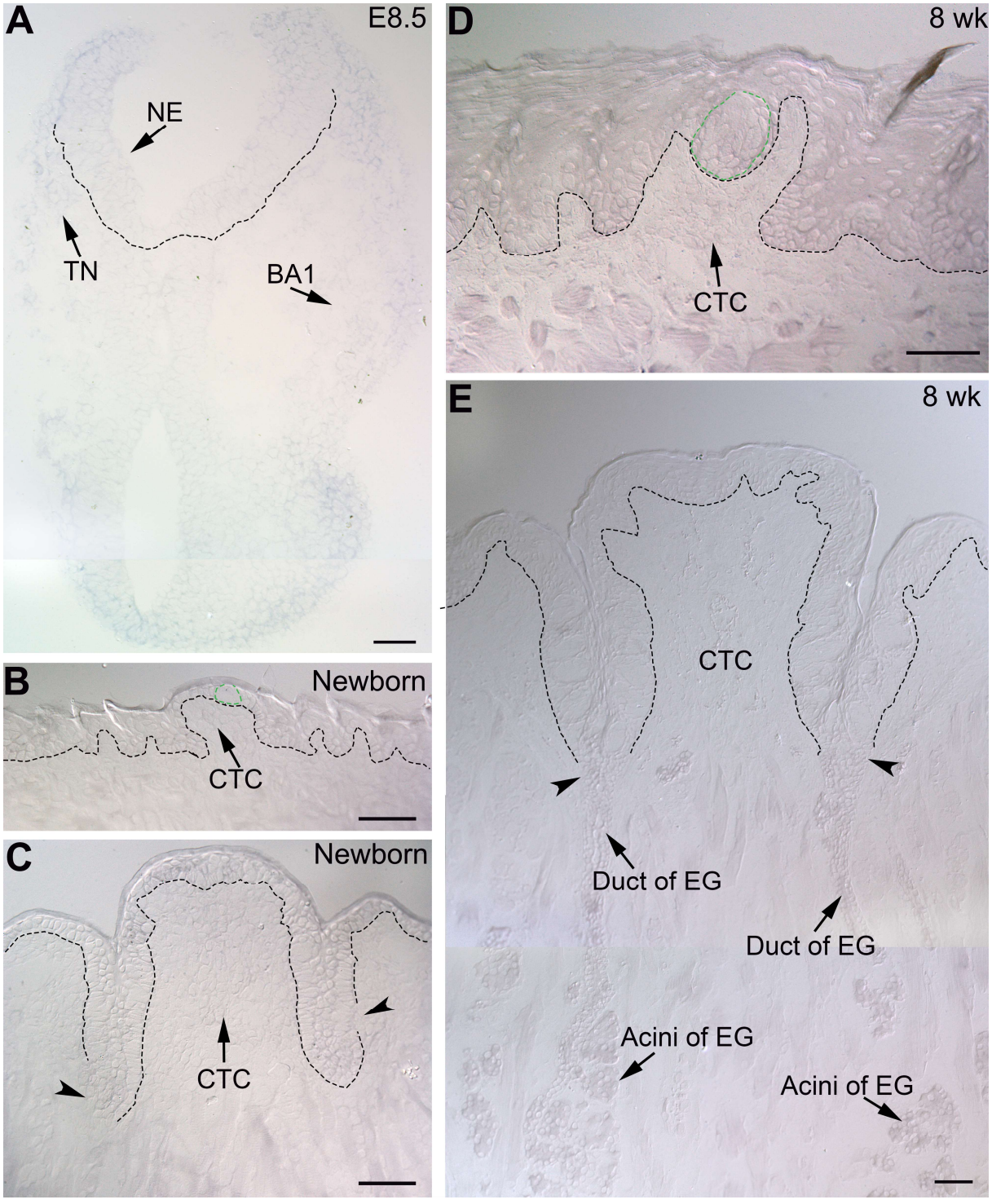

Figure S2.3. No in situ hybridization signals were detected using Sox10 sense RNA probe. Tissue sections adjacent to those in Figure 2.5 were used for Sox10 sense RNA probe. The images are corresponding to the images with in situ signals in Figure 2 5. **A**:

An E8.5 embryo; **B**: newborn fungiform papillae; **C**: newborn circumvallate papillae; **D**: fungiform papilla at 8 weeks; **E**: circumvallate papilla at 8 weeks. Green dashed lines in B and D bracket a taste bud. Black dashed lines in (A) demarcate the NE from surrouding tissue. Arrowheads in (C,E) point to the openings of ducts of von Ebner's glands. Black dashed lines in (B-E) mark the borders between the epithelium and underlying tissue. Scale bars: 50 μm for all images. BA1, rranchial arch1; CTC, connective tissue core; NE, neuroepithelium; OE, optic eminence; TN, trigeminal neural crest stream.

In newborn and 8-week-old mouse tongue, Sox10 mRNA was found in the connective tissue core of taste papillae, e.g., fungiform (Figure 2.5B, D) and circumvallate (Figure 2.5C, E), although the staining was less intense in the adult compared to the newborn. Sox10 mRNA was also observed in the ducts and acini (Figure 2.5C, E) of von Ebner's glands adjacent to the circumvallate papilla. Also, signals were seen in the opening of the ducts of von Ebner's glands at the bottom trench areas of circumvallate papilla (Figure 2.5C, E, arrowheads).

Of note, Sox10 mRNA was not detected in the tongue epithelium - neither in the taste buds nor surrounding tongue epithelium. Furthermore, signals were not observed in lamina propria outside of the taste papillae. This included the filiform papillae and the surrounding tissue of the circumvallate papilla. Again, no signals were detected in the control sections of tongue tissue with sense RNA probe (Figure S2.3B-E).

2.5 Discussion

2.5.1 Sox10-Cre$^+$ cells: newly discovered progenitors for taste buds in postnatal mice

Previous studies have reported that taste bud progenitor cells reside in the basal layer of the surrounding lingual epithelium and express Krt14, Krt5, TRP63, Sox2 and LGR5 [6, 8, 9]. However, our recently published data revealed that a population of taste bud cells are labeled concurrently with cells under, but not within, the tongue epithelium [16, 153]. In the present study, using a model of Cre under the control of endogenous Sox10 promoter (Sox10-Cre), we found that in mature taste buds of adult mice, Sox10-Cre/tdT labeled a large population (up to around 35%) of taste bud cells. These taste bud cells had a significantly low level of immunoproducts of Keratin (Krt) 8, a widely used pan-taste cell marker. Sox10 mRNA was not detected in taste buds nor in the stratified lingual epithelium suggesting the taste bud cells labeled by Sox10-Cre are derived from cells in tissue other than tongue epithelium. Together, our data indicate that the Sox10-Cre$^+$ cells are a previously unrecognized source of progenitors for taste bud cells.

Lineage tracing of sonic hedgehog (Shh)$^+$ cells in the epithelium of tongue rudiment with Shh-CreER mouse model demonstrated that early taste buds are from Shh$^+$Krt8$^+$ epithelial cells of the tongue primordium, not the surrounding tissue compartments [18, 34]. Our data from the present study showing that Sox10-Cre/tdT labeled cells within taste buds are progressively more abundant with age in postnatal mice indicate a dual origin of taste buds during maturation and maintenance after birth, i.e., from both surrounding basal cells of stratified tongue epithelium and Sox10-Cre$^+$ cells under the tongue epithelium. Further studies are needed to demonstrate whether Sox10-

Cre$^+$ cells temporarily transit to Krt14$^+$ basal epithelial cells, which, if so, will reconcile the seemingly contradictory reports [6].

2.5.2 Tissue locations of Sox10-expressing taste bud progenitors

Sox10 has been detected in multiple tissues and cell types including migrating neural crest cells [145] and neural crest-derived cell populations from embryo to adult, including glial cells [129, 130], melanocytes [146], peripheral ganglia in the gut [154, 155], dorsal root ganglia [156-158], and stem cells in cranial bone marrow [158]. Sox10 expression has also been detected in submandibular salivary glands [133]. Moreover, Sox10 expression has been found in non-neural crest derived cell lineages such as glial cells in the central nervous system in postnatal mice [159-162].

To identify the tissue compartments that contain Sox10$^+$ cells, in situ hybridization was performed and robust expression of Sox10 mRNA in migrating neural crest cells was detected in the migrating neural crest cells in E8.5 embryos, which is consistent with the previous reports [145]. Of particular interest, Sox10$^+$ cells were detected in taste bud-surrounding tissue compartments in postnatal mouse tongues -- the connective tissue core of taste papillae and von Ebner's glands under the circumvallate papilla, which add two novel reservoirs of Sox10$^+$ cells.

Of note, Sox10 mRNA was not detected in the tongue epithelium including taste buds and surrounding stratified tongue epithelium, nor the connective tissue outside of the taste papillae. These results lead us to propose three candidates of Sox10$^+$ taste bud progenitors: neural crest or non-neural crest derived connective tissue cells in the core of taste papillae, or Von Ebner's glands. To further define the specific tissue compartments

that host Sox10$^+$ taste bud progenitors, it will be necessary to mark lineages of each specific cell population.

2.5.3 Krt8 does not label all taste bud cells and Sox10-Cre$^+$ progenitor-derived taste bud cells are not noticeably Krt8$^+$

Taste bud cells are intragemmal, simple epithelial cells that are distinguishable from the surrounding stratified squamous epithelium. Krt8, a type II intermediate filament, is specifically expressed in simple epithelial cells and has been widely used as a pan taste bud cell marker [163]. We have observed that the intensity of Krt8 immunosignals is considerably variable in individual taste bud cells. Measurements of corrected total cell fluorescence (CTCF) in individual taste bud cells to represent the intensity of Krt8 immunosignals showed a broad range of CTCF values distribution. Of note, the CTCF values in a small population of taste bud cells are below 0 suggesting the absence of Krt8 immunoproducts in these cells. Also, over half the population of taste bud cells had very low CTCF values. Our results indicate that taste bud cells vary remarkably in Krt8 expression which prompts a re-evaluation to address the question whether Krt8 can serve as a pan-taste bud cell marker.

Interestingly, Sox10-Cre/tdT labeled taste bud cells were faint in Krt8 immunolabeling. The CTCF values in tdT$^+$ taste bud cells were significantly lower than those in tdT$^-$ ones. Intermediate filaments including Krt8 are key elements of cytoskeleton [164-166] and provide mechanical support for the plasma membrane to withstand the stress [167], which enhances cell structural and morphological integrity. In taste bud cells, the intermediate filaments are organized into bundles around the nucleus and in the

periphery of the cytoplasm [168]. The difference of Krt8 levels in individual taste bud cells may represent the status/phase, type, or functions of taste cells.

Quantitative analyses demonstrated that Sox10-Cre$^+$ cells contribute mainly to type III (74%), and a small proportion of type I (16%) and type II (10%) taste bud cells. indicating that Sox10-Cre$^+$ cells tend to differentiate into neuronal-like taste bud cells (Type III). In our previous study using P0-Cre/tdT to trace the lineage of neural crest and derived connective tissue cells, 30% of tdT$^+$ taste bud cells were SNAP25$^+$ type III taste bud cells in the circumvallate papilla [16], suggesting that the Sox10-Cre$^+$ cells represent an overlapping but different progenitor cell population from P0-Cre$^+$ cells. Additionally, among type III taste bud cell population, 79% of them are labeled by Sox10-Cre/tdT, indicating that Sox10-Cre$^+$ cells serve as a major progenitor source for type III taste bud cells. This complements with the previous finding that only type I and II taste bud cells are found as offspring of taste papilla placodal cells expressing sonic hedgehog (Shh) [29, 34, 149]. Overall, our data demonstrate that Sox10-Cre$^+$ cells in the connective tissue and/or von Ebner's glands represent another source of progenitors, as well as those in the tongue epithelium, that give rise to a significant population of taste bud cells.

Acknowledgements

The authors give thanks to Drs. Shi-You Chen, Luke Mortensen, and Franklin West, (The University of Georgia, Athens, Georgia) for the discussion and feedbacks; Dr. William Pavan for the Sox10 probe template; Dr. Guiqian Chen and Mr. Brett Marshall for assistance in mouse maintenance. This study was supported by the National Institutes of Health, grant number R01DC012308 and R21DC018089 to H.X.L.

CHAPTER 3

TASTE BUDS ARE NOT DERIVED FROM NEURAL CREST IN MOUSE, CHICKEN, AND ZEBRAFISH [1]

[1] Wenxin Yu, Zhonghou Wang, Brett Marshall, Yuta Yoshida, Renita Patel, Xiaogang Cui, Rebecca Ball, Linlin Yin, Fuminori Kawabata, Shoji Tabata, Wenbiao Chen, Robert N. Kelsh, James D. Lauderdale, and Hong-Xiang Liu. 2021. *Developmental Biology*. 471:76-88. Reprinted here with permission of publisher.

3.1 Abstract

Our lineage tracing studies using multiple Cre mouse lines showed a concurrent labeling of abundant taste bud cells and the underlying connective tissue with a neural crest origin, warranting a further examination on the issue of whether there is an neural crest derivation of taste bud cells. In this study, we mapped neural crest cell lineages in three different models, Sox10-iCreER^{T2}/tdT mouse, GFP^{+} neural fold transplantation to GFP^{-} chickens, and Sox10-Cre/GFP-RFP zebrafish model. We found that in mice, Sox10-iCreER^{T2} specifically labels neural crest cell lineages with a single dose of tamoxifen at E7.5 and that the labeled cells were widely distributed in the connective tissue of the tongue. No labeled cells were found in taste buds or the surrounding epithelium in the postnatal mice. In the GFP^{+}/GFP^{-} chicken chimera model, GFP^{+} cells migrated extensively to the cranial region of chicken embryos ipsilateral to the surgery side but were absent in taste buds in the base of oral cavity and palate. In zebrafish, Sox10-Cre/GFP-RFP faithfully labeled known neural crest-derived tissues but did not label taste buds in lower jaw or the barbel. Our data, together with previous findings in axolotl, indicate that taste buds are not derived from neural crest cells in rodents, birds, amphibians or teleost fish.

Key words: Taste buds, neural crest, progenitors, mouse, chicken, zebrafish.

3.2 Introduction

Taste buds are taste sensory organs located on the tongue and inside the oral cavity of all vertebrates. In some fishes and amphibians, particularly species with barbels, taste buds are also found in the skin. A large proportion of taste bud cells are glial-like (type I) [21, 22, 24-26, 169] and a small subset is neuronal-like (type III) [48, 69-72, 169].

Given that glial cells in the peripheral nervous system are derived from the neural crest [170-173] and neurons are from either neural crest [171-176] or epibranchial placodes [173, 177-182], a question has been asked whether taste buds could plausibly have been derived either from the neural crest, or from the epibranchial placodes, or from the local epithelium [183]. Barlow and Northcutt used grafting experiments between pigmented and non-pigmented axolotl embryos and showed that neither the neural crest nor epibranchial placodes contribute to taste buds, whereas DiI-labeled endoderm formed both taste buds and the surrounding epithelium in the oropharynx, confirming an endoderm-derived local epithelial origin for taste buds in axolotl [183].

Although compelling evidence demonstrates a non-neural crest origin of taste bud cells in axolotl [183], studies in rodents indicate that, in addition to the lingual epithelium [3, 6, 12, 14, 141, 144], neural crest may also contribute to taste bud cells [17, 184, 185]. This difference between axolotl and rodents suggests that there may be a difference in taste bud development between non-mammals and mammals.

In mice, evidence that taste bud progenitors arise from local epithelium is solid [3, 6, 12, 14, 141, 144, 183]. Stone and colleagues identified local epithelium as taste progenitor source using mosaic X-inactivation chimera mouse model [12], which was later reiterated studies that traced the lineage of local epithelium to taste buds using Cre-LoxP transgenic mouse model [6]. However, the question remains whether surrounding epithelium is the “sole” source of taste bud progenitors.

In the past several years, the use of transgenic mouse lines to trace the lineage of cranial neural crest cells has raised new speculations regarding neural crest derivatives, e.g., tooth bud [186] and olfactory [187, 188] epithelial cells. In the tongue organ, neural

crest has been found to be the major contributor to the mesenchyme [123] and connective tissue under the epithelium [17, 184, 185]. Our recent findings revealed that a significant proportion of taste bud cells are labeled with P0-Cre [17, 185], Dermo1-Cre [185], Sox10-Cre [184] concurrently with the underlying connective tissue cells in the absence of labeling in the surrounding lingual epithelium. In contrast, Wnt1-Cre-labeled cells are rarely seen in taste buds although labeled cells are extensive in the underlying connective tissue [17]. Therefore, the published data suggest the possibility of a neural crest derivation of taste buds [17, 184, 185] but this fundamental issue has not yet settled. Given that none of these models labels all neural crest cells, nor do they label neural crest cells exclusively [113, 124], animal models that specifically and exclusively label neural crest cell lineages and detailed examinations are imperative.

To address the fundamental issues of whether taste bud cells have a derivation from neural crest cells and whether this contribution is species-specific, we performed lineage tracing for neural crest cells in three model species, using Sox10-iCreER^{T2}/tdT mice, GFP^{+}/GFP^{-} chicken chimeras, and Sox10-Cre/GFP-RFP zebrafish. We found that in these three models neural crest cell lineages were extensively marked but not found in taste buds. Together with previous findings in axolotl [183], the data from these different model species provide support for the idea that taste buds do not have a neural crest derivation.

3.3 Materials and methods

3.3.1 Animals

Animal use was approved by The University of Georgia Institutional Animal Care and Use Committee and was in accordance with the National Institutes of Health

Guidelines for care and use of animals for research. Three species of animals were used: mouse, chicken and zebrafish.

Mice were maintained and bred in the animal facility of the Animal and Dairy Science department at the University of Georgia at 22℃ under 12-hour day/night cycles. Sox10-iCreER^{T2} (CBA;B6-Tg(Sox10-icre/ER^{T2})388Wdr/J, Stock#027651) [189] and R26-tdTomato (hereafter tdT) Cre reporter mice (B6.Cg-Gt(ROSA)26Sor$^{tm14(CAG-tdTomato)Hze}$/J, Stock#007914) [190] were obtained from The Jackson Laboratory. The hemizygous Sox10-iCreER^{T2} mice and homozygous tdT reporter breeders were crossed to generate Sox10-iCreER^{T2}/tdT mice. No significant difference was found in the distribution pattern of labeled cells between males and females; therefore, males and females were grouped together and used at the examined stages. Cre negative littermates served as controls. FVB/NJ wild type mice (The Jackson Laboratory, Stock#001800) were used to breed in parallel for fostering caesarean born Sox10-iCreER^{T2}/tdT pups.

Chicken embryos were produced by incubating fertilized eggs horizontally in the cabinet incubator (Cat#1502 “SPORTSMAN”, GQF Manufacturing Company, Inc, Savannah, GA) in the lab room at the University of Georgia. Fertilized Roslin GFP^{+} donor [191] and Roslin GFP^{-} host chicken eggs were purchased from Clemson University.

Zebrafish were housed in the Paul D. Coverdell Building Fish Facility at the University of Georgia at 28.5℃ under 12-hour day/night cycles. Sox10-EGFP zebrafish (TG(-4.9sox10:egfp)^{ba2} and Sox10-Cre zebrafish (TG(-4725sox10:Cre)^{ba74} were obtained from Dr. Robert N. Kelsh, University of Bath, Bath, UK) [192-194]. Hemizygous Sox10-Cre zebrafish (TG(-4725sox10:Cre)^{ba74} were crossed with homozygous GFP-RFP Cre reporter zebrafish (Tg(eab2:[EGFP-T-mCherry]), from Dr. Wenbiao Chen, Vanderbilt

University, Nashville, TN) [195] to generate Sox10-Cre/GFP-RFP zebrafish. Timed pairings were allowed for 30 min for synchronized embryo development.

PCR genotyping was performed using the following primers: (1) mouse Cre allele forward 5'-ATT GCT GTC ACT TGG TCG GC-3' and reverse 5'-GGA AAA TGC TTC TGT CCG TTT GC-3' to detect the mouse Cre recombinase allele; (2) zebrafish Cre allele forward 5'-CCA TGT CCA AAT TTA CTG ACC GTA C-3' and reverse 5'-CAT CTT CAG GTT CTG CGG GAA AC-3' to detect the zebrafish Cre recombinase allele; (3) zebrafish EGFP allele forward 5'-GTT CAT CTG CAC CAC CGG C-3' and reverse 5'-TTG TGC CCC AGG ATG TTG C -3' to detect the zebrafish EGFP reporter allele; (4) iCreER^{T2} allele forward 5'-GAG ACG GAC CAA AGC CAC T-3' and reverse 5'-CTG CAG CCT CCT CCA CTG-3' to detect the mouse iCreER^{T2} recombinase allele; (5) msSRYz_SexDet forward, 5'-TTG TCT AGA GAG CAT GGA GGG CCA TGT CAA-3' and reverse 5'-CCA CTC CTC TGT GAC ACT TTA GCC CTC CGA-3' to determine the sex of mouse embryos; and tdT allele forward, 5'-CTG TTC CTG TAC GGC ATG G-3' and reverse 5'-GGC ATT AAA GCA GCG TAT CC-3' to determine the expression of tdT reporter.

3.3.2 Tamoxifen treatment of mice and pups fostering

Timed pregnant mice were used for labeling neural crest cell lineages specifically. Noon of the day of vaginal plug detection in mice was designated embryonic (E) day 0.5. To induce Cre recombination in embryos at E8.0, tamoxifen (Tmx) (Cat No. T5648; Sigma-Aldrich, Inc, St. Louis, MO) was dissolved in corn oil at a concentration of 11.1 mg/mL, and a single dose of 0.1 mL tamoxifen solution was given through oral gavage using 16 G x 38 mm polyurethane feeding tubes (Cat No. FTPU-16-50, Instech Laboratories, Inc, Plymouth Meeting, PA) to the pregnant dams carrying E7.5 embryos

($Tmx^{E7.5}$). Vehicle (Veh) controls were treated with corn oil at the same stage.

Tamoxifen injection in pregnant mice has been reported to cause dystocia. To resolve this problem, caesarean sections were performed to deliver the Sox10-iCreER^{T2}/tdT embryos at E18.5. The delivered pups were fostered by a FVB/J nursing dam immediately after caesarean birth.

3.3.3 GFP$^+$ neural fold transplantation in GFP$^-$ chicken embryos

At Hamburger Hamilton 9 stage (29-33 hours post-incubation), a window on the eggshell was opened above the embryos. A drop of sterile 0.5% neutral red (Cat No. N2889-100ML, Sigma-Aldrich, Inc, St. Louis, MO) in 0.9% NaCl was used to stain and stage the embryos under a dissection microscope. According to the previous report that an “insertion” instead of “replacement” of neural folds for graft transplantation increased the survival rate while maintaining the normal development of neural crest and neural crest-derived organs [196], a single side of neural fold at the levels of posterior midbrain and anterior hindbrain were dissected from a GFP$^+$ chicken embryo and inserted into the lesion made laterally adjacent to the counterpart of a GFP$^-$ chicken embryo at the same somite stage. After the surgery, embryos were incubated until desired stages ranging from 1 to 19 days post-surgery (DPS).

3.3.4 Tissue collections

Mouse embryos at embryonic E8.0-8.5 were collected between 10am and 4pm. The embryos were also staged by counting somite pairs. Embryos at 7~15-somite stages (n=4 for both vehicle- and tamoxifen-treated groups) were selected and used for further analyses. Pregnant dams were euthanized with CO_2 followed by cervical dislocation. The uterus was removed and placed in a petri dish containing 0.1 M phosphate buffered saline

(PBS) (Cat No. CP4390-48, Denville Scientific, Inc, Metuchen, NJ). Embryos were dissected from the uterus under a stereomicroscope and fixed with 4% paraformaldehyde (PFA) (Cat No. AAJ19943k2, Thermo Fisher HealthCare, Pittsburgh, PA) in 0.1 M PBS at 4℃ for 2 hours. Postnatal mice were harvested at 2 weeks, 4 weeks, and 8 weeks (n=3 for both vehicle- and tamoxifen-treated at each stage). Mice were euthanized with CO_2 followed by transcardial perfusion using 10 mL warm 0.1 M PBS, followed by 10 mL warm and 20 mL cold 2% PFA in 0.1 M PBS. Tongues, soft palates, heads, and dorsal root ganglia were dissected and further fixed in 2% PFA at 4℃ for 2 hours.

GFP^+/GFP^- chicken chimeras with successful transplantation were collected at 1 (n=5), 2 (n=2), 14 (n=2), and 19 (n=5) DPS. Palates and base of oral cavities were dissected from embryos at 14 and 19 DPS. Whole embryos at 1 and 2 DPS and dissected tissues at 14 and 19 DPS were then fixed with 4% PFA in 0.1 M PBS at 4℃ for 2 hours.

Zebrafish eggs were collected after 1 hour pairing and incubated in 28.8℃ egg water until collections at 7- (n=3), 10- (n=3), and 12-somite (n=3) stages and 5.5 (n=3), 15 (n=3), and 30 (n=3) days post fertilization (dpf) and adult (90 days to 2 years) (n=3). Zebrafish were anesthetized with a neutrally-buffered solution of 0.016% Tricaine (Cat No. T0941, TCI AMERICA, Inc, Portland, OR), followed by decapitation and fixation in 4% PFA at 4℃ for 2 hours. For 30-day-old and adult fish, fixed heads were further treated with 0.5 M EDTA (Cat No. RES3002E, Sigma-Aldrich, Inc, St. Louis, MO) for bone softening, with medium change every other day for 2 weeks.

3.3.5 Immunohistochemistry

All fixed tissues were cryoprotected in 30% sucrose in 0.1 M PBS for at least 48 hours at 4℃. Tissues were trimmed and dissected, embedded in O.C.T. (Cat No. 23-730-

571, Thermo Fisher Scientific, Pittsburgh, PA) and rapidly frozen as such for: (1) Mice: transverse sections of cranial region of E8.5 embryos, sagittal sections of whole tongue of E12.5 embryos, sagittal sections of the left and right halves of the anterior 2/3 of postnatal oral tongue where fungiform papillae are distributed, sagittal sections of both foliate papillae, left and right halves of soft palate, and coronal sections of single circumvallate papilla; (2) Chickens: transverse sections of cranial region of embryos at 1 DPS, sagittal sections of whole embryos at 2 DPS, base of oral cavities of embryos at 14 and 19 DPS, and palates of embryos at 19 DPS; (3) Zebrafish: horizontal sections of zebrafish embryos, sagittal sections of heads of 5.5- and 15-dpf-old fish, sagittal sections of lower jaws, barbels, and body segments of 30-dpf and adult fish.

Frozen sections were cut at 8 μm in thickness and mounted onto charged slides (Fisher brand™ Superfrost™ Plus Microscope Slides, Cat No. 12-550-15, Thermo Fisher Scientific, Pittsburgh, PA). Non-specific binding was blocked with 10% normal donkey serum (Cat No. SLBW2097, Sigma-Aldrich, Inc, St. Louis, MO) in 0.1 M PBS containing 0.3% Triton X-100 (Cat No. X100-100ML, Sigma-Aldrich, Inc, St. Louis, MO) for 30 min, followed by overnight incubation with primary antibody diluted with 0.1 M PBS containing 0.3% Triton X-100 and 1% normal donkey serum. Primary antibodies used in this study are listed in Table 3.1.

Table 3.1. Primary antibodies that were used.

Antibodies	Dilution	Source
mouse anti-Calretinin clone 6B3	1:5000 (section) 1:1000 (whole mount)	Cat No. 010399, Swant, Inc, Switzerland
goat anti-Cre	1:500	Cat No. sc-83398, Santa Cruz Biotechnology, Inc. Dallas, TX
rabbit anti-dsRed	1:500	Cat No. ab62341, Abcam, Inc, Cambridge, MA
goat anti-E-cadherin	1:500	Cat No. AF748, R&D systems, Inc, Minneapolis, MN
chicken anti-GFP	1:500 (section) 1:250 (whole mount)	Cat No. GFP-1010, Aves Labs, Inc, Tigard, OR
rat anti-Keratin 8 (Krt8)	1:1000	Cat No. TROMA-1, Developmental Studies Hybridoma Bank, Iowa city, IA
goat anti-SOX10	1:500	Cat No. sc-365692, Santa Cruz Biotechnology, Inc, Dallas, TX
mouse anti-HNK1(1C10)	1:10	Cat No. AB_10570406, Developmental Studies Hybrydoma Bank, Iwoa city, IA
rabbit anti-Epithelial Cell Adhesion Molecule markers (EpCAM)	1:200	Cat No. MBS2027145, Mybioresource Inc, San Diego, CA
rabbit anti-α-Gustducin	1:500	Generated by Dr. Shoji Tabata's lab
mouse anti-Vimentin (Vim3B4)	1:250	Cat No. ab28028, Abcam, Inc, Cambridge, MA

After rinses in 0.1 M PBS (3 times, 10 min each), sections were incubated in Alexa Fluor® 488 (for E-cadherin, GFP), Alexa Fluor® 546 (for dsRed), and/or Alexa Fluor® 647 (for all the other markers)-labeled secondary antibody (1:500, Invitrogen, Eugene, OR) for 1 hour at room temperature. Sections were rinsed and then counterstained with DAPI (200 ng/mL, Cat No. D1306, Thermo Fisher Scientific, Pittsburgh, PA). After rinses with 0.1 M PBS followed by dipping in Milli-Q water (Direct-Q® 3 UV water purification system, Millipore, MA). Sections were air dried and coverslipped with Prolong® diamond antifade mounting medium (Cat No. P36970, Thermo Fisher Scientific, Pittsburgh, PA).

3.3.6 Photomicroscopy

Immunoreacted sections on slides were analyzed under a fluorescent light microscope (EVOS FL, Thermo Fisher Scientific, Pittsburgh, PA) and images were taken using a laser scanning confocal microscope (Zeiss LSM 710, Zeiss, Germany). Whole mount tissues were examined and images taken using a stereomicroscope (SZX116, Olympus, Japan). Images were assembled using Adobe Photoshop with minimal editing.

3.4 Results

3.4.1 In mice, Sox10-iCreER^{T2} specifically and extensively labels neural crest cell lineages with a single dose of tamoxifen at E7.5 and labeled cells are not found in taste buds

In mouse embryos, Sox10 expression has been found specifically in neural crest cells during early embryonic stages [129, 145]. To exclusively map the lineages of Sox10^{+} neural crest cells, we utilized a Sox10-iCreER^{T2} mouse model [189] in which iCreER^{T2} is driven by endogenous Sox10 promoter and tamoxifen administration was performed at E7.5 when neural crest cells were about to be generated [197, 198] and express Sox10

[129, 145]. To validate the specificity and recombination efficiency of Sox10-iCreER^{T2} in labeling neural crest cell lineages, Sox10-iCreER^{T2} expression were analyzed in vehicle and tamoxifen-treated mice (n=3 for each group). In transverse sections of E8.5 (12-somite) Sox10-iCreER^{T2} embryos at 1 day after a single-dose vehicle (corn oil) treatment to the pregnant dam at E7.5 (Veh$^{E7.5}$), Cre recombinases were detected exclusively in Sox10^{+} cranial neural crest cells (Figure 3.1A-B), including the cells in the trigeminal neural crest tissue [199] (Figure 3.1A), branchial arch 1 (Figure 3.1A), and optic eminence (Figure 3.1A). Importantly, Cre immunosignals were restricted to the cytoplasm (arrowheads) of the neural crest cells (Figure 3.1B). In the E8.5 (9-somite) Sox10-iCreER^{T2} embryos with tamoxifen treatment to the pregnant dam at E7.5 (Tmx$^{E7.5}$), Cre immunosignals were found within the nuclei (arrows) of Sox10^{+} neural crest cells (Figure 3.1C). In Tmx$^{E7.5}$ E12.5 Sox10-iCreER^{T2}/tdT embryos (n=3), tdT signals were obvious in the spatulate tongue (Figure 3.1D$_1$) and extensively distributed in the tongue mesenchyme under the epithelium (Figure 3.1D$_2$). In young adult (8 weeks, n=3) Sox10-iCreER^{T2} mice (Tmx$^{E7.5}$), tdT signals were found in tissue compartments that are known to arise from neural crest, including the dorsal root ganglia (Figure 3.1E). No tdT signals were found in corresponding Cre-negative control (data not shown). Together, a single dose of tamoxifen treatment to Sox10-iCreER^{T2} dam at E7.5 was sufficient to label neural crest cell lineages specifically and extensively.

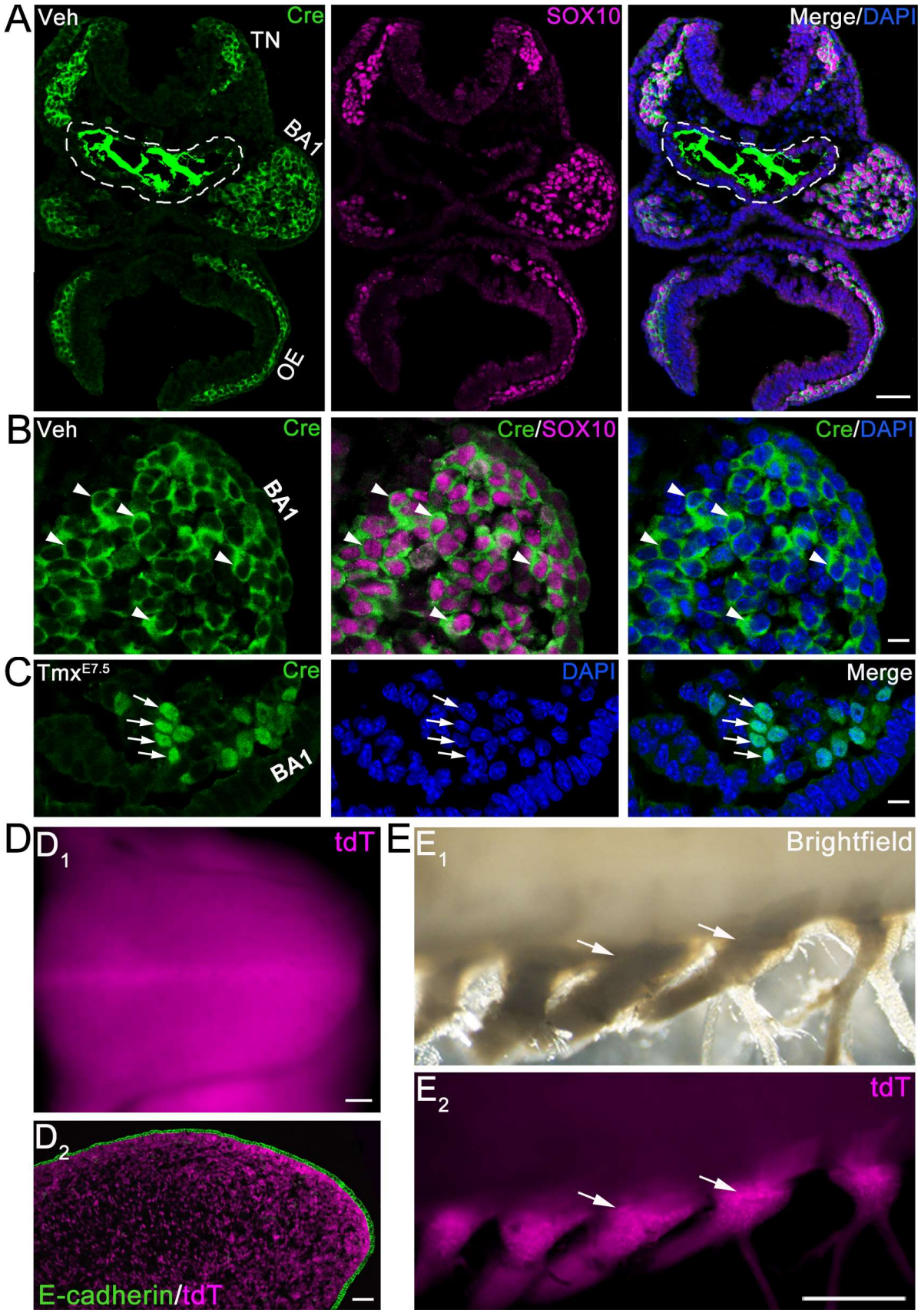
A
Veh
Cre
TN
BA1
OE
SOX10
Merge/DAPI
B
Veh
Cre
BA1
Cre/SOX10
Cre/DAPI
C
Tmx$^{E7.5}$
Cre
BA1
DAPI
Merge
D
D$_1$
tdT
D$_2$
E-cadherin/tdT
E
E$_1$
Brightfield
E$_2$
tdT

Figure 3.1. Sufficiency of a single dose of tamoxifen (Tmx) in activating the nuclear translocation of Cre recombinase that triggered DNA recombination to drive tdT expression in neural crest and neural crest-derived tissues. **A-B:** Low (A) and high (B) -power images of transverse sections of the cranial region of a vehicle (Veh)-treated Sox10-iCreER^{T2} mouse embryo at E8.5 (12-somite). Immunosignals of Cre (green) in the cytoplasm (arrowheads in B) and Sox10 (magenta) in the nuclei were visualized. White dashed lines in A outline the foregut diverticulum with non-specific staining [113]. TN: trigeminal neural crest tissue; BA1: branchial arch 1; OE: optic eminence. **C:** High-magnification images of the BA1 region in a transverse section of an E8.5 (9-somite) Sox10-iCreER^{T2} mouse embryo with tamoxifen activation of Cre (Tmx$^{E7.5}$). Arrows point to the Cre immunosignals (green) within nuclei. **D:** Images of whole mount (D_1) and sagittal section (D_2) of the tongue from a E12.5 Sox10-iCreER^{T2}/tdT mouse embryo with tamoxifen activation of Cre (Tmx$^{E7.5}$). Tongue epithelium was immunoreacted with antibody against E-cadherin (green) in D_2. **E:** Bright field (E_1) and tdT fluorescent (E_2) images of mouse dorsal root ganglia (arrows) of a Sox10-iCreER^{T2}/tdT mouse at 8 weeks with tamoxifen activation of Cre (Tmx$^{E7.5}$). Arrows point to the dorsal root ganglia. Scale bars: 50 μm in A and D (single-plane laser scanning confocal); 10 μm in B and C (single-plane laser scanning confocal); 1 mm in E (stereomicroscopy).

To map the lineage of Sox10^{+} neural crest-derived cells in taste buds, the distribution of Sox10-iCreER^{T2}/tdT-labeled cells (Tmx$^{E7.5}$) was thoroughly analyzed in the major tissues containing taste buds including the soft palate and all three types of lingual taste papillae, i.e., fungiform, foliate, and circumvallate, in 2-week, 4-week and 8-week-old mice (n=3 for each stage). In serial sections of the soft palate and tongue tissues,

Sox10-iCreER^{T2} driven tdT^{+} cells were extensively distributed in the connective tissue (Figure 3.2A-C). In contrast, Sox10-iCreER^{T2}/tdT-labeled cells were not observed in taste buds located by the immunosignals of Krt8 in the soft palate (Figure 3.2C), and in all three types of lingual taste papillae, i.e., fungiform (Figure 3.2A-C), foliate (Figure 3.2C), circumvallate (Figure 3.2A-C). Additionally, tdT^{+} cells were not found in the taste bud-surrounding tongue epithelium, including basal epithelial cells that are known as progenitors of taste bud cells [3, 6, 12, 14, 141, 144].

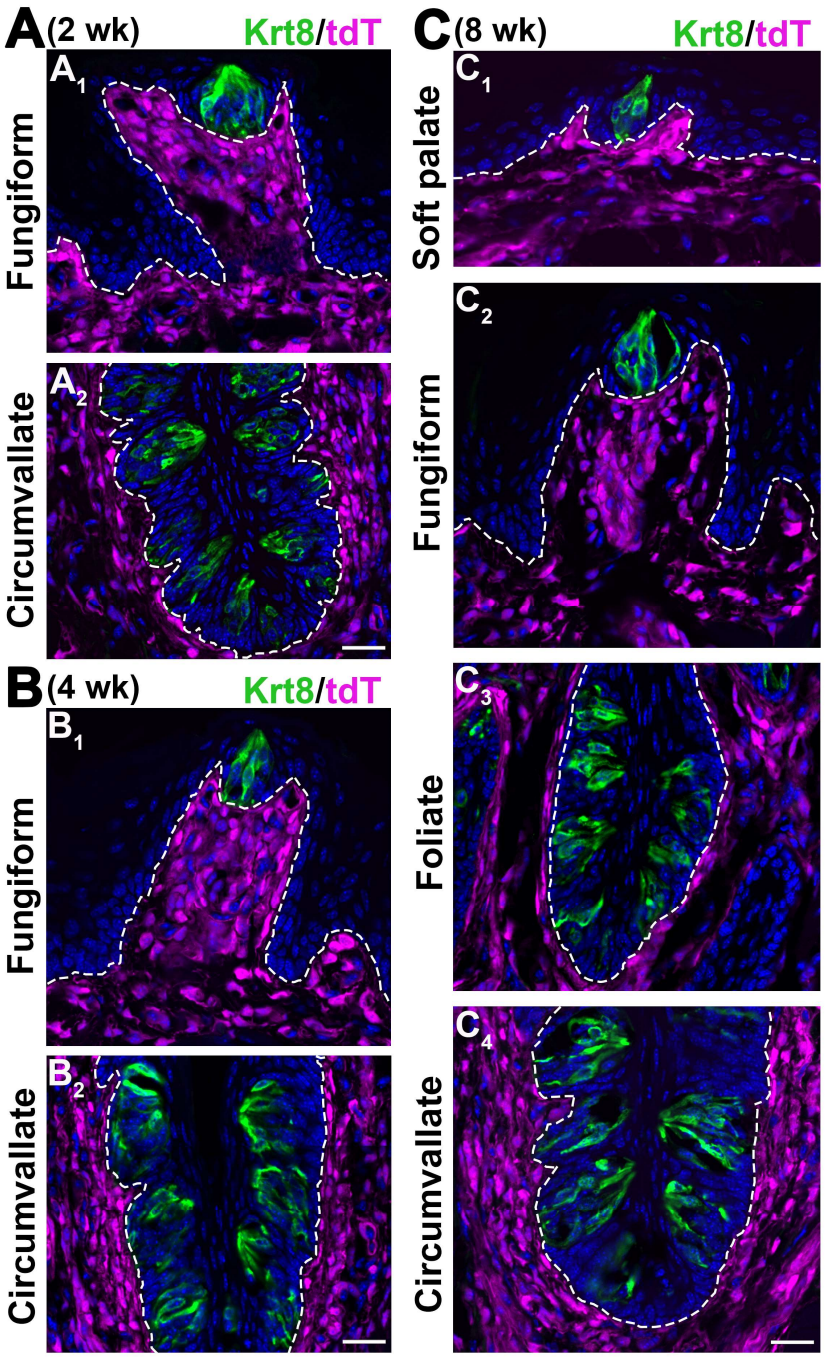

Figure 3.2. Single-plane laser scanning confocal photomicrographs to demonstrate the distributions of Sox10-iCreER^{T2}/tdT-labeled cells in the tongue and soft palate in postnatal mice (Tmx$^{E7.5}$) at different stages. **A-B:** Images of a fungiform papilla on a sagittal section (A_1, B_1) and circumvallate on a coronal section (A_2, B_2) of tongue at 2 weeks (A) and 4 weeks (B). **C:** Images of soft palate (C_1), fungiform papilla (C_2), foliate

papilla on a sagittal section (C_3), and circumvallate papilla on a coronal section (C_4) of tongue tissue at 8 weeks. Taste buds were marked by the immunosignals of Keratin 8 (Krt8, green). White dashed lines demarcate lingual epithelium from the underlying connective tissue. Scale bars: 50 μm for all images.

3.4.2 In GFP^+/GFP^- chicken chimera model, GFP^+ neural crest cell lineages were labeled and sustained in the craniofacial regions, but not found in taste buds

To map GFP^+ neural crest cell lineages in craniofacial regions, a GFP^+/GFP^- chimera chicken model was used. One side of neural folds at the posterior midbrain and anterior hindbrain levels was dissected from a transgenic GFP^+ chicken [191] and then inserted into an incision lateral to the dorsal neural fold of a GFP^- chicken at the corresponding level of rostral-caudal axis (Figure 3.3A). At 1 day post-surgery (DPS) (n=5), ventrally migrating streams of GFP^+ neural crest cells were observed in the transplantation side of the embryos (Figure 3.3B). To further validate the identity of GFP^+ cells, HNK1 [200] was used to label migrating neural crest cells. GFP^+ cells were largely, if not all, labeled by HNK1 (Figure 3.3C). Moreover, GFP^+ neural crest cells were in the vicinity of ventral side of mesencephalon, which specifically contributes to oral tissues that host taste buds (Figure 3.3C).

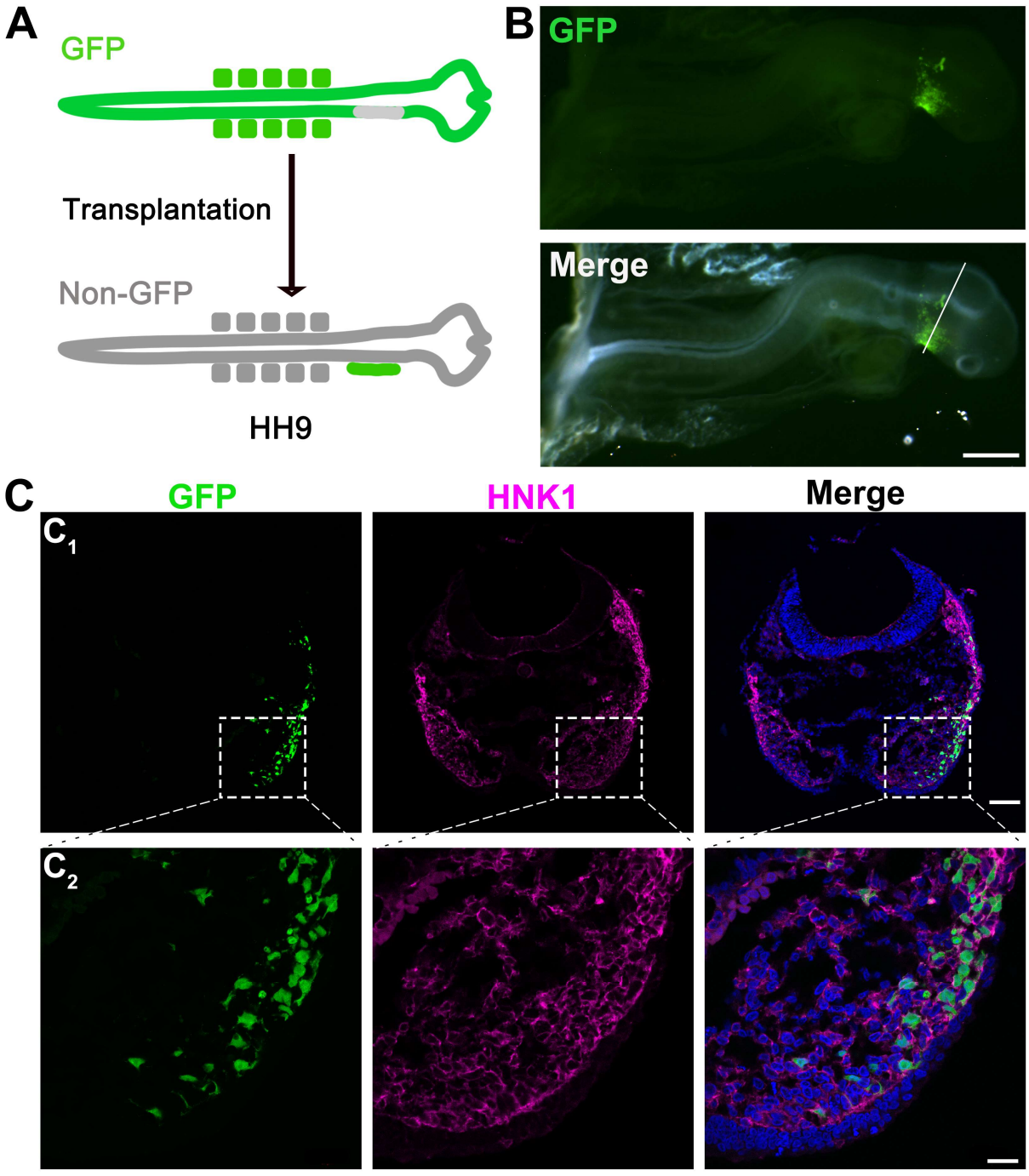

Figure 3.3. Migration of GFP$^+$ NC cells ventrally in GFP$^-$ host chicken after the insertion of the GFP$^+$ neural fold. **A**: A schematic graph illustrating the insertion of GFP$^+$ neural fold to GFP$^-$ host chicken embryo. **B**: Photomicrographs of a GFP$^+$/GFP$^-$ chicken chimera at 1 DPS. Top: fluorescent image to show GFP signals; Bottom: merged fluorescent and

bright-field images. **C**: Single-plane laser scanning confocal images of a section (C_1) from the position indicated by white line in B and higher power images (C_2) from the area indicated by dashed square shown in C_1. Sections were immunoreacted for neural crest cell marker HNK1 (magenta). Scale bars: 500 μm in B; 80 μm in C_1 and 20 μm in C_2.

To characterize the migration of neural crest lineages, chimeric embryos were collected at various stages. At 2 DPS (n=2), GFP^+ cells populated at the ipsilateral side of pharyngeal arch to the neural fold insertion (Figure 3.4A), which would eventually give rise to oral tissues including beaks. At 14 (n=2) and 19 DPS (n=5), GFP signals were detected in multiple craniofacial regions (Figure 3.4A). Of note, the GFP signals were remained restricted to the surgical side, which could be appreciated by a clear boundary in the midline separating GFP^+ and GFP^- tissues in the lower (Figure 3.4A) and upper (Figure 3.4A) beaks. Absence of GFP signals on the contralateral side of surgery was consistent in all examined chimeric embryos (Figure 3.4A).

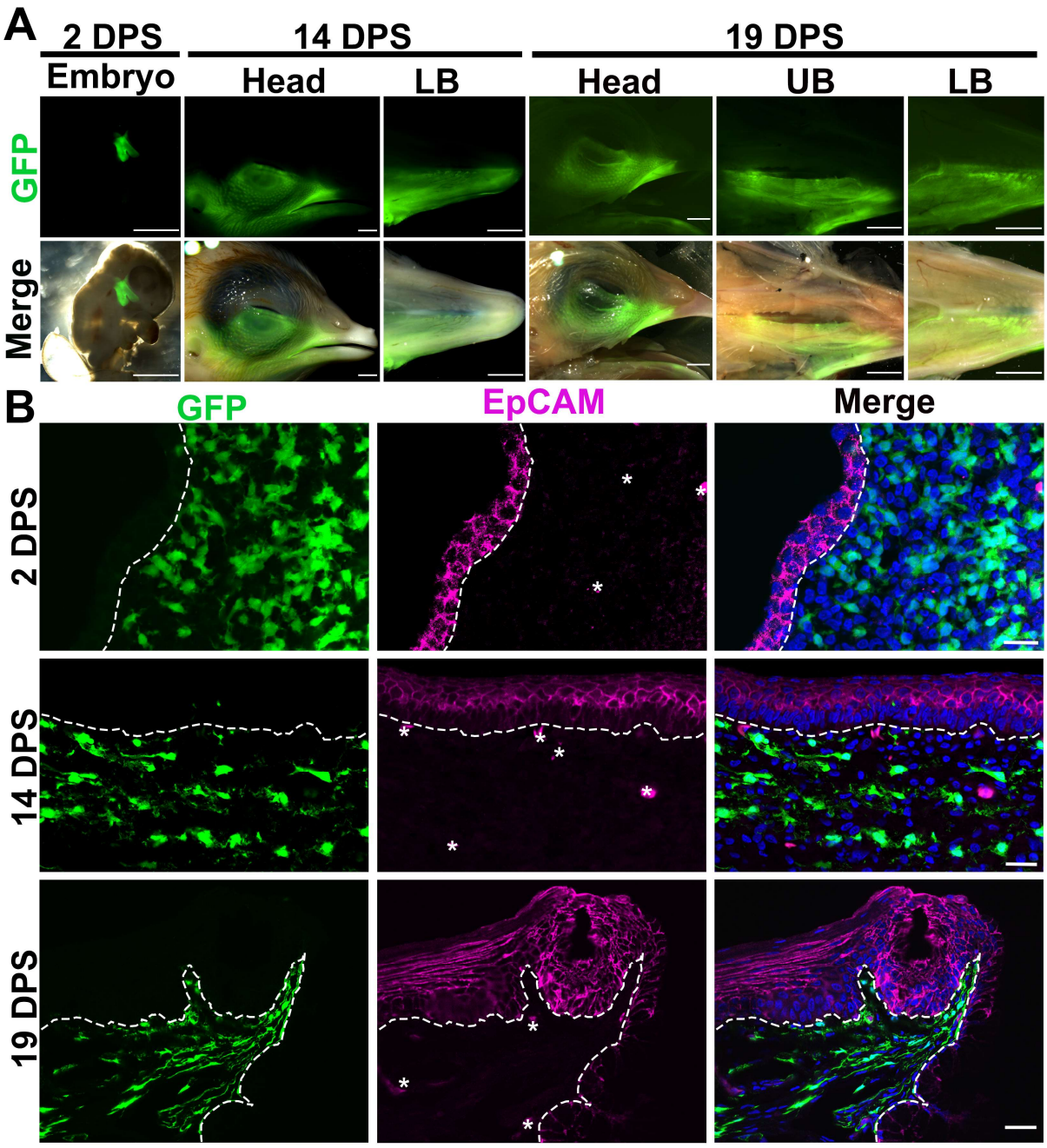

Figure 3.4. Distribution of GFP$^+$ neural fold-derived cells in the craniofacial regions ispilateral to the surgery side. **A**: Photomicrographs of a chimeric embryo at 2 DPS, side view of heads and dorsal view of the lower beak (LB) at 14 and 19 DPS, and upper beak (UP) at 19 DPS. Top panel: fluorescent images to show the GFP signals; Bottom panel: merged fluorescent and bright-field images. **B**: Single-plane laser scanning

confocal images of sagittal sections of pharyngeal arch of chimeric embryo at 2 DPS and base of oral cavities of chimeric embryos at 14 and 19 DPS. Sections were immunoreacted for the epithelial cell marker EpCAM (magenta). White dashed lines demarcate the epithelium from the underlying mesenchyme. Scale bars: 2 mm in A; 20 μm in B.

In sagittal sections of surgical side of pharyngeal arch at 2 DPS and the bases of oral cavities at 14 and 19 DPS, GFP^+ cells were extensively and exclusively distributed in connective tissues immediately beneath the epithelium marked by EpCAM (Figure 3.4B). To further confirm whether there were GFP^+ cells in taste buds or not, thorough examinations were performed in serial sections of GFP^+ gustatory tissues in all surviving 19 DPS chimeric embryos (n=5) in which early taste buds have emerged. In the sections immunostained with a specific taste bud cell marker α-Gustducin, only the taste buds that were surrounded by GFP^+ connective tissue cells were included for analysis. A total of 40 taste buds from serial sections of GFP^+ base of oral cavities and 37 taste buds from serial sections of GFP^+ palates were imaged and analyzed. In contrast to the abundant distribution in the underlying connective tissue (Figure 3.5), GFP^+ cells were not observed in oral epithelium including taste buds and adjacent salivary glands in either the base of oral cavities (Figure 3.5A) or palates (Figure 3.5B).

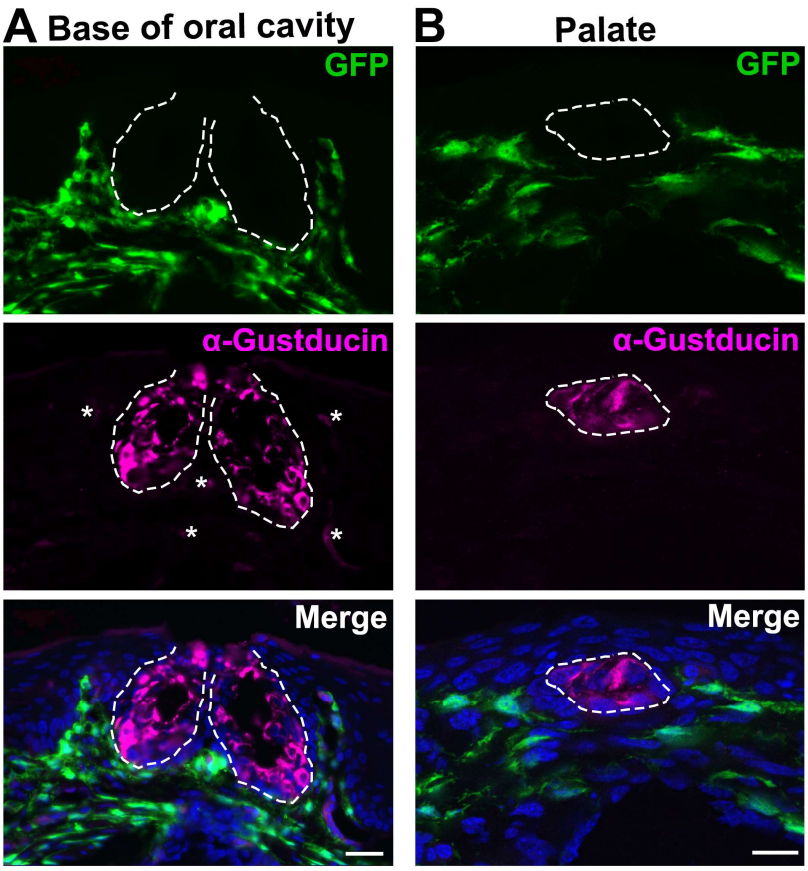

Figure 3.5. Distribution of GFP⁺ labeled cells in the tissue of oral cavity of chimeric embryos at 19 DPS. **A**: Representative images of a sagittal section of the base of oral cavity. **B**: Images of a sagittal section of the palate. Sections were immunoreacted for taste bud cell marker α-Gustducin (magenta). White dashed lines encircle taste buds. Autofluorescence in α-Gustducin immunoreacted sections were identified and are marked by asterisks (*). Scales bars: 20 μm for all images (single-plane laser scanning confocal images).

3.4.3 In zebrafish, Sox10⁺ neural crest cell lineage was not observed in taste buds

In addition to the use of mice and chickens, we introduced zebrafish, another widely used animal model for neural crest fate mapping [193, 201-206], to trace the lineage of Sox10⁺ neural crest cells in taste buds. To verify the Sox10 expression in neural

crest cells and not in taste buds, Sox10-EGFP zebrafish [193, 194] were used (n=3 for each embryonic stage). In early embryos, EGFP signals emerged in the trunk region at 7-somite stage (Figure 3.6A) and later appeared in cranial regions in 10- and 12-somite embryos (Figure 3.6A). Importantly, those signals were exclusively found in $Sox10^{+}$ neural crest cells (Figure 3.6B) in transverse sections of cranial region of 12-somite fish. Of note, in fish at 5.5 dpf (n=3), EGFP signals were absent in the taste buds marked by calretinin (Figure 3.6C).

The specific expression of Sox10 in neural crest while being absent in fish taste buds allowed the use of Sox10-Cre fish model [192] to perform lineage tracing of $Sox10^{+}$ neural crest to taste buds. The use of GFP-RFP [195], in which the ubiquitous and constitutive GFP expression could be effectively switched to RFP upon Cre induced recombination, gave us a sharp contrast of signals for an easy recognition of Cre-labeled cells. Sox10-Cre driven RFP signals could be found in well-known neural crest-derived organs such as gills (Figure 3.6D) [207, 208]. In lower jaw where most taste buds reside in zebrafish, Sox10-Cre driven RFP signals were not found in taste buds at 15 dpf (n=3), 30 dpf (n=3), and adult stages (n=3) (Figure 3.6E). However, RFP expression was readily observed in cells within the connective tissue in all tissues examined (Figure 3.6E). Similar labeling patterns were also found in adult barbels (Figure 3.6E).

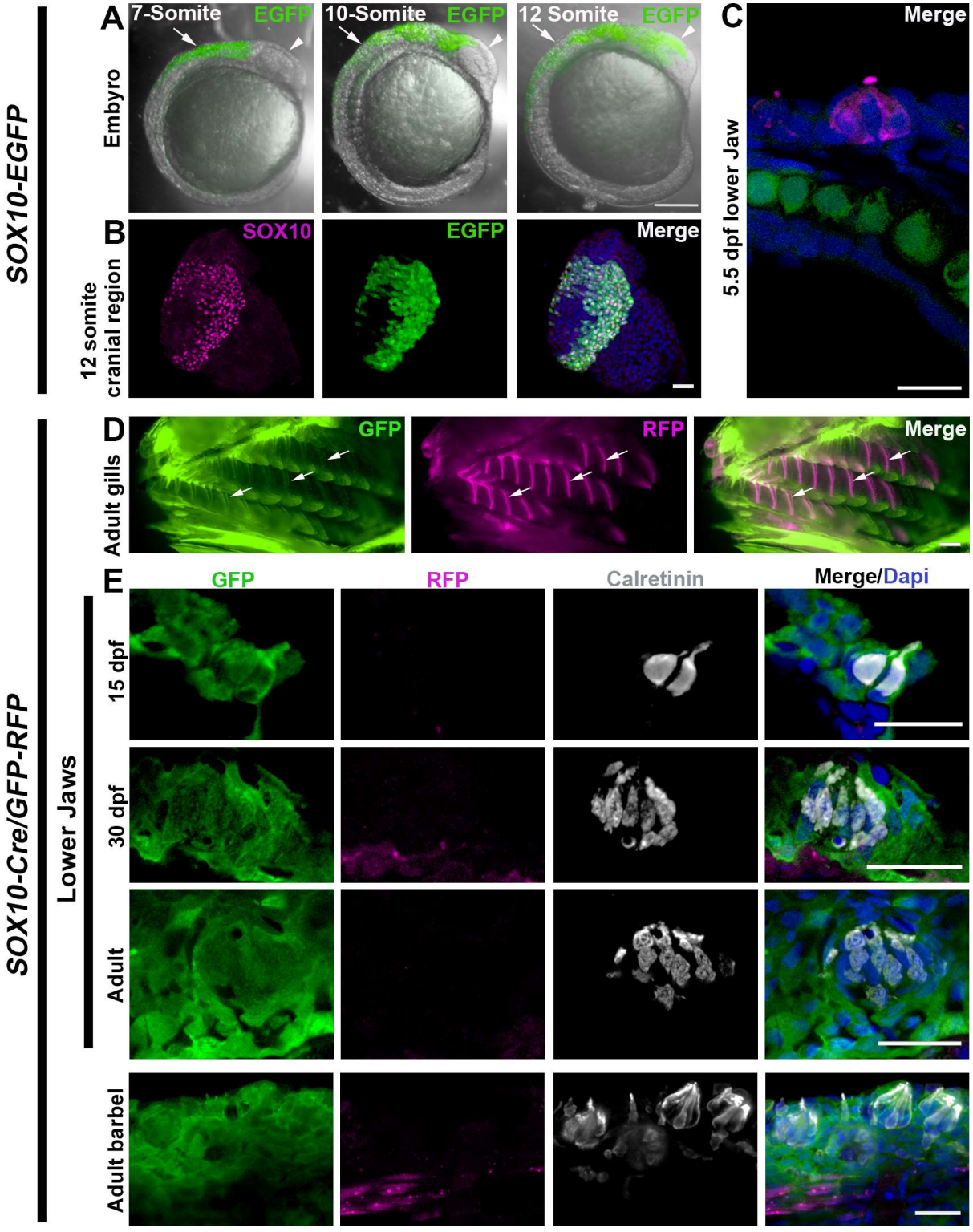

Figure 3.6. Mapping neural crest cell lineages in zebrafish. **A-C**: Sox10-EGFP expression was in neural crest but not in taste buds. **A**: Merges EGFP and bright-field images of

lateral views of Sox10-EGFP fish embryos at 7, 10, and 12-somite stages. Arrowheads point to heads and arrows point to truck regions. **B**: Photomicrographs of transverse sections of cranial regions of a 12-somite Sox10-EGFP fish embryo. Migrating neural crest cells were immunostained for Sox10 (magenta). **C**: Photomicrographs of a sagittal section of a taste bud in lower jaw of a 5.5 dpf fish embryo. **D-E**: Sox10-Cre/GFP-RFP labeled known neural crest-derived tissues but not taste buds. **D**: Whole mount images of gills (arrows) of Sox10-Cre/GFP-RFP adult zebrafish. **E**: Photomicrographs of sagittal sections of lower jaws at 15 dpf, 30 dpf, and adult and adult barbel of Sox10-Cre/GFP-RFP zebrafish. GFP and RFP signals were amplified by applying antibodies against GFP (green) and RFP (magenta). Calretinin (gray) indicates presence of taste buds. Scale bars: 200 μm in A and D; 50 μm in B; 20 μm in C and E (single-plane laser scanning confocal).

3.5 Discussion

3.5.1 Taste bud cells are not derived from neural crest

The neural crest is a multipotent cell population derived from the lateral ridges of the neural plate in early vertebrate embryos [209]. By the fusion of neural folds, neural crest cells leave the dorsal part of the neural epithelium, migrate extensively and give rise to a wide variety of differentiated cell types, including neurons and glial cells of the peripheral nervous system and connective tissue of the head [170, 174-176, 210]. For years, the use of transgenic mouse lines has facilitated the fate mapping of cranial neural crest, and findings have led to new speculated neural crest derivatives, e.g., tooth bud [186] and olfactory [187, 188] epithelial cells. Taste buds have been regarded as solely derived from the surrounding epithelium [3, 6, 12, 14, 141, 144]. However, recent findings

revealed a potential of neural crest derivation of taste buds in mammals [17, 184, 185], thereby suggesting a potential difference in how taste buds from in mammals compared to non-mammalian vertebrate.

In the present study we tested the contribution of neural crest lineage to taste buds in mammals, birds, and teleost fish using Sox10-iCreER^{t2}/tdT mouse model, GFP^{+}/GFP^{-} chicken chimera model, and Sox10-Cre/GFP-RFP zebrafish model. We report that each of these models marks neural crest lineage specifically or/and extensively. Despite careful examination of multiple individuals in each model, we were unable to find any examples where the neural crest has contributed to cells in the taste buds. Our data, in combination with those from axolotl [183], provide solid evidence that taste buds, composed largely of glial-like (type I) and neuronal-like (type III) cells, are not derived from neural crest in mammalian and non-mammalian animals.

Our recent lineage tracing results using Sox10-Cre mice have indicated three candidates of Sox10-expressing taste bud progenitors: neural crest or non- neural crest derived connective tissue cells in the core of taste papillae, or von Ebner's glands [184]. The absence of Sox10-iCreER^{T2} (Tmx$^{E7.5}$) labeled cells in taste buds and surrounding epithelium rules out neural crest cells as Sox10-expressing progenitors for taste buds. This leaves two candidates for future work required to assess the Sox10-expressing cell types under the lingual epithelium [184], including non- neural crest-derived connective tissue and/or von Ebner's gland [184].

Even though neural crest does not give rise to taste bud cells, the connective tissue cells in tongue are largely derived from neural crest [17, 184, 185]. Neural crest-derived mesenchymal cells interact with the overlying epithelium and play essential roles in taste

bud and taste papilla development [211-213]. For examples, mesenchymal FGF10 has been reported to control the size of fungiform papillae via modulating epithelial Wnt/β-catenin signals [211]; and mesenchymal Follistatin modulates epithelial BMP7 signaling to control size and spacing of fungiform papillae and inhibits gustatory fate of intermolar eminence [212]. Future studies using high throughput techniques will be beneficial for identifying novel factors from neural crest derivatives that are required for taste bud formation and maintenance.

3.5.2 Neural crest lineage tracing: limitations of Cre mouse models and ideal using Sox10-iCreER^{T2}

Cre/loxP site-specific recombination system is a noninvasive approach that enables long-term lineage tracing. In the past several years, a number of Cre mouse lines have been generated for neural crest lineage tracing [124]. For many lines, labeling specificity has been a problem because of ectopic expression of the Cre transgene and/or labeling of markers in cells/tissues beyond neural crest. Additionally, the use of non-inducible Cre can lead to labeling of cell lineages from more than one specific cell type. For example, Wnt1-Cre mainly labeled the mesencephalic stream of neural crest [113, 124], which only partially contributes to pharyngeal arch 1 [123], i.e., the primordium of the tongue. In addition, ectopic Wnt1 expression from Wnt1-Cre transgene impaired midbrain development [125], and subsequently affected overall development of the mouse. P0-Cre mainly labels rhombencephalic stream of neural crest [113], which is a major contributor to pharyngeal arches [123]. However, the expression of P0-Cre was not neural crest lineage-restricted, e.g., P0-Cre labeled cells were also found in notochord [113], and ectoderm-derived non-gustatory lingual epithelium at embryonic stages [17,

115]. Dermo1-Cre has frequently been used to target mesenchymal cell lineages [116, 117, 119, 120], however, instead of neural crest-derived cell labeling only, Dermo1-Cre also labeled mesoderm-derived mesenchymal cells, e.g., osteoblasts, chondrocytes [121], perichondrial, and periosteal cells in the trunk and part of the head region [122]. Sox10 is a specific marker for neural crest cells during early embryonic stages [129, 145]. In a previous study using Sox10-Cre to trace the lineage of Sox10-expressing cells in mouse model, Sox10 expression was found in cells beyond neural crest cell lineage, e.g., von Ebner's gland cells under taste papillae [184]. Together, careful attention must be paid when using these Cre mouse models for tracing neural crest cell lineages in order to avoid erroneous conclusions about the labeled cell types [17]. Indeed, inconsistent observations were obtained in our previous mouse studies using Wnt1-Cre [17], P0-Cre [17, 185], Dermo1-Cre [185], and Sox10-Cre [184] driver lines to trace the lineage of neural crest to taste buds, which raises suspicions about the specificity of those models in labeling the neural crest lineage.

To test our findings of potential neural crest origin of taste buds in Sox10-Cre as well as other Cre-driver lines in previous studies, we introduced an inducible Cre model Sox10-iCreER^{T2} [189] to specifically target Sox10-expressing neural crest lineage. CreER^{T2} is a fusion protein of Cre recombinase and mutant form of the human estrogen receptor that blocks the nuclear translocation of Cre without exposure to tamoxifen [214]. We showed that tamoxifen administration in a given time window when Sox10 expression was exclusive in migrating neural crest cells triggered Cre recombination in neural crest cells, labeling them and their derivatives. We found that a single dose of tamoxifen administration at E7.5 was reliable and sufficient for DNA recombination in neural crest

cells, and that well-known neural crest derivatives were extensively labeled. Our data suggest that use of the Sox10-iCreER^{T2} line in this way is ideal for neural crest lineage mapping in mice. This model enables us to generate definitive data to answer whether neural crest gives rise to particular cell types, e.g., taste bud cells.

3.5.3 GFP$^+$ neural fold insertion in chicken embryos is ideal for longitudinally tracking neural crest cell lineages *in ovo*

Chickens share the common marker Vimentin with humans in labeling taste bud cells [215], which makes it unique for neural crest lineage mapping in taste buds and facilitates comparison of findings between these two species. The low survival rate of chimeras up to hatch after neural fold transplantation may limit the neural crest lineage mapping in post-hatch birds. However, taste buds in chickens develop well before hatching, which makes it a good model to use in the present study.

Neural fold transplantation in avian embryos is a well-established, but technically challenging, method to trace cell lineages of the neural crest [216-219]. The development of lines of transgenic chickens in which GFP is ubiquitously expressed facilitates assessment of migrating neural crest and their contribution to tissues without staining in GFP$^+$/GFP$^-$ chimeras [191]. Such a model system allows for longitudinal *in ovo* observations for neural crest cell migration and lineage tracing. Even though assays involving dye labeling and retroviral infection of neural crest cells can facilitate the experimental procedures and increase the post-surgery survival rate, neural fold transplantation is more advantageous in providing a highly specific method in labeling neural crest cells. Moreover, we compared GFP$^+$ neural fold insertion into the tissue lateral to the neural fold of GFP$^-$ host embryo with neural fold replacement, and found that

insertion increased the embryo survival rate and GFP^+ cells from inserted neural fold precede the GFP^- host cells and occupy the target tissue extensively.

3.5.4. Sox10-Cre zebrafish model is useful for labeling cranial neural crest cell lineages

Zebrafish is an emerging model with advantages of easily accessible and transparent embryos for genetic manipulation and observation of dynamic developmental processes [193, 201-206]. Here we used lines of fish harboring transgenes for Sox10-EGFP or Sox10-Cre to label neural crest cells. Sox10-derived transgenes in zebrafish have been used by a number of investigators to image neural crest cells and neural crest lineages throughout the developing zebrafish embryo [192, 194, 220-222]. As a consequence, the expression characteristics of the two established transgenic lines used in the current study are well known. Both lines are known to drive expression in migratory neural crest cells and their derivatives at all axial levels of the embryo and have been used to study the role of neural crest in the development of a number of tissues, including craniofacial cartilage, pigment cells, and dorsal root ganglia [192, 194, 220-222]. Additionally, both lines are known to drive expression in cells that are not derived from neural crest, such as in the pectoral fin cartilage, otic epithelium, some neurons and oligodendrocytes of the central nervous system, and in some muscle tissues [124, 192, 194, 220]. Several of these non- neural crest derived cells normally express Sox10 [223]. We confirmed that both the Sox10-EGFP and Sox10-Cre lines are expressed extensively in cranial neural crest cells and their lineages in developing and adult zebrafish, including cells that could potentially contribute to taste buds. The complete absence of Sox10-Cre–

labeled cells in all taste buds in juvenile and adult fish demonstrates that the taste buds in zebrafish did not receive a contribution from neural crest.

In the present study, the use of Sox10-Cre/GFP-RFP zebrafish allowed us to map neural crest derivatives in taste buds. Unlike the Sox10-Cre mouse line, Sox10-Cre labeled cells were not found in zebrafish taste buds. One possible explanation for the differential expression of these transgenes in mice and zebrafish is that there are species-specific differences in Sox10 expression outside of the neural crest. Of note, potential distinct ectopic expression of Cre cannot be ignored. Careful attention needs to be paid to validating the behavior of transgenic constructs both within a species and especially when comparing results across species.

Acknowledgments

The authors give thanks to Shi-You Chen, Luke Mortensen, Steven Stice, and Franklin West, (Regenerative Bioscience Center, The University of Georgia, Athens, Georgia) for the discussion and feedbacks; to Mary Redmond Hutson (Duke University, Durham, NC) and Richard Schneider (University of California at San Francisco, San Francisco, CA) as consultants for chicken chimera surgery; to Paul Trainor (Stowers Institute for Medical Research), Prasangi Rajapaksha (University of Kentucky, Lexington, KY), Jason Payne and Robert Beckstead (University of Georgia, Athens, GA) for technical assistance of labeling neural crest cells in chicken model, and The Jackson Laboratory for transgenic mouse lines. This study was supported by the National Institutes of Health, grant number R01DC012308 and R21DC018089 to HXL; R01NS090645 to JDL.

CHAPTER 4

VON EBNER'S GLANDS CONTAIN PROGENITORS FOR TASTE BUDS IN THE CIRCUMVALLATE PAPILLA

Wenxin Yu, Naomi Kramer, and Hong-Xiang Liu. To be submitted to *Proceedings of the National Academy of Sciences of the United States of America.*

4.1 Abstract

We have recently demonstrated that Sox10-expressing cells located in two tissue compartments under lingual epithelium, i.e., connective tissue core of taste papillae and von Ebner's glands, give rise to taste bud cells that are mainly type III. The recently reported finding that taste buds are not derived from neural crest cell lineages (including the majority of connective tissue cells) leave two progenitor candidates to be determined: non-neural crest-derived connective tissue cells and von Ebner's glands. In this study, we aimed to identify which cell type(s) in the Sox10-expressing tissue compartments contribute to taste buds using inducible Cre mouse models to map the lineage of cells in connective tissue (including stromal cells and Schwann cells) and cells in von Ebner's glands, respectively. We found that the distribution of labeled cells in circumvallate taste buds was concurrent with that in von Ebner's glands, but not in the connective tissue. More specifically, the absence of labeled cells in circumvallate taste buds and von Ebner's glands were consistent in Sox10-iCreER^{T2}/tdT mice for mapping neural crest cell lineages, Vimentin-CreER/tdT mice for stromal cells, and Plp1-CreER^{T} for Schwann cells. On the contrary, when von Ebner's glands was fully labeled in Sox10-iCreER^{T2}/tdT mice after prolonged tamoxifen injection at perinatal stages, circumvallate taste buds were labeled concurrently. Our data strongly support the idea that von Ebner's glands contain progenitors for circumvallate taste buds. Ongoing studies are being undertaken to collect direct evidence.

Key words: taste buds, progenitor, Sox10, von Ebner's gland, connective tissue, Plp1,Schwann cells, Vimentin, stromal cells.

4.2 Introduction

Taste bud cells mostly have a short lifespan requiring continuous turnover [1, 2, 4, 5, 25]. Thus, active progenitors in tissue compartments surrounding taste buds are necessary to maintain the homeostasis of taste buds. Beyond the well-established progenitor cell population residing in lingual epithelium surrounding taste buds [3, 4, 6, 11-14], Sox10-expressing tissue compartments under lingual epithelium, i.e., connective tissue core and von Ebner's glands, have been recently reported as potential progenitor sources for taste buds [15]. However, the specific type(s) of Sox10-expressing cells that contribute to taste buds have not yet been identified.

In a recent study using Sox10-iCreER^{T2} to map the lineage of neural crest-derived connective tissue cells to taste buds, labeled cells were extensively distributed in underlying connective tissue but not in taste buds [44], suggesting the absence of direct contribution of neural crest cells and their derivatives to taste buds. However, question remains whether non-neural crest-derived connective tissue and von Ebner's glands contain progenitor cells for taste buds.

Von Ebner's glands are minor serous salivary glands specifically connecting to the bottom of the trenches of circumvallate and foliate papillae in posterior tongue [135, 136]. Indeed, taste buds has been observed in the circular structure that were speculated to be derived from von Ebner's glands in transplanted circumvallate papillae to mouse eyes [140]. Verification of whether taste buds originate from von Ebner's glands necessitate the use of a mouse model to label cell lineage of von Ebner's glands.

In this study, we used multiple inducible Cre mouse models to map the lineage of cells in connective tissue (including stromal cells and Schwann cells) and cells in von

Ebner's glands, respectively. We found a consistent concurrent distribution of labeled cells in circumvallate taste buds and that in von Ebner's glands, but not that in connective tissue. Our data suggest that von Ebner's glands, but not connective tissue core of taste papillae, contain progenitors for taste buds.

4.3 Materials and methods

4.3.1 Animals

Animal use in this study was approved by The University of Georgia Institutional Animal Care and Use Committee and was in compliance with the National Institutes of Health Guidelines for care and use of animals for research.

Mice were maintained in the animal facility of the Animal and Dairy Science department at the University of Georgia at 22℃ under 12-hour day/night cycles. Sox10-iCreER^{T2} (CBA; B6-Tg (Sox10-icre/ER^{T2}) 388Wdr/J; Jackson Laboratory Stock#027651) [189], Vimentin-CreER mice [127], and Plp1-CreER^{T} (heterozygotes, B6.Cg-Tg$^{(Plp1\text{-}cre/ERT)3Pop}$/J, Jackson Laboratory Stock # 005975) mice were bred with R26-tdTomato (hereafter tdT) Cre reporter mice (homozygotes, B6.Cg-*Gt(ROSA)26Sor*$^{tm14(CAG\text{-}tdTomato)Hze}$/J; Jackson Laboratory Stock #007914) respectively to generate Sox10-iCreER^{T2}/tdT, Vimentin-CreER/tdT, and Plp1-CreER^{T}/tdT mice. No significant difference was found between females and males regarding the distribution of labeled cells in each line; therefore, females and males were grouped together for analyses. Cre-negative littermates served as controls. FVB/NJ wild type mice (The Jackson Laboratory, Stock#001800) were used to breed in parallel for fostering caesarean born Sox10-iCreER^{T2}/tdT pups.

PCR genotyping was performed using the following primers: (1) CreER allele forward 5'-ATT GCT GTC ACT TGG TCG GC-3' and reverse 5'-GGA AAA TGC TTC TGT CCG TTT GC-3' to detect the mouse CreER and CreER^{T} recombinase allele; (2) iCreER^{T2} allele forward 5'-GAG ACG GAC CAA AGC CAC T-3' and reverse 5'-CTG CAG CCT CCT CCA CTG-3' to detect the mouse iCreER^{T2} recombinase allele; (3) msSRYz_SexDet forward, 5'-TTG TCT AGA GAG CAT GGA GGG CCA TGT CAA-3' and reverse 5'-CCA CTC CTC TGT GAC ACT TTA GCC CTC CGA-3' to determine the sex of mouse embryos; and (4) tdT allele forward, 5'-CTG TTC CTG TAC GGC ATG G-3' and reverse 5'-GGC ATT AAA GCA GCG TAT CC-3' to determine the expression of tdT reporter.

4.3.2 Tamoxifen administration and pups fostering

Tamoxifen (Tmx) (Cat No. T5648; Sigma-Aldrich, Inc, St. Louis, MO) was dissolved in corn oil at the working concentration of 11.1 mg/mL. Timed pregnant mice were used for labeling neural crest cell lineages in embryos. Noon of the day of vaginal plug detection in mice was designated embryonic (E) day 0.5. To induce Cre recombination in embryos at E8.0, a single dose of 0.1 mL tamoxifen solution was given through oral gavage using 16 G x 38 mm polyurethane feeding tubes (Cat No. FTPU-16-50, Instech Laboratories, Inc, Plymouth Meeting, PA) to the pregnant dams carrying E7.5 embryos. To activate Cre recombination in perinatal mice, 0.1 mL tamoxifen solution was given through oral gavage to nursing dams daily for consecutive 10 days from P1 to P10. For mice with prolonged tamoxifen administration, 0.1 mL tamoxifen solution was given through oral gavage to nursing dams for every three days until weaning at day 28, followed by oral gavage to weaned mice for every three days until 8 weeks or 16 weeks. Vehicle controls were treated with corn oil in the Cre- and reporter-positive littermates at

the same stages in parallel. A list of the tamoxifen administrations and subsequent tissue collections is shown in Table 4.1.

Table 4.1: Time points of tamoxifen administration and tissue collection

Stage and dose of tamoxifen	Tissue collection
E7.5 (single dose to dam)	8 week
P1-P10 day (10 daily doses)	P11 day and 8 week
P1- 8 week (a dose for every 3 day)	8 week
P1- 16 week (a dose for every 3 day)	16 week

To resolve the dystocia problem caused by tamoxifen injection to pregnant mice, caesarean sections were performed to deliver the Sox10-iCreER^{T2}/tdT embryos at E18.5. The delivered pups were fostered by a FVB/J nursing dam immediately after caesarean birth.

4.3.3 Tissue collection

Postnatal mice were harvested at P11 day, 8 weeks, or 16 weeks (n=3 for both vehicle- and tamoxifen-treated at each stage). Mice were euthanized with CO_2 followed by transcardial perfusion using 10 mL warm 0.1 M PBS, 10 mL warm and 20 mL cold 2% PFA in 0.1 M PBS. Tongues were dissected and further fixed in 2% PFA at 4℃ for 2 hour.

4.3.4 Immunohistochemistry

Fixed tongues were cryoprotected in 30% sucrose in 0.1 M PBS for at least 48 hours at 4℃. The circumvallate papilla was dissected from the tongues and trimmed under a stereomicroscope, embedded in O.C.T. (Cat No. 23-730-571, Thermo Fisher Scientific, Pittsburgh, PA) and rapidly frozen for coronal sections. Frozen sections were cut at 8 μm in thickness and mounted onto charged slides (Fisher brand™ Superfrost™ Plus Microscope Slides, Cat No. 12-550-15, Thermo Fisher Scientific, Pittsburgh, PA). Non-specific binding was blocked with 10% normal donkey serum (Cat No. SLBW2097, Sigma-Aldrich, Inc, St. Louis, MO) in 0.1 M PBS containing 0.3% Triton X-100 (Cat No.

X100-100ML, Sigma-Aldrich, Inc, St. Louis, MO) for 30 min, followed by overnight incubation with primary antibody against Keratin (Krt) 8 (1:500, Developmental Studies Hybridoma Bank, TROMA-1, RRID: AB_531826) diluted with 0.1 M PBS containing 0.3% Triton X-100 and 1% normal donkey serum. After rinses in 0.1 M PBS (3 times, 10 min each), sections were incubated with Alexa Fluor® 647 secondary antibody (1:500, Invitrogen, Eugene, OR) for 1 hour at room temperature. Sections were rinsed and then counterstained with DAPI (200 ng/mL, Cat No. D1306, Thermo Fisher Scientific, Pittsburgh, PA) for 10 min at room temperature. After rinses with 0.1 M PBS followed by dipping in Milli-Q water (DirectQ® 3 UV water purification system, Millipore, MA). Sections were air dried and coverslipped with Prolong® diamond antifade mounting medium (Cat No. P36970, Thermo Fisher Scientific, Pittsburgh, PA).

4.3.5 Photomicroscopy

Immunoreacted sections on slides were thoroughly examined under a fluorescent light microscope (EVOS FL, Thermo Fisher Scientific, Pittsburgh, PA) and images were taken using a laser scanning confocal microscope (Zeiss LSM 710, Zeiss, Germany).

4.3.6 Quantification and data analysis

Quantitative analyses (n=3) were performed using single-plane confocal images and Photoshop software to quantify the total cells and Sox10-iCreER^{T2}/tdT-unlabeled cells in connective tissue immediate under circumvallate taste buds in 8-week-old Sox10-iCreER^{T2}/tdT mice with tamoxifen administration at E7.5. The region of underlying connective tissue within 100 μm in distance to basement membrane of the circumvallate papilla epithelium was included for the quantification. For each mouse, three sections were selected for analyses, i.e., the section with the deepest trench and biggest area of

circumvallate papilla, and the one 40 μm anterior and 40 μm posterior to the section with the deepest trench. Only the cells with a clear DAPI$^+$ nucleus was counted. A clear DAPI$^+$ nucleus without any tdT signals surrounded was regarded as a Sox10-iCreER^{T2}/tdT non-labeled cell. The proportion of connective tissue cells labeled by Sox10-iCreER^{T2}/tdT was calculated using the formula of [(total DAPI$^+$ cells – DAPI$^+$ tdT$^-$ cells) / total cells].

4.4 Results

4.4.1 Sox10-iCreER^{T2}-labeled neural crest cell lineages were distributed in the connective tissue core of circumvallate papilla, but absent in both circumvallate taste buds and von Ebner's glands

Sox10 expression is restricted to migrating neural crest cells during a short time window of early embryonic development [15, 128, 129]. In postnatal mouse tongue Sox10 expression has been found to be in two tissue compartments that's are adjacent to taste buds: the connective tissue core of taste papillae and von Ebner's glands [15]. To answer the question of to what extent cells in the papilla connective tissue core and von Ebner's glands are neural crest-derived, we revisited the Sox10-iCreER^{T2}/tdT mouse model in labeling Sox10$^+$ migrating neural crest cells with tamoxifen administration at E7.5 (Figure. 4.1A). In 8-week-old young adult when most circumvallate taste buds are mature, Sox10-iCreER^{T2}/tdT-labeled cells were widely distributed in the connective tissue surrounding the trenches of circumvallate papillae (Figure. 4.1B). In contrast, tdT$^+$ cells were neither found in the ducts and acini of von Ebner's glands, nor circumvallate taste buds located by the immunosignals of Krt8 (Figure. 4.1B). tdT$^+$ cells were not absent in the taste bud-surrounding tongue epithelium, including basal epithelial cells that are known as progenitors of taste buds [3, 4, 6, 11-14].

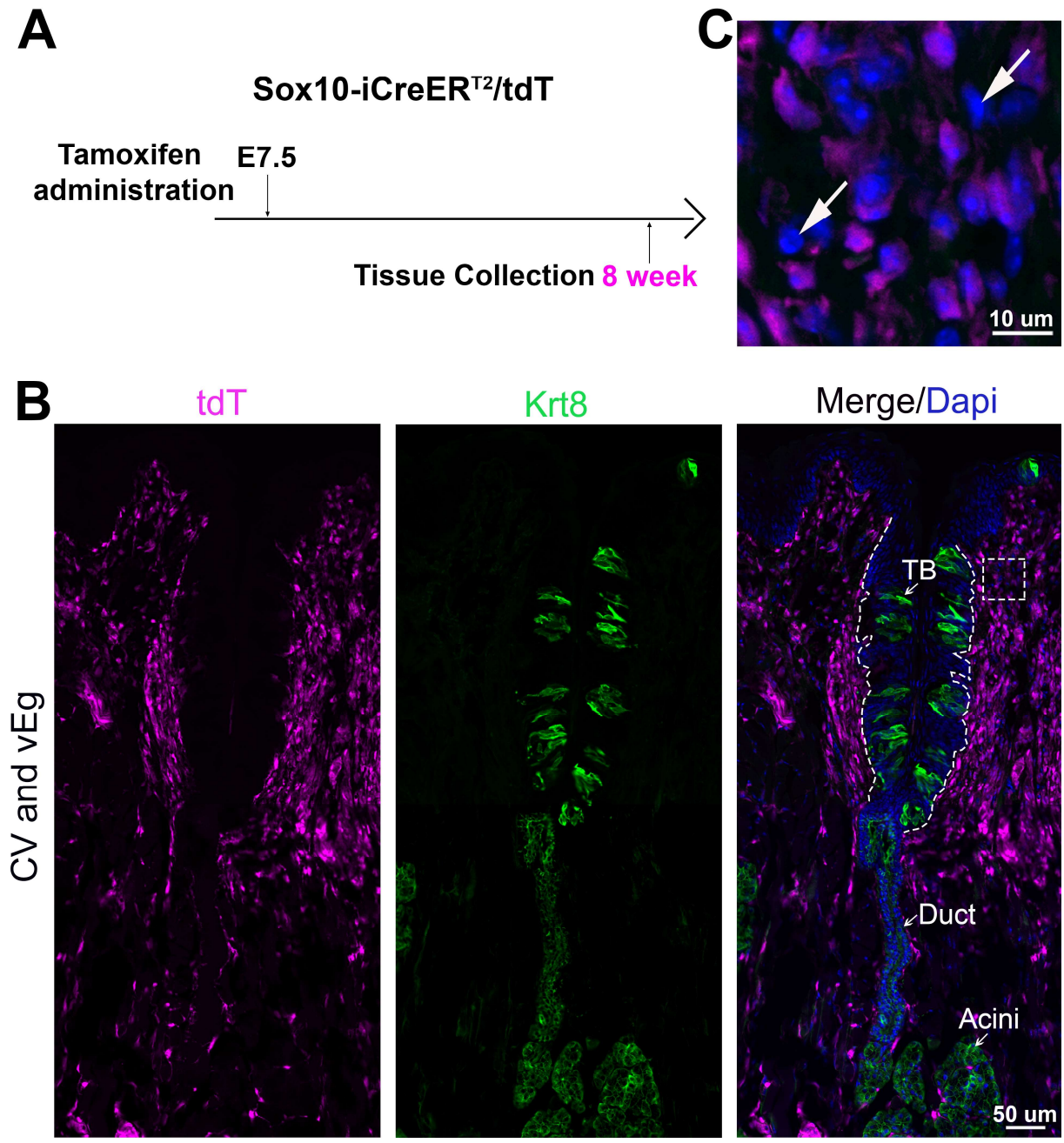

Figure 4.1. Neural crest lineage mapping in the circumvallate papilla. **A:** Schematic diagram showing the timeline of tamoxifen administration to Sox10-iCreER^{T2}/tdT mice at E7.5 for neural crest cell labeling and tongue tissue collection at 8 weeks. **B:** Single-plane laser scanning confocal photomicrographs on a coronal section of circumvallate papilla to demonstrate the distribution of Sox10-iCreER^{T2}/tdT-labeled cells (magenta) in tongue

of 8-week-old mice with tamoxifen administration at E7.5. **C:** High power images from the area indicated by dashed square shown in B. Arrows point to the cells without any tdT signal surrounded. Taste buds (TB) and ducts (Duct) and acini (Acini) of von Ebner's gland were marked by the immunosignals of Keratin 8 (Krt8, green). White dashed lines mark the borders between the epithelium and underlying tissue. Scale bars: 50 μm in B and 10 μm in C.

In connective tissue, not all the cells are labeled by Sox10-iCreER^{T2}/tdT (Figure. 4.1C). To understand the proportion of the connective tissue cells that are labeled by Sox10-iCreER^{T2}/tdT, the coronal sections of circumvallate papillae were used to visualize the connective tissue cells immediate under circumvallate taste buds for quantification. The percentage of Sox10-iCreER^{T2}/tdT-labeled cells versus total cells in the defined area of connective tissue was 89.2% (89.2±6.15).

4.4.2 Plp1-CreER^{T} and Vimentin-CreER labeled cells were extensively distributed in the connective tissue but not in circumvallate taste buds and von Ebner's glands

Labeling Sox10^{+} migrating neural crest cells with tamoxifen administration at E7.5 in Sox10-iCreER^{T2}/tdT mouse model has demonstrated that taste buds are not derived from neural crest [44]. Questions remain whether all neural crest cells are labeled due to the tamoxifen-induced DNA recombination and whether the non-neural crest derived connective tissue cells give rise to taste buds. In order to verify the potential contribution of connective tissue cells to taste buds, we utilized the Plp1-CreER^{T}/tdT and Vimentin-CreER/tdT mouse models to map the lineage of Plp1^{+} Schwann cells and Vimentin^{+} stromal cells respectively in circumvallate papillae and von Ebner's glands.

In the P11 Plp1-CreER^T/tdT mice, tdT$^+$ cells were abundantly distributed in the connective tissue core of circumvallate papilla after daily tamoxifen treatments from P1 to P10 (Figure. 4.2). In contrast, no tdT$^+$ cell was found in taste buds and von Ebner's glands (Figure. 4.2). The data demonstrated the efficient DNA recombination in labeling Schwann cell lineage and the extensive distribution of Schwann cells and derived cells in the connective tissue. To give sufficient time for taste bud cell reviewal according to the lifespan (~8-12 days on average) of taste bud cells, young adult mice at 8 weeks were harvested for analyses after daily tamoxifen treatments from P1 to P10. Similarly to the data from P11 mouse tongues, tdT$^+$ cells were extensively present in the connective tissue, but remained absent from both taste buds and von Ebner's glands (Figure. 4.3). Taste bud-surrounding epithelium was free of Plp1-CreER^T/tdT labeling at all stages examined (Figure. 4.2, 4.3).

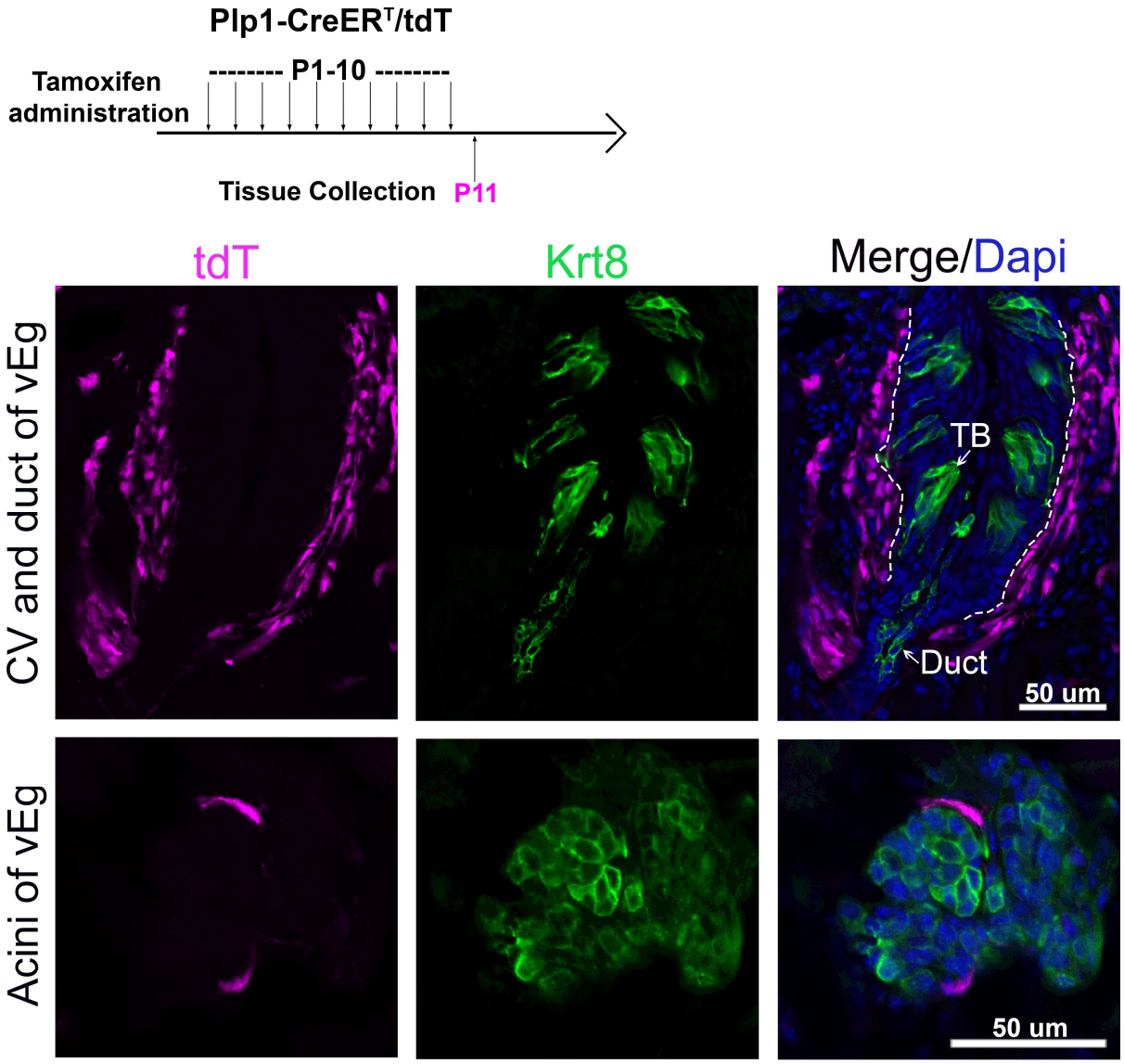

Figure 4.2. Schwann cell lineage mapping in the circumvallate papilla using P11 Plp1-CreER^T/tdT mice with tamoxifen administration from P1 to P10. Schematic diagram showing the timeline of daily tamoxifen administration from P1-10 and tissue collection at P11 day of stage. Single-plane laser scanning confocal images of circumvallate papilla and von Ebner's gland on a coronal section of P11 mice demonstrate the distribution of Plp1-CreER^T/tdT-labeled cells (magenta). Taste buds (TB) and ducts (Duct) and acini of von Ebner's gland were marked by the immunosignals of Keratin 8 (Krt8, green). White

dashed lines mark the borders between the epithelium and underlying tissue. Scale bars: 50 μm in all images.

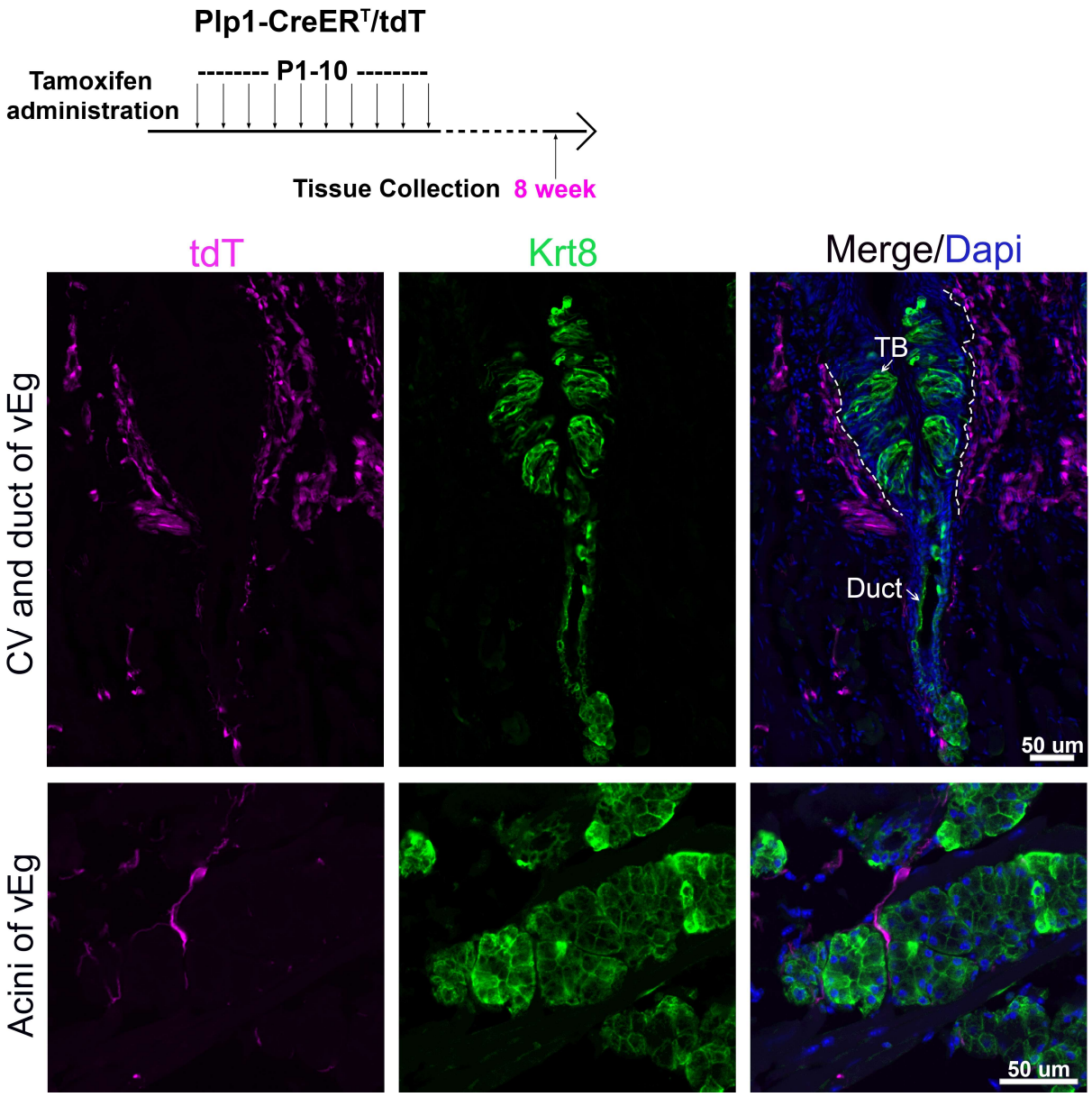

Figure 4.3. Schwann cell lineage mapping in the circumvallate papilla using 8-week-old Plp1-CreER^T/tdT mice with tamoxifen administration from P1 to P10. Schematic diagram showing the timeline of daily tamoxifen administration from P1-10 and tissue collection at 8 weeks of age. Single-plane laser scanning confocal images of circumvallate papilla and von Ebner's gland on a coronal section of 8-week-old mice demonstrate the distribution of Plp1-CreER^T/tdT-labeled cells (magenta). Taste buds (TB) and ducts (Duct) and acini of von Ebner's gland were marked by the immunosignals of Keratin 8 (Krt8, green). White

dashed lines mark the borders between the epithelium and underlying tissue. Scale bars: 50 μm in all images.

To map the lineage of Vimentin^{+} stromal cells and avoid confusion caused by membrane-bound fluorescent signals [16], Vimentin-CreER/tdT mice were used. Using the same tamoxifen treatment regimen as that aforementioned to the Plp1-CreER^{T}/tdT, tamoxifen-induced DNA recombination and labeling of Vimentin^{+} stromal cell lineages were highly efficient. In Vimentin-CreER/tdT tongue at P11, tdT^{+} cells were widely distributed in the underlying connective tissue of circumvallate taste buds (Figure. 4.4). Similar to the distribution pattern found in Plp1-CreER^{T}/tdT mice, tdT^{+} cells were neither observed in circumvallate taste buds nor in von Ebner's glands (Figure. 4.4). Moreover, tdT^{+} cells were not seen in taste buds and von Ebner's glands except in the connective tissue core of circumvallate in 8-week-old mice (Figure. 4.5). Vimentin-CreER/tdT did not label taste bud-surrounding epithelium at all stages examined (Figure. 4.4, 4.5).

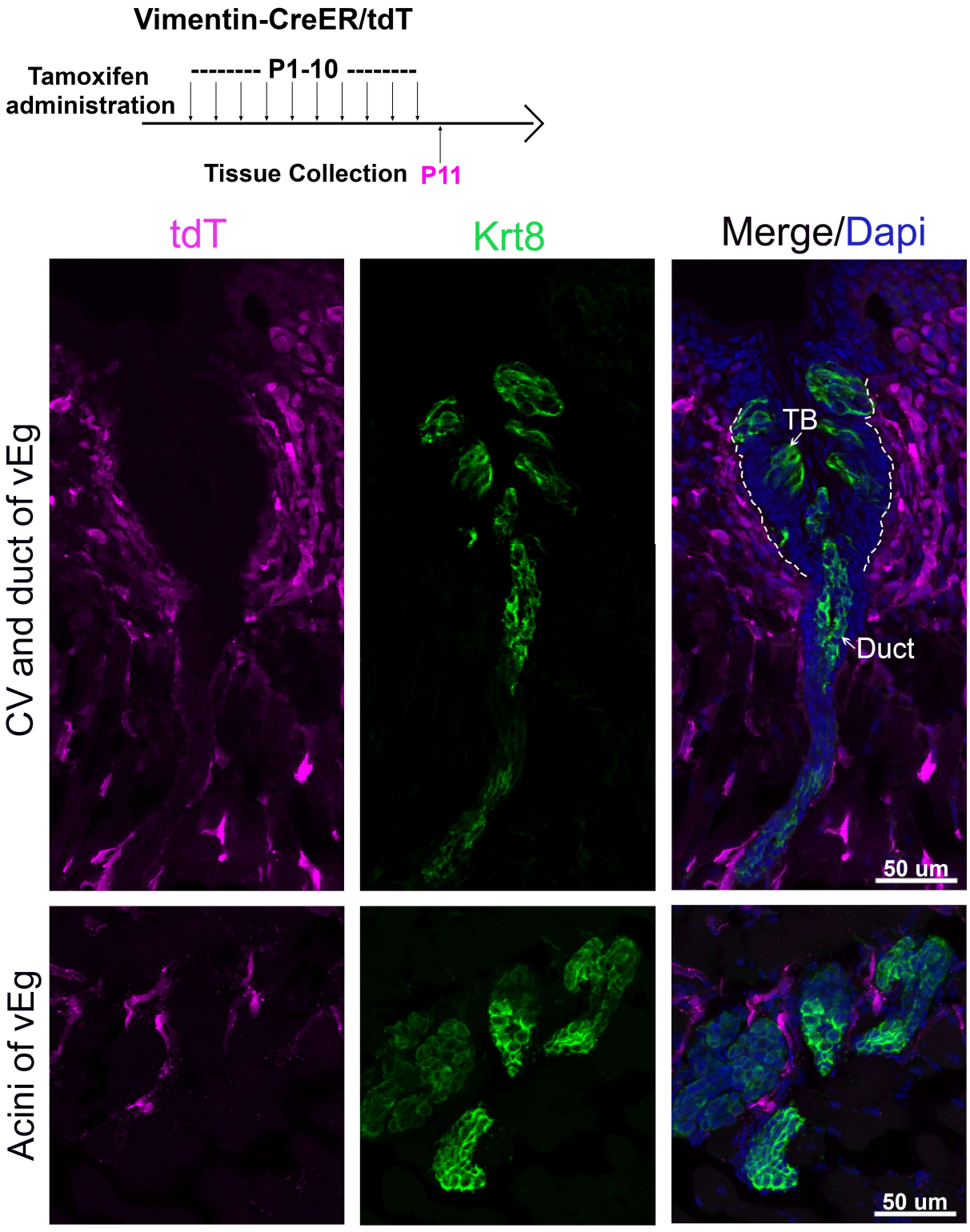
Vimentin-CreER/tdT
Tamoxifen administration
-------- P1-10 --------
Tissue Collection P11
tdT
Krt8
Merge/Dapi
CV and duct of vEg
TB
Duct
50 um
Acini of vEg
50 um

Figure 4.4. Stromal cell lineage mapping in circumvallate papilla using P11 Vimentin-CreER/tdT mice with tamoxifen administration from P1 to P10. Schematic diagram showing the timeline of daily tamoxifen administration from P1-P10 and tissue collection at P11. Single-plane laser scanning confocal photomicrographs of circumvallate papilla and von Ebner's gland were taken from a coronal section of a P11 mouse circumvallate papilla to demonstrate the distribution of Vimentin-CreER/tdT-labeled cells (magenta). Taste buds (TB) and ducts (Duct) and acini of von Ebner's gland were marked by the immunosignals of Keratin 8 (Krt8, green). White dashed lines mark the borders between the epithelium and underlying tissue. Scale bars: 50 μm in all images.

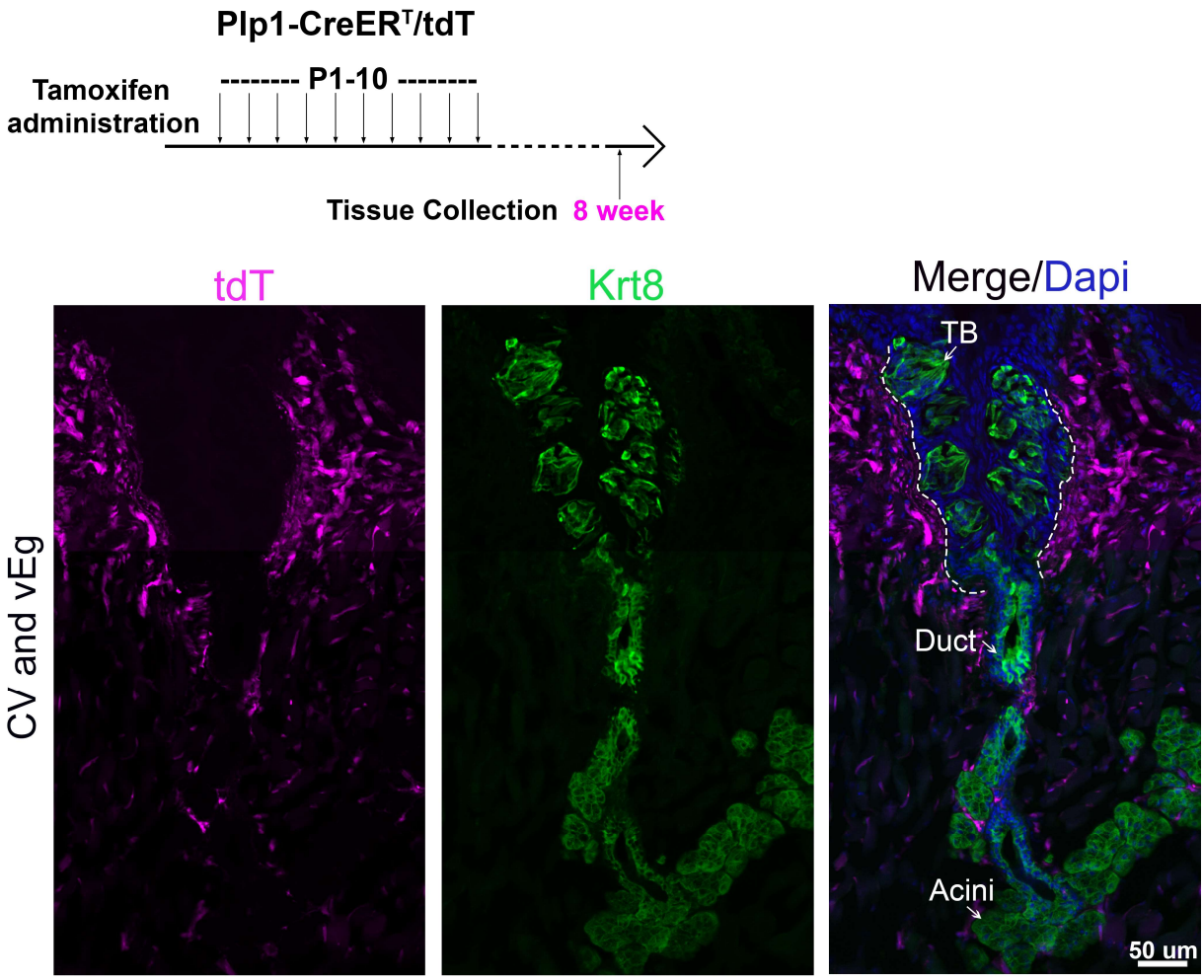

Figure 4.5. Stromal cell lineage mapping in circumvallate papilla using 8-week-old Vimentin-CreER/tdT mice with tamoxifen administration from P1 to P10. Schematic diagram showing the timeline of daily tamoxifen administration from P1-P10 and tissue collection at 8 weeks. Single-plane laser scanning confocal photomicrographs of circumvallate papilla and von Ebner's gland were taken from a coronal section of a 8-week-old mouse circumvallate papilla to demonstrate the distribution of Vimentin-CreER/tdT-labeled cells (magenta). Taste buds (TB) and ducts (Duct) and acini (Acini) of von Ebner's gland were marked by the immunosignals of Keratin 8 (Krt8, green). White dashed lines mark the borders between the epithelium and underlying tissue. Scale bars: 50 μm in all images

4.4.3 Sox10-iCreER^{T2}-labeled cells were concurrently distributed in von Ebner's glands and circumvallate taste buds in 8- and 16-week-old mice after consecutive tamoxifen administration

As aforementioned, Sox10 expression is in two tissue compartments that are adjacent to taste buds in postnatal mouse tongue: the connective tissue core of taste papillae and von Ebner's glands [15]. The data from three mouse models used to define the cell types of Sox10^{+} taste bud progenitors indicate that distribution of labeled cells in circumvallate taste buds is not correlated with that in the connective tissue, which leaves von Ebner's gland as the only candidate of progenitor source for taste bud cell renewal. To track the lineage of potential progenitor cells for circumvallate taste buds in von Ebner's glands, we used Sox10-iCreER^{T2}/tdT mouse model with daily tamoxifen administration from P1 to P10. In P11 mice, von Ebner's glands and connective tissue were abundantly labeled by Sox10-iCreER^{T2}/tdT right after tamoxifen injection while Sox10-iCreER^{T2}/tdT-labeled cells were not found in circumvallate taste buds (Figure. 4.6). Given that Sox10^{+} progenitors give rise mainly to type III taste bud cells [15] that have a half-life of 22 days [5], a long time window was given after the termination of tamoxifen treatments and 8-week-old mice were harvested for examination. Von Ebner's glands and circumvallate taste buds were concurrently labeled by Sox10-iCreER^{T2}/td after perinatal administration of tamoxifen (Figure. 4.7). Importantly, Sox10-iCreER^{T2}/tdT-labeled cells were found, although infrequently, in taste buds (Figure. 4.7).

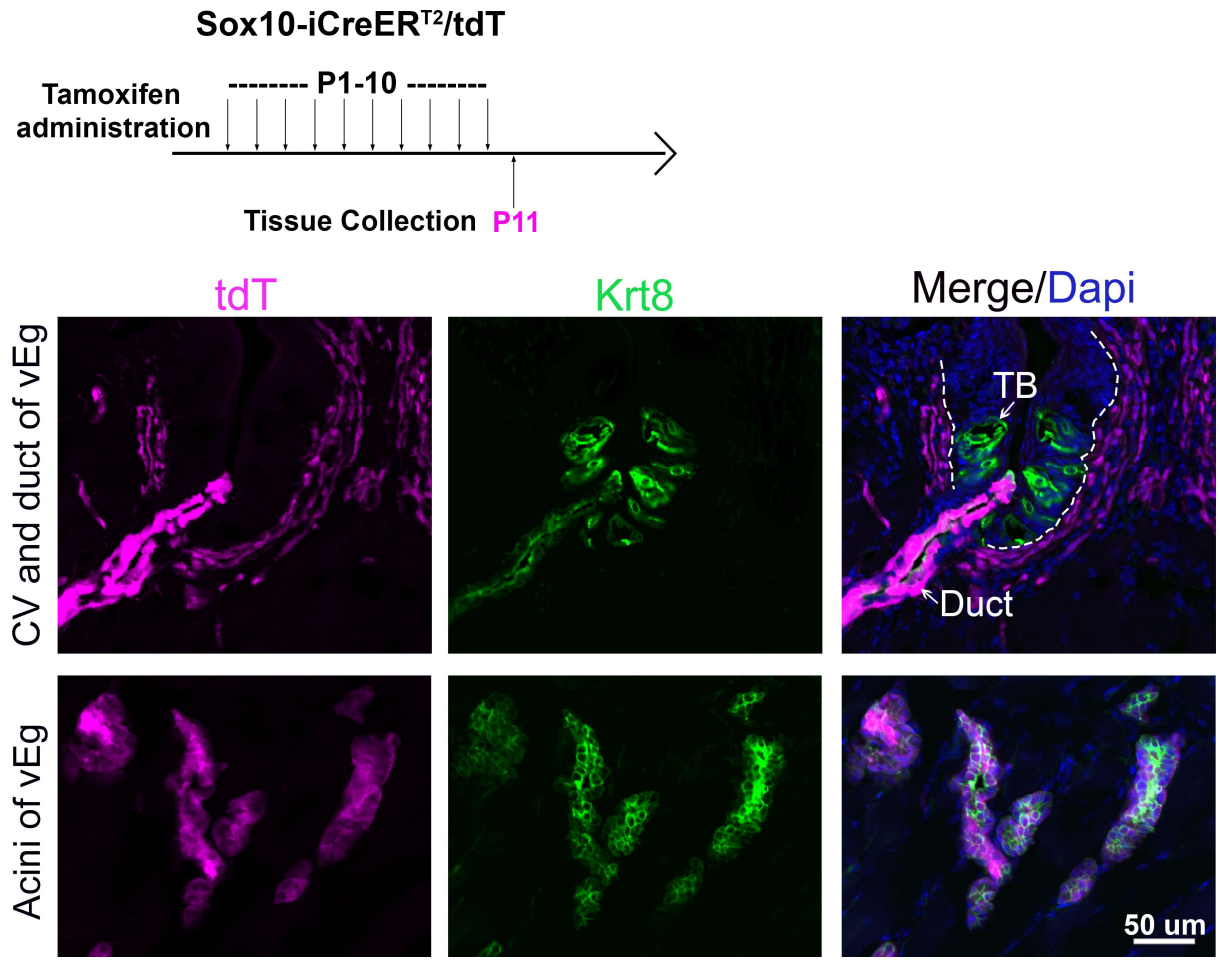

Figure 4.6. Lineage tracing of Sox10^{+} cells (von Ebner's gland and connective tissue cells) in the circumvallate papilla using P11 Sox10-iCreER^{T2}/tdT mice with tamoxifen administration from P1 to P10. Schematic diagram showing the timeline of daily tamoxifen administration from P1 to P10 and tissue collection at P11. Representative images of circumvallate papilla and von Ebner's gland are single-plane laser scanning confocal from a coronal section of P11 mouse tongue. Taste buds (TB) and ducts (Duct) and acini of von Ebner's gland were marked by the immunosignals of Keratin 8 (Krt8, green. White dashed lines mark the borders between the epithelium and underlying tissue. Scale bars: 50 μm in all images.

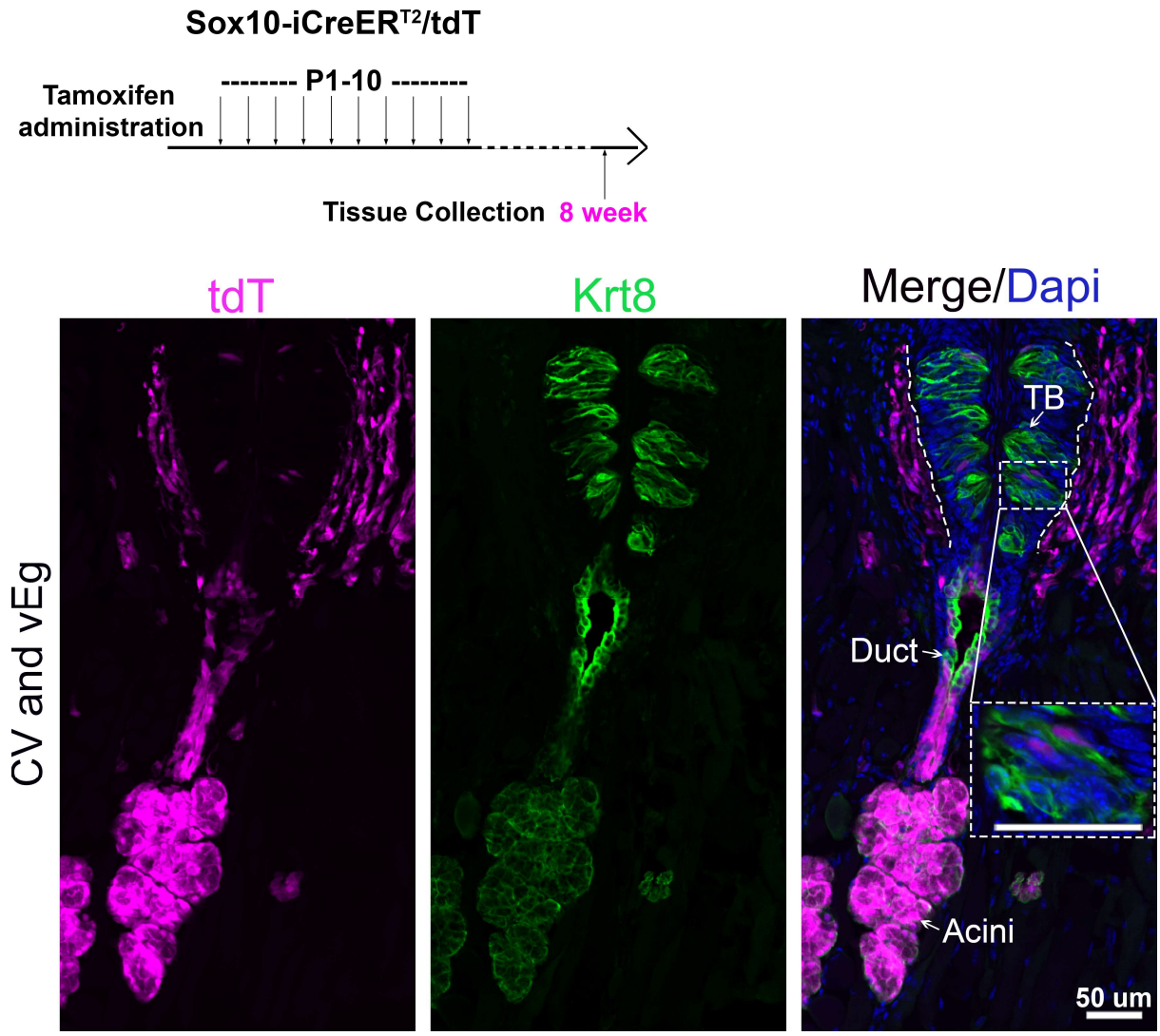

Figure 4.7. Lineage tracing of Sox10^{+} cells (von Ebner's gland and connective tissue cells) in the circumvallate papilla using 8-week-old Sox10-iCreER^{T2}/tdT mice with tamoxifen treatment from P1 to P10. Schematic diagram showing the timeline of daily tamoxifen administration from P1 to P10 and tissue collection at 8 weeks. Representative images of circumvallate papilla and von Ebner's gland are single-plane laser scanning confocal from a coronal section of 8-week-old mouse tongue. Taste buds (TB) and ducts (Duct) and acini (Acini) of von Ebner's gland were marked by the immunosignals of

Keratin 8 (Krt8, green). White dashed lines mark the borders between the epithelium and underlying tissue. Scale bars: 50 μm in all images.

To test whether the infrequent Sox10-iCreER^{T2}/tdT labeling of taste bud cells was caused by transient Sox10 expression in taste bud progenitors, consecutive tamoxifen administration was performed in Sox10-iCreER^{T2}/tdT mice from P1 day to 8 week or up to 16 week. Indeed, after 8 week of tamoxifen treatment, circumvallate taste buds were abundantly labeled concurrently with von Ebner's glands in Sox10-iCreER^{T2}/tdT mice (Figure. 4.8). The labeled taste bud cells were clearly visualized with the typical fusiform shape of differentiated taste cells (Figure. 4.8). Similar labeling pattern was found in 16-week-old mice (Figure. 4.9). In addition, Sox10-iCreER^{T2}/tdT-labeled cells were abundantly distributed in connective tissue but not in taste bud-surrounding lingual epithelium in all stages examined (Figure. 4.8, 4.9).

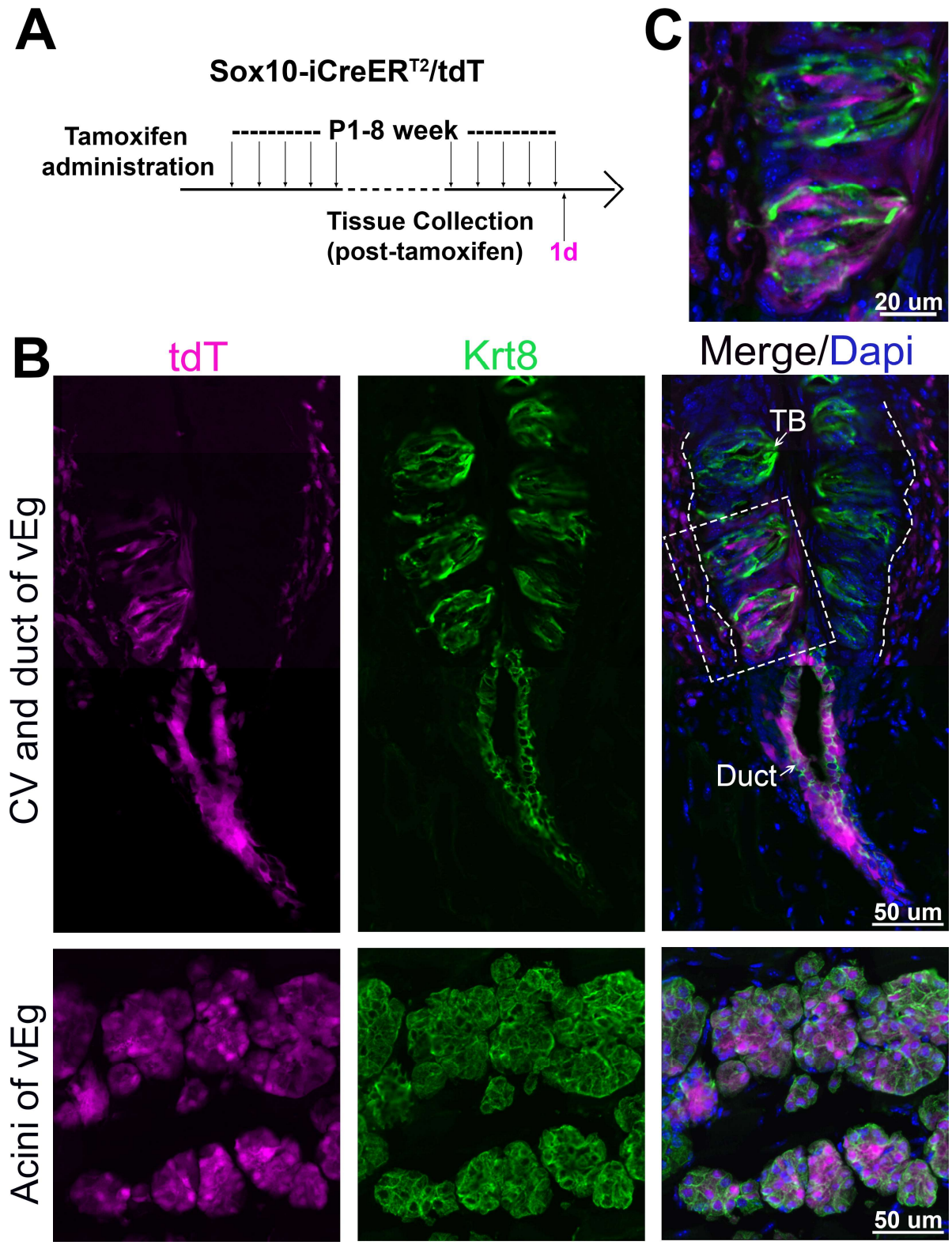
A
Sox10-iCreER^{T2}/tdT
Tamoxifen administration
---------- P1-8 week ----------
Tissue Collection (post-tamoxifen)
1d
C
20 um
B
tdT
Krt8
Merge/Dapi
CV and duct of vEg
TB
Duct
50 um
Acini of vEg
50 um

Figure 4.8. Lineage tracing of Sox10^{+} cells (Von Ebner's gland and connective tissue cells) in the circumvallate papilla using 8-week-old Sox10-iCreER^{T2}/tdT mice with prolonged tamoxifen treatments. **A:** Schematic diagram showing the timeline of tamoxifen administration to Sox10-iCreER^{T2}/tdT mice from P1 to 8 week and tongue tissue was collected 1 day after the termination. **B:** The representative images of circumvallate papilla and von Ebner's gland were from a coronal section of an 8-week-old mouse. Single-plane laser scanning confocal images of a coronal section of circumvallate papilla illustrate a concurrent distribution of tdT^{+} cells in circumvallate taste buds and von Ebner's gland in addition to that in connective tissue. **C:** High power images from the area indicated by dashed square shown in B. Taste buds (TB) and ducts (Duct) and acini of von Ebner's gland were marked by the immunosignals of Keratin 8 (Krt8, green). White dashed lines mark the borders between the epithelium and underlying tissue. Scale bars: 50 μm in B and 20 μm in C.

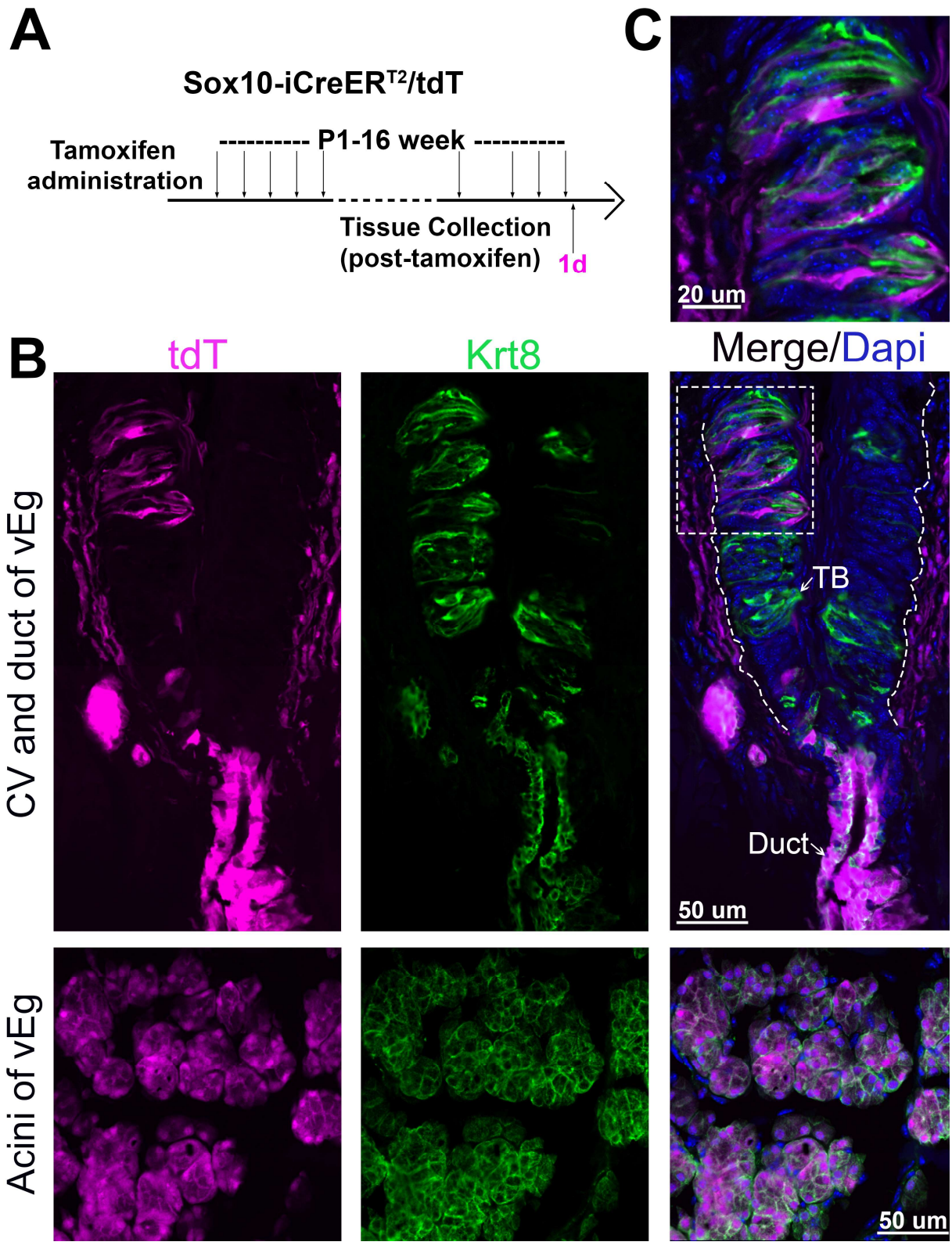
A
Sox10-iCreER^{T2}/tdT
Tamoxifen administration
---------- P1-16 week ----------
Tissue Collection (post-tamoxifen)
1d
C
20 um
B
tdT
Krt8
Merge/Dapi
CV and duct of vEg
TB
Duct
50 um
Acini of vEg
50 um

Figure 4.9. Lineage tracing of Sox10$^+$ cells (Von Ebner's gland and connective tissue cells) in the circumvallate papilla using 16-week-old Sox10-iCreER^{T2}/tdT mice with prolonged tamoxifen treatments. **A:** Schematic diagram showing the timeline of tamoxifen administration to Sox10-iCreER^{T2}/tdT mice from P1 to 16 week and tongue tissue was collected 1 day after the termination. **B:** The representative images of circumvallate papilla and von Ebner's gland were from a coronal section of a 16-week-old mouse. Single-plane laser scanning confocal images of a coronal section of circumvallate papilla illustrate a concurrent distribution of tdT$^+$ cells in circumvallate taste buds and von Ebner's gland in addition to that in connective tissue. **C:** High power images from the area indicated by dashed square shown in B. Taste buds (TB) and ducts (Duct) and acini of von Ebner's gland were marked by the immunosignals of Keratin 8 (Krt8, green). White dashed lines mark the borders between the epithelium and underlying tissue. Scale bars: 50 μm in B and 20 μm in C.

4.5 Discussion

4.5.1 Sox10$^+$ cells in von Ebner's glands, but not those in connective tissue, serve as progenitors for circumvallate taste buds

Our recent studies have demonstrated that Sox10$^+$ cells serve as progenitors for taste buds [15]. We have identified three tissue compartments that contain Sox10$^+$ cells, i.e., migrating neural crest cells, connective tissue core of taste papillae, and von Ebner's glands [15]. Among them, migrating neural crest lineages, including the neural crest-derived connective tissue in tongue, have been excluded from the candidacy [44], leaving non-neural crest-derived cells in connective tissue and/or von Ebner's glands for further studies.

In present study, we aimed to answer the question which tissue compartment, non-neural crest-derived connective tissue cells and/or von Ebner's glands, contain progenitors for taste buds. Combining the data from multiple inducible CreER mouse models to specifically label the lineages of different cell types in distinct tissue compartments, we provide evidence that von Ebner's gland, but not connective tissue, is the progenitor source for taste buds. The distribution of labeled cells in circumvallate taste buds is correlated with that in von Ebner's gland, not with that in the connective tissue core of circumvallate papilla.

In the connective tissue core, we found two abundant and largely distinct subpopulations of cells that express Vimentin, an intermediate filament protein widely used as a marker for mesenchymal stromal cells [224] including both neural crest and non-neural crest lineages, and S100, low-molecular-weight proteins found in vertebrates that are expressed in glial cells [225]. To mark the cells in connective tissue core of taste papillae, we used Cre-ER mouse lines in which CreER is under the control of promoter of Vimentin and Proteolipid protein 1 (Plp1) that is specifically expressed in immature Schwann cells [226], the known neural crest derivatives [227]. In both Plp1-CreER^{T}/tdT and Vimentin-CreER/tdT mice, labeled cell lineages of Plp1^{+} Schwann cells and Vimentin^{+} stromal cells were abundant in the connective tissue core of circumvallate papilla but not in taste buds, suggesting the absence of direct contribution of non-neural crest-derived connective tissue cells to circumvallate taste buds. Meanwhile, these data provide a clear reference for the observations in previous study using membrane-bound GFP reporter [16], in which mGFP signals in taste buds may attribute to the extended nerve fiber or fibroblast lamellipodia from connective tissue. Of note, the labeled cells

were also absent in von Ebner's glands along with taste buds in both Plp1-CreER^{T}/tdT and Vimentin-CreER/tdT mice.

However, in Sox10-iCreER^{T2}/tdT mice with postnatally tamoxifen administration, labeled cells were concurrently distributed in both von Ebner's glands and circumvallate taste buds. The concurrent lineage labeling of taste buds and von Ebner' glands, but not connective tissue, indicates a contribution of von Ebner's glands to taste buds. The efficiency of Sox10-iCreER^{T2} in labeling von Ebner's glands is granted by the early induction of Cre recombination. But the limited labeled cells in taste buds suggests the transient Sox10 expression in taste bud progenitors, which is confirmed in following studies with prolonged tamoxifen treatment. Overall, our data support the idea that von Ebner's glands are potential progenitor source for circumvallate taste buds, which still need solid evidence to be verified.

4.5.2 Not all connective tissue cells are from Sox10^{+} neural crest in the tongue

Neural crest cells have been found to be the major contributors of mesenchyme/connective tissue of tongue at both embryonic and postnatal stage [15-17, 44, 123]. However, question remains whether they are the sole player in genesis of mesenchyme/connective tissue in tongue. Our recently published data have demonstrated that a single dose tamoxifen administration to the pregnant dam with E7.5 Sox10-iCreER^{T2}/tdT embryos resulted in a labeling of most, if not all, of tongue mesenchymal cells at E12.5 [44]. In present study, 89.2% (89.2$\pm$6.15) of the connective tissue cells were labeled in the adult Sox10-iCreER^{T2}/tdT with tamoxifen treatment at E7.5, suggesting that Sox10^{+} neural crest cells give rise to most, but not all, of the connective tissue cells.

Acknowledgments:

This study was supported by the National Institutes of Health, grant number R01DC012308 and R21DC018089 to HXL.

CHAPTER 5

CELL DISSOCIATION FROM TONGUE EPITHELIUM AND MESENCHYME/CONNECTIVE TISSUE OF EMBRYONIC-DAY 12.5 AND 8-WEEK-OLD MICE [1]

[1] Wenxin Yu, Mohamed Ishan, Zhonghou Wang, and Hong-Xiang Liu. 2021. *JoVE Journal of Visualized Experiments*. (167), e62163. Reprinted here with permission of publisher.

5.1 Abstract

Cell dissociation has been an essential procedure for studies researching at the individual-cell level and/or at a cell-population level, e.g., single cell RNA sequencing and primary cell culture. Yielding viable, healthy cells in large quantities is critical, and the optimal conditions to do so are tissue-dependent. Cell populations in the tongue epithelium and underlying mesenchyme/connective tissue are heterogeneous and tissue structures vary in different regions and at different developmental stages. We have tested protocols for isolating cells from mouse tongue epithelium and mesenchyme/connective tissue in the early developmental [embryonic day 12.5 (E12.5)] and young adult (8-week) stages. A clean separation between the epithelium and underlying mesenchyme/connective tissue was easy to accomplish. However, to further process and isolate cells, yielding viably healthy cells in large quantities, careful selection of enzymatic digestion buffer, incubation time period, and centrifugation speed and time is critical. Incubation of separated epithelium or underlying mesenchyme/connective tissue in 0.25% Trypsin-EDTA for 30 min at 37 ℃, followed by centrifugation at 200 x g for 8 min resulted in a high yield of cells at a high viability rate (>90%) regardless of the mouse stages and tongue regions. Moreover, we found that both dissociated epithelial and mesenchymal/connective tissue cells from embryonic and adult tongues could survive in our cell culture-based medium for at least 3 hours without a significant decrease of cell viability. Our protocols will be useful for studies that require the preparation of isolated cells from mouse tongues at early developmental (E12.5) and young adult (8-week) stages requiring cell dissociation from different tissue compartments.

5.2 Introduction

The mammalian tongue is a complex organ critical for taste, speaking, and food processing. It is comprised of multiple types of highly organized tissues compartmentalized by mesenchyme/connective tissue and covered by a stratified epithelial sheet containing taste papillae and taste buds. Cell populations in both tongue epithelium and mesenchyme/connective tissue are heterogeneous. To better understand the functions and distribution of a particular type of cells in the tongue, studies using dissociated cells are necessary. For example, single cell RNA sequencing is a powerful and high-throughput method for transcriptomic profiling in individual cells, which is designed to understand the transcriptome of complex tissue at a single-cell resolution [228-231]. Primary cell culture has been proved to be a useful tool to study the function and differentiation of stem/progenitor cells for taste buds [10, 232]. These studies require a large quantity of high quality isolated cell populations, e.g., sufficient total cell number with proper concentration and high viability.

Thus, there is a need to isolate cells from lingual tissues in different regions and at different developmental stages. Currently there is not a detailed protocol available for cell dissociation from tongue epithelium and underlying mesenchyme/connective tissue. Here we report an optimized cell dissociation method to prepare cells for experiments requiring a high quality of live cells such as for single cell RNA sequencing and primary stem cell cultures. We found that selection of enzymatic digestion buffer, gentle pipetting, selection of resuspension medium, and optimal centrifugation time and speed are crucial to generate these large quantities of high quality cells.

5.3 Protocol

5.3.1. Animal usage

Animal use (C57BL/6 mice throughout the study) was approved by The University of Georgia Institutional Animal Care and Use Committee and was in accordance with the National Institutes of Health Guidelines for care and use of animals for research.

Note: Mice were maintained and bred in the animal facility of the Animal and Dairy Science department at the University of Georgia at 22℃ under 12-h day/night cycles. Noon of the day of vaginal plug detection in mice was designated as embryonic (E) day 0.5. Embryos at E12.5 and postnatal mice at 8 weeks of age were used for the following experiments.

5.3.2. Preparation before experiment

Note: The instruments required for this protocol include dissecting scissors, mini-scissors, surgical forceps, fine forceps, spatula, 1mL syringes, 30 G needles, 0.22-μm syringe filter, 35- and 100- mm culture dishes, plastic wrap, 5-mL low binding microcentrifuge tube, 35- and 70-μm cell strainer, hemocytometer, inverted microscope with imaging system. The reagents required are 70% ethanol, 0.1 M Phosphate-Buffered Saline (PBS, pH 7.4), stock solutions of dispase (5.0 mg/mL) and collagenase (2.0 mg/mL) in 0.1 M PBS, Tyrode's solution, 0.25% typsin-EDTA, fetal bovine serum (FBS), DMEM/F12, bovine serum albumin (BSA), Trypan blue.

(1) Autoclave instruments before the experiment. Sterilize instruments using bead sterilizer during the experiment.

(2) Clean the surgical area, dissecting microscope, and biosafety cabinet using 70% alcohol wipes. Turn on the UV light of biosafety cabinet and keep it on for 20 min prior experimental procedure.

(3) Make enzyme mixture of 1:1 dispase (5.0 mg/mL) and collagenase (2.0 mg/mL) to a final concentration of 2.5 and 1.0 mg/mL respectively, and filter the solution using 0.22-μm syringe filter [233]. Prepare 1 mL of enzyme mixture for an adult tongue or 0.5 mL for a specific region of tongue (e.g., posterior or anterior tongue). Prepare 2 mL enzyme mixture for embryonic tongues.

(4) Make 10 mL 2.5% BSA in 0.1 M PBS and filter the solution using 1-mL syringe and 0.22-μm syringe filter.

(5) Make 500 μL 5% FBS in DMEM/F12.

(6) Make 3 mL DMEM/F12 containing 10% FBS and 1% BSA and filter the solution using 1-mL syringe and 0.22-μm syringe filter.

5.3.3. Separation of tongue epithelium from mesenchyme/underlying connective tissue.

5.3.3.1 Separation of epithelium from mesenchyme of an E12.5 mouse tongue.

(1) Euthanize timed pregnant female mice carrying E12.5 embryos by placing it in a CO_2 chamber followed by cervical dislocation.

Note: Mouse embryos at E12.5 are collected after 12pm (afternoon) on the 12th day after detection of vaginal plug in the pregnant female mice.

(2) Transfer mice to surgical area. Wet mouse abdomen using 70% ethanol to prevent fur from getting into the operating site.

(3) Open the abdomen using dissecting scissors to expose the uterine horns carrying embryos. Dissect the uterine horns using dissecting scissors and transfer it to 15 mL fresh Tyrode's solution in a 100-mm culture dish.

(4) Dissect the embryos (Figure 1A$_1$) out from uterine horns under a dissecting microscope using mini-scissors and fine forceps.

(5) Open the mouth cavity widely by carefully using fine forceps and dissect the tongues with mandible and further dissect the tongues off from mandible using mini-scissors (Figure 1A$_2$).

(6) Wash tongues in biosafety cabinet in Tyrode's solution in 100-mm culture dish and then transfer the tissues to 2 mL of enzyme mixture of dispase (2.5 mg/mL) and collagenase (1.0 mg/mL) in a 35-mm culture dish using spatula and fine forceps for a 20-min incubation at 37 ℃.

(7) Transfer tongues to 15 mL fresh sterile Tyrode's solution in a 100-mm culture dish and gently remove mesenchyme from epithelium from the ventral side using fine forceps.

Note: Epithelial sheets may be separated without mechanical force during the incubation.

(8) Wash the separated epithelia and mesenchyme twice in 15 mL fresh sterile Tyrode's solution in a 100-mm culture dish.

Note: The activities of dispase and collagenase will be inhibited by EDTA in the cell dissociation procedure.

5.3.3.2 Separation of tongue epithelium from underlying connective tissue of adult mice.

(1) Euthanize mouse at 8 weeks of age by placing it in a CO_2 chamber. Confirm that the mouse is euthanized with no breaths and forepaw-pinch response.

(2) Transfer mice to surgical area. Wet mouse head using 70% ethanol to prevent fur from getting into the oral cavity.

(3) Cut the corners of the mouth along the cheek using dissecting scissors to open the oral cavity. Dissect the tongue with mandible (Figure $1B_1$) and place it in a plastic dish with a layer of plastic wrap.

(4) Using surgical forceps to hold the tongue under a dissecting microscope, inject the enzyme mixture of dispase (2.5 mg/mL) and collagenase (1.0 mg/mL) in the sub-epithelial space of tongue through the cutting edge (Figure $1B_1$, arrows) of the posterior tongue. Inject 1 mL enzyme mixture evenly to the whole tongue for tissue collection from both anterior and posterior tongue. Inject 0.5 mL enzyme mixture locally to the anterior tongue for tissue collection from tongue tip or to the posterior tongue for circumvallate papilla tissue collection.

Note: Tongue will swell as enzyme accumulates (Figure $1B_2$). Gentle injection of the enzyme can prevent pressure from damaging epithelium and keep as much enzyme as possible in the tongue.

(5) Wrap the tongue with plastic wrap and incubate the tongue for 30 min at 37 ℃.

(6) Use mini-scissors to dissect the tongue tip and/or circumvallate papilla, and use spatula and fine forceps to transfer tissue to 15 mL fresh sterile Tyrode's solution in a 100-mm culture dish.

(7) Separate epithelium from underlying connective tissue in enzyme-digested sub-epithelial space using mini-scissors. Trim the tissues into a proper size according to the requirement of downstream experiments.

(8) Wash the separated epithelium and underlying connective tissue twice in 15 mL fresh sterile Tyrode's solution in a 100-mm culture dish.

Note: The activities of dispase and collagenase will be inhibited by EDTA in the cell dissociation procedure

5.3.3. Cell dissociation

Note 1: Cell dissociation protocol described here can be applied to tongue epithelium and mesenchyme/connective tissue in both E12.5 embryonic and 8-week-old mice.

Note 2: To reduce the cell loss during agitation and transfer of cell suspension, use commercial low retention pipette tips or pre-coated pipette tips with 2.5% BSA in 0.1 M PBS at pH 7.4 [234].

(1) Transfer the tissues using spatula and fine forceps to 3 mL 0.25% typsin-EDTA in a new 35-mm culture dish for 30-min incubation at 37 °C. Agitate gently the tissues every 5 min with 1 mL pipette tips.

Note: Do not cut the pipette tip, as the cutting edge can physically damage the dissociated cells.

(2) Add 500 µL 5% FBS in DMEM/F12 to stop the reaction and transfer the medium to 5-mL low binding centrifuge tube.

(3) Centrifuge cell suspension at 200 x g for 8 min at room temperature and remove the supernatant.

(4) Re-suspend cells gently in 3 mL of DMEM/F12 containing 10% FBS and 1% BSA using 1 mL pipette tips and filter the cells using a 70-μm cell strainer, followed by a 35-μm cell strainer.

(5) Centrifuge cell suspension at 200 x g for 8 min at room temperature. Remove most of the medium and leave 50-300 μL as final volume to re-suspend cells.

Note: Adjust the concentration of cells according to requirements of downstream experiments by changing the final volume of single cell suspension.

5.3.4 Cell counting and viability test using hemocytometer

Note: To improve measurement accuracy, 3 technical replicates are recommended for each sample.

(1) Gently mix 5-10 μL single cell suspension with an equal volume of Trypan blue and add onto hemocytometer.

Note: Clean the hemocytometer thoroughly using 70% ethanol before use. Dusts particles on the hemocytometer will be stained in dark blue and affect the accuracy of viability test. Check the hemocytometer under a microscope.

(2) Count the total cell number, the number of live cells (white), and the number of dead cells (dark blue) stained by Trypan blue (Figure 5.2, arrows) respectively in 4 squares with 16 grids (Figure 5.2) using inverted microscope with imaging system.

(3) Calculate the cell concentration and viability:

Cell concentration:

$$\frac{\text{Total cell number of all 4 squares}}{4} \times 2\ (\text{diluted factor}) \times 10^4\ \text{cells/mL}$$

Viability:

$$\frac{\text{Number of live cells of 4 squares}}{\text{Total cell number of all 4 squares}} \times 100\%$$

5.4 Representative results

5.4.1 Separation of tongue epithelium from underlying mesenchyme/connective tissue.

In embryonic mouse tongue, a gap in the sub-epithelial space is visible after proper enzyme digestion. Epithelial sheets of some tongues are separated without mechanical force during the incubation.

In adult mouse tongue, a successful enzyme injection is indicated by the swelling in injected areas (Figure 5.1B_2), which suggests that the enzyme can be held by the tongue. Insufficient enzyme and/or deep needle insertion to the mesenchyme and/or tongue epithelial penetration by needle will induce a partial swelling of the injection area or no swelling at all. After enzyme digestion, underlying connective tissues with proper enzyme digestion become loose and sticky. A gap in sub-epithelial space is visible when gently lifting the edge of the epithelial sheet.

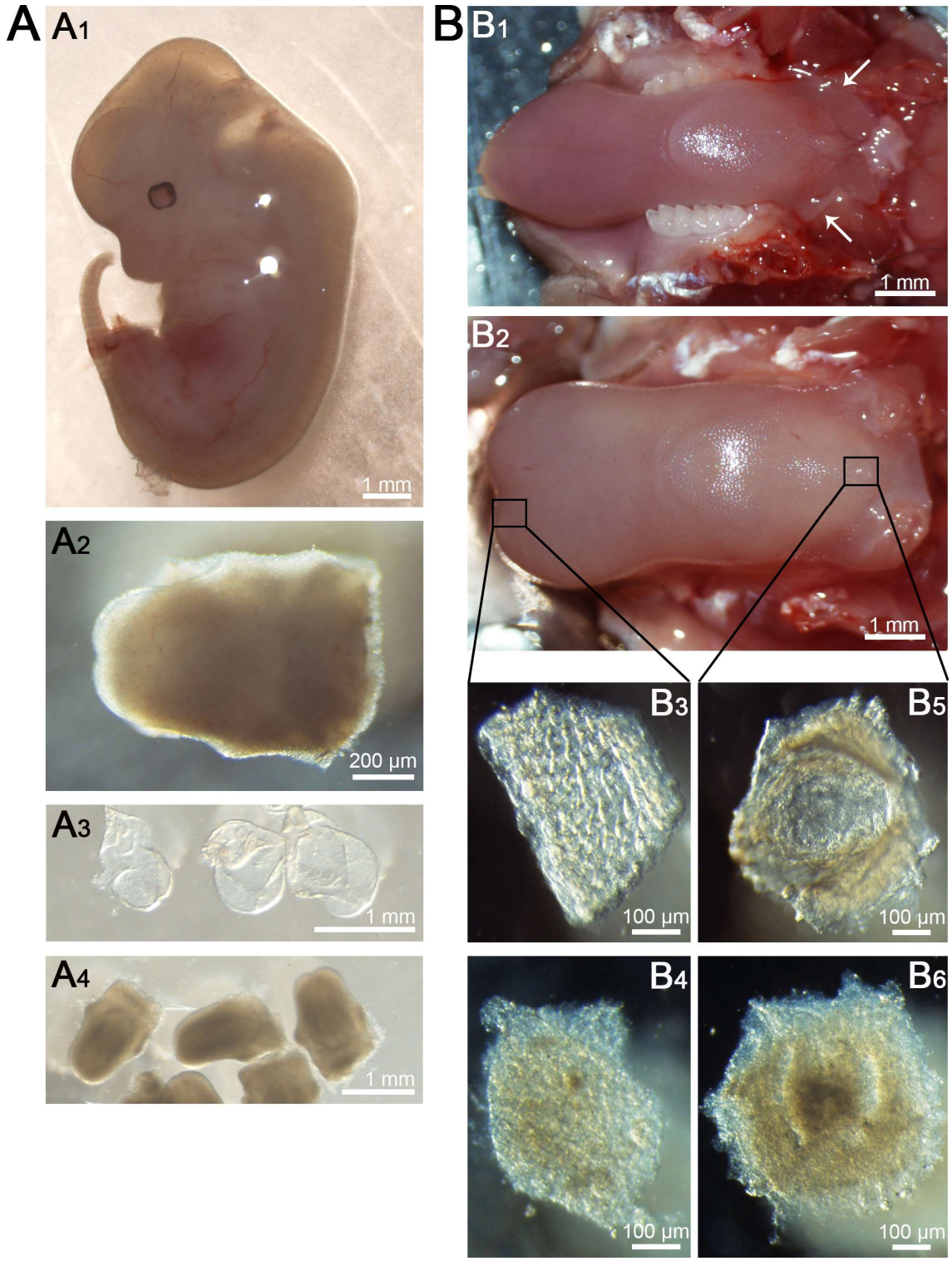

Figure 5.1. Tissue preparation for cell dissociation. **A**: Representative images of an E12.5 whole embryo (A_1), dorsal view of the dissected tongue (A_2), and epithelial sheets (A_3) and mesenchyme (A_4) separated from tongues. **B**: Representative images of an adult

tongue before (B_1) and after enzyme injection (B_2). Dorsal view of an epithelial sheet (B_3) and mesenchyme (B_4) of tongue tip, and an epithelial sheet (B_5) and underlying connective tissue (B_6) of circumvallate papilla. Scale bars: 1 mm in A_1, A_3, A_4, B_1, B_2; 200 μm in A_2; 100 μm in B_3, B_4, B_5, and B_6.

5.4.2 Effect of cell dissociation on total cell number and viability

With 4 E12.5 tongues, the epithelial sheets and thin layers of mesenchyme immediately under the epithelium of tongues were pooled respectively. Manual cell counting using hemocytometer (Figure 5.2) demonstrated that our protocol yielded 63,917 cells in total with the viability of 95.2% from epithelial sheets (around 0.3 mm^2 in size per tongue) (Figure 5.1A_3), and 294,333 cells in total with the viability of 96.3% from mesenchyme (around 0.3 mm^2 in size per tongue) (Figure 5.1A_4).

Using 10 adult tongues at 8 weeks of age, the pieces of the epithelial sheets of the tongue tip (where taste buds are densely distributed), epithelial sheets of circumvallate papillae, and thin layers of connective tissue immediately under the epithelium of circumvallate papillae were pooled respectively. A manual cell count using the hemocytometer (Figure 5.2) demonstrated that our protocol yielded 187,333 cells in total with the viability of 95.4% from epithelial sheets of tongue tip (around 0.075 mm^2 in size per tongue) (Figure 5.1B_3), 544,000 cells in total with the viability of 96.3% from epithelial sheets of circumvallate papillae (around 0.1 mm^2 in size per tongue) (Figure 5.1B_5), and 150,500 cells in total with the viability of 93% from connective tissues (around 0.1 mm^2 in size per tongue) (Figure 5.1B_6).

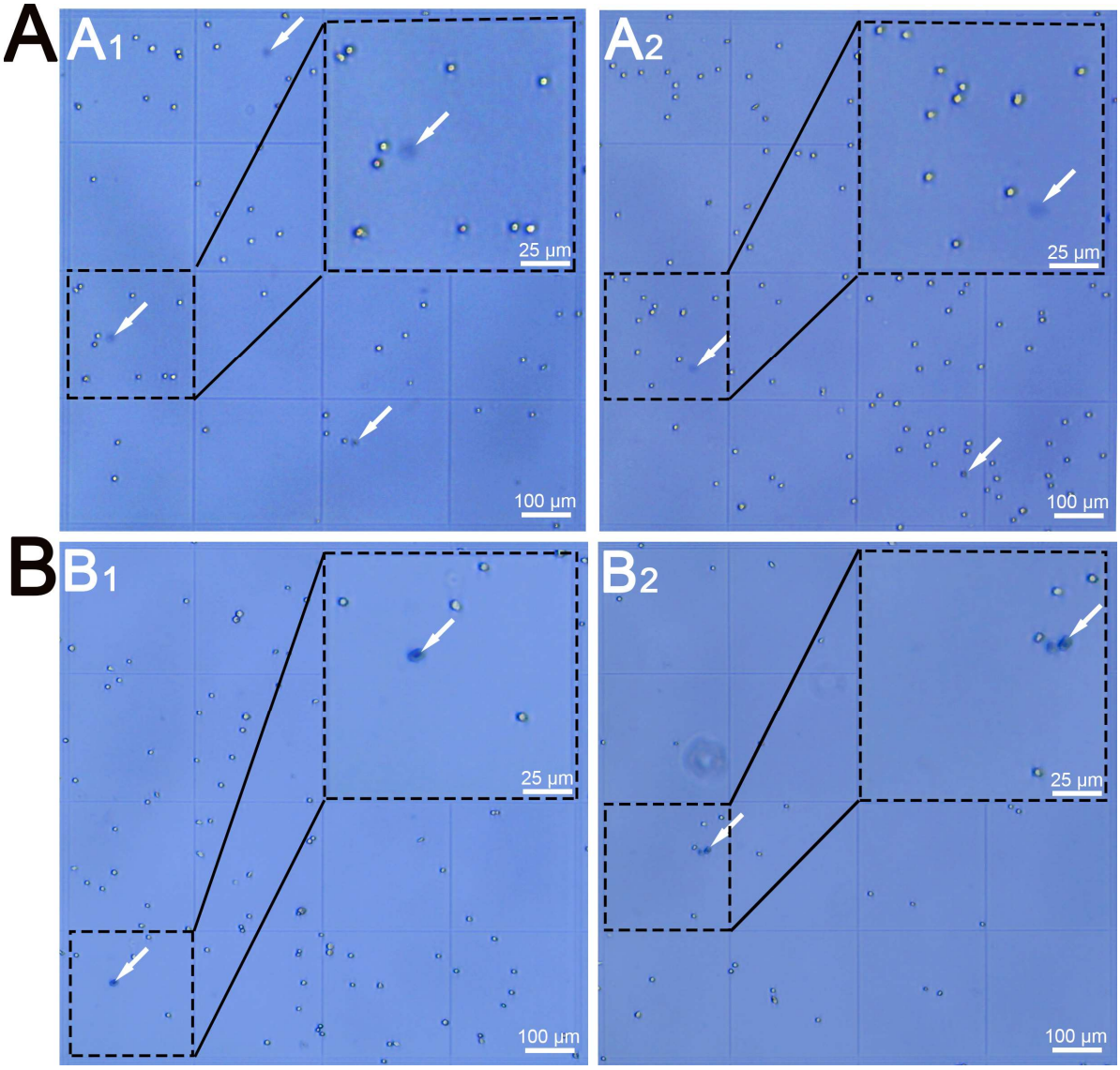

Figure 5.2. Representative images of isolated cells visualized in hemocytometer. **A**: Isolated cells from epithelial sheets (A_1) and mesenchyme (A_2) of embryos at E12.5. **B**: Isolated cells from epithelial sheets (B_1) and underlying connective tissue cores (B_2) of circumvallate papillae at 8 weeks of age. Dash lines encircle the grids amplified in top right corner. Arrows point to dead cells stained by trypan blue. Scale Bars: 100μm for B_1, B_2, B_3, and B_4; 25 μm for high power images in top right corner.

5.5 Discussion

So far there has not been a detailed protocol available for cell dissociation from tongue epithelium and underlying mesenchyme/connective tissue. This current cell dissociation protocol provides a reproducible procedure to generate single cell suspension with a high cell viability (>90%) from mouse tongue tissues, including epithelial sheets and mesenchyme/connective tissues at both embryonic and postnatal stages even though isolated cells from E12.5 and adult are different in size. For example, isolated cells from epithelium and mesenchyme of E12.5 tongue are consistent and small in contrast to a large variability (from small to large) of cells from 8-week-old tongue. With the advantage of the high viability (>90%) of isolated cells, the yielded single cell suspension can facilitate the downstream experiments requiring high quality of viable cells, e.g., single cell RNA sequencing and primary cell cultures.

To guarantee the high viability of cells, careful attention must be paid to several important factors. A proper digestion time with dispase and collagenase mixture can effectively separate epithelium from mesenchyme/underlying connective tissue while preserve the viable cells. A 20-min incubation for embryonic tongue and 30-min incubation for adult tongue are recommended. Even though epithelial sheets can be easily peeled after enzyme digestion, cutting with scissors for the separation is recommended, which may preserve stem cell population in the basal area of the tongue epithelium [6]. The choice of 0.25% Trypsin-EDTA over Trypsin alone is highly recommended for dissociating cells as 0.25% Trypsin-EDTA can dissociate cells more efficiently and keep cells in separation compared to the Trypsin alone. The use of cell culture based medium (DMEM/F12 containing 10% FBS and 1% BSA) to re-suspend cells

after enzymatic digestion is crucial, and contributes to the higher viability of isolated cells compared to cell suspension medium, i.e., 1% BSA in 0.1 M PBS. In addition, isolated cells have a higher survival rate in this medium over time - at least 3 hours without significant decrease of cell viability. Pipetting technique is another critical factor to ensure a high cell viability. Gently aspirating supernatant and re-suspending cells using pipette can reduce extra cell loss and physical damage to cells.

Concentration of isolated cells in a single cell suspension is another important consideration for downstream experiments. In a total given cell number, cell concentration can be adjusted based on the final volume of resuspended solution. For the first trial when total cell number is unknown, resuspension of isolated cells should start at a low volume. Then, isolated cells can be diluted based on the requirements of downstream experiments. Of note, in our culture medium based solution, cellular aggregates were found when the concentration was higher than 4000 cells/μL (around 200 cells per square in hemocytometer). The optimal concentrations range from 500 to 2500 cells/μL.

Acknowledgments:

This study was supported by the National Institutes of Health, grant number R01DC012308 and R21DC018089 to HXL. We give thanks to Brett Marshall (University of Georgia, Athens, GA) and Egon Ranghini (10X GENOMICS, Pleasanton, CA) for technical assistance and consultation regarding the cell dissociation; to Francisca Gibson Burnley (University of Georgia, Athens, GA) for English editing.

CHAPTER 6

CONCLUSION AND FUTURE DIRECTION

Taste bud is an aggregate of epithelial cells that mostly have a short lifespan and undergo continuous turnover [1-5]. Thus, progenitor sources surrounding taste buds are necessary. Lingual taste buds reside in a specialized structure called taste papilla, in which taste bud is surrounded by lingual epithelium, underlying connective tissue core, and minor salivary gland, i.e., von Ebner's gland.

Taste bud-surrounding basal epithelium have been considered as sole progenitor source for taste buds [3, 6, 11, 12, 14, 141]. However, our previous study using various mouse models have suggested a contribution of tissue compartments under the lingual epithelium of taste buds [16, 17]. To better understand the occurrence of taste disorders and development of therapeutic regimen such as stem-cell therapies, a clear understanding of the distribution of progenitor sources for taste buds is necessary. The overall goal of this PhD dissertation was to explore the potential progenitor sources for taste buds under lingual epithelium.

6.1 Sox10-expressing cells are progenitors for taste bud cells

In chapter 2, *in-vitro* and *in-vivo* experiments using a transgenic mouse model were conducted respectively to identify the $Sox10^+$ tissue compartments around taste buds and map the lineage of $Sox10^+$ cells to taste buds. Several points are drawn based on our results:

(1) In addition to the known migrating neural crest, Sox10 mRNA is also expressed in connective tissue and von Ebner's glands.

(2) $Sox10^+$ cells give rise to cells within taste buds in all three types of taste papillae (fungiform, circumvallate, and foliate) as well as in the soft palate in postnatal mice.

(3) $Sox10^+$ cells mainly give rise to type III taste bud cells, less so to type I and II.

(4) The proportion of $Sox10^+$ cells-derived taste bud cells increases from virtually zero at birth to over 35% in adults.

(5) $Sox10^+$ cells-derived taste bud cells represent an unconventional population of taste bud cells with low intensity of immunosignals of Keratin 8 (a widely used taste bud cell marker).

6.2 Neural crest cells are not the progenitors for taste bud cells

In chapter 3, *in-vivo* experiments using three model species were recruited to map the lineage of neural crest and their derivatives to taste buds. Two conclusions were reached based on our observations:

(1) $Sox10^+$ neural crest cells give rise to connective tissue cells in tongue.

(2) Taste buds are not derived from $Sox10^+$ neural crest cells and their derivatives in connective tissue in rodent, birds, and teleost fish.

6.3 Sox10-expressing cells in von Ebner's glands are potential progenitors for taste bud cells

In chapter 4, *in-vivo* experiments using different transgenic mouse models were performed to map the lineage of cells in connective tissue and von Ebner's glands to taste bud cells. Several conclusions are drawn based on our results:

(1) $Sox10^+$ neural crest cells are not the progenitor for von Ebner's glands, but give rise to most, but not all, of the connective tissue cells around circumvallate taste buds in the tongue.

(2) $Plp1^+$ Schwann cells and $Vimentin^+$ stromal cells in connective tissue are not the progenitors for circumvallate taste bud cells

(3) Von Ebner's glands are most likely a progenitor source for circumvallate taste bud cell renewal.

6.4 High quality and quantity of dissociated cells can be generated from tissue compartments in embryonic and adult tongue

In chapter 5, a protocol was developed to dissociate cells from the mouse tongue epithelium and mesenchyme/connective tissue in the early developmental (embryonic day 12.5) and young adult (8-week) stages, which warrants the future studies in tongue at the individual-cell and/or cell-population level (e.g., single cell RNA sequencing and primary cell culture).

(1) 0.25% Trypsin-EDTA is the ideal digestion buffer for cell dissociation from tongue

(2) Centrifugation at 200 x g for 8 min result in a high yield of cells at a high viability rate (>90%)

(3) Dissociated cells can survive in culture cell-based medium for at least 3 hours.

6.5 Future direction

The current findings in this dissertation raise additional important questions which remain to be addressed in future studies:

(1) Taste bud cells derived from $Sox10^{+}$ progenitors display low intensity of immunosignal of Keratin 8, which suggests their characteristics as a subset of unconventional taste bud cells. Transcriptomic analysis such as single cell RNA sequencing will be an efficient method to reveal the category of progenitor cells and identify the specific markers for them, which will benefit from the cell dissociation protocol as shown in chapter 5.

(2) In fungiform taste buds where no salivary glands directly connect to, Sox10 mRNA is solely expressed in connective tissue core. Given that connective tissue cells do not contribute to taste buds, the potential $Sox10^{+}$ progenitor candidates for fungiform taste buds may be some migratory cell types, e.g., immune cells, which deserves detailed studies in the future.

(3) Due to lack of specific marker for von Ebner's glands, our observation in Sox10-iCreER^{T2} model is implicated but not enough to draw a conclusion that von Ebner's glands are progenitor sources for circumvallate taste buds. It will be important to collect solid evidence to demonstrate the contribution of von Ebner's glands to circumvallate taste buds and identify specific cell type(s) of progenitors in von Ebner's glands, for which studies are ongoing using 3D organoid culture.

REFERENCES

1. Beidler, L.M. and R.L. Smallman, *Renewal of cells within taste buds.* Journal of Cell Biology, 1965. **27**(2): p. 263-272.
2. Conger, A.D. and M.A. Wells, *Radiation and aging effect on taste structure and function.* Radiation research, 1969. **37**(1): p. 31-49.
3. Hamamichi, R., M. Asano-Miyoshi, and Y. Emori, *Taste bud contains both short-lived and long-lived cell populations.* Neuroscience, 2006. **141**(4): p. 2129-2138.
4. Cohn, Z.J., et al., *Lipopolysaccharide-induced inflammation attenuates taste progenitor cell proliferation and shortens the life span of taste bud cells.* BMC neuroscience, 2010. **11**(1): p. 1-16.
5. Perea-Martinez, I., T. Nagai, and N. Chaudhari, *Functional cell types in taste buds have distinct longevities.* PloS one, 2013. **8**(1): p. e53399.
6. Okubo, T., C. Clark, and B.L. Hogan, *Cell lineage mapping of taste bud cells and keratinocytes in the mouse tongue and soft palate.* Stem cells, 2009. **27**(2): p. 442-450.
7. Ohmoto, M., et al., *Genetic lineage tracing in taste tissues using Sox2-CreERT2 strain.* Chemical Senses, 2017. **42**(7): p. 547-552.
8. Yee, K.K., et al., *Lgr5-EGFP marks taste bud stem/progenitor cells in posterior tongue.* Stem cells, 2013. **31**(5): p. 992-1000.
9. Takeda, N., et al., *Lgr5 identifies progenitor cells capable of taste bud regeneration after injury.* PLoS One, 2013. **8**(6): p. e66314.

10. Ren, W., et al., *Single Lgr5-or Lgr6-expressing taste stem/progenitor cells generate taste bud cells ex vivo.* Proceedings of the National Academy of Sciences, 2014. **111**(46): p. 16401-16406.
11. Nguyen, H.M. and L.A. Barlow, *Differential expression of a BMP4 reporter allele in anterior fungiform versus posterior circumvallate taste buds of mice.* BMC neuroscience, 2010. **11**(1): p. 1-17.
12. Stone, L.M., et al., *Taste receptor cells arise from local epithelium, not neurogenic ectoderm.* Proceedings of the National Academy of Sciences, 1995. **92**(6): p. 1916-1920.
13. Sullivan, J.M., A.A. Borecki, and S. Oleskevich, *Stem and progenitor cell compartments within adult mouse taste buds.* European Journal of Neuroscience, 2010. **31**(9): p. 1549-1560.
14. Miura, H. and L.A. Barlow, *Taste bud regeneration and the search for taste progenitor cells.* Archives italiennes de biologie, 2010. **148**(2): p. 107.
15. Yu, W., et al., *SOX10-Cre-Labeled cells under the tongue epithelium serve as progenitors for taste bud cells that are mainly type III and Keratin 8-low.* Stem cells and development, 2020. **29**(10): p. 638-647.
16. Boggs, K., et al., *Contribution of underlying connective tissue cells to taste buds in mouse tongue and soft palate.* PLoS One, 2016. **11**(1): p. e0146475.
17. Liu, H.-X., et al., *Neural crest contribution to lingual mesenchyme, epithelium and developing taste papillae and taste buds.* Developmental biology, 2012. **368**(2): p. 294-303.

18. Kramer, N., et al., *Early taste buds are from Shh+ epithelial cells of tongue primordium in distinction from mature taste bud cells which arise from surrounding tissue compartments.* Biochemical and biophysical research communications, 2019. **515**(1): p. 149-155.
19. Cobourne, M.T., et al. *How to make a tongue: Cellular and molecular regulation of muscle and connective tissue formation during mammalian tongue development*. in *Seminars in cell & developmental biology*. 2019. Elsevier.
20. Doty, R.L., *Handbook of olfaction and gustation*. 2015: John Wiley & Sons.
21. Farbman, A.I., *Electron microscope study of the developing taste bud in rat fungiform papilla.* Developmental biology, 1965. **11**(1): p. 110-135.
22. Pumplin, D.W., C. Yu, and D.V. Smith, *Light and dark cells of rat vallate taste buds are morphologically distinct cell types.* Journal of Comparative Neurology, 1997. **378**(3): p. 389-410.
23. Barlow, L.A. and O.D. Klein, *Developing and regenerating a sense of taste.* Current topics in developmental biology, 2015. **111**: p. 401-419.
24. Bartel, D.L., et al., *Nucleoside triphosphate diphosphohydrolase‐2 is the ecto‐ATPase of type I cells in taste buds.* Journal of Comparative Neurology, 2006. **497**(1): p. 1-12.
25. Miura, H., et al., *Sonic hedgehog–expressing basal cells are general post‐mitotic precursors of functional taste receptor cells.* Developmental Dynamics, 2014. **243**(10): p. 1286-1297.
26. Lawton, D.M., et al., *Localization of the glutamate–aspartate transporter, GLAST, in rat taste buds.* European Journal of Neuroscience, 2000. **12**(9): p. 3163-3171.

27. AhPin, P., et al., *Prenatal development and innervation of the circumvallate papilla in the mouse.* Journal of anatomy, 1989. **162**: p. 33.

28. Jitpukdeebodintra, S., Y. Chai, and M.L. Snead, *Developmental patterning of the circumvallate papilla.* International Journal of Developmental Biology, 2003. **46**(5): p. 755-763.

29. Mistretta, C.M. and H.-X. Liu, *Development of fungiform papillae: patterned lingual gustatory organs.* Archives of histology and cytology, 2006. **69**(4): p. 199-208.

30. Jung, H.-S., V. Oropeza, and I. Thesleff, *Shh, Bmp-2, Bmp-4 and Fgf-8 are associated with initiation and patterning of mouse tongue papillae.* Mechanisms of development, 1999. **81**(1-2): p. 179-182.

31. Harada, S., et al., *Maturation of taste buds on the soft palate of the postnatal rat.* Physiology & behavior, 2000. **68**(3): p. 333-339.

32. Hall, J.M., J.E. Hooper, and T.E. Finger, *Expression of sonic hedgehog, patched, and Gli1 in developing taste papillae of the mouse.* Journal of Comparative Neurology, 1999. **406**(2): p. 143-155.

33. Heussler, H. and M. Suri, *Sonic hedgehog.* Molecular Pathology, 2003. **56**(3): p. 129.

34. Thirumangalathu, S., et al., *Fate mapping of mammalian embryonic taste bud progenitors.* Development, 2009. **136**(9): p. 1519-1528.

35. Ohtubo, Y., M. Iwamoto, and K. Yoshii, *Subtype‐dependent postnatal development of taste receptor cells in mouse fungiform taste buds.* European Journal of Neuroscience, 2012. **35**(11): p. 1661-1671.

36. Nelson, W.G. and T.-T. Sun, *The 50-and 58-kdalton keratin classes as molecular markers for stratified squamous epithelia: cell culture studies.* The Journal of cell biology, 1983. **97**(1): p. 244-251.

37. Zhang, S., et al., *FGF10 is required for circumvallate papilla morphogenesis by maintaining Lgr5 activity.* Frontiers in physiology, 2018. **9**: p. 1192.

38. Suzuki, Y., *Expression of Sox2 in mouse taste buds and its relation to innervation.* Cell and tissue research, 2008. **332**(3): p. 393-401.

39. Nakayama, A., et al., *During development intense Sox2 expression marks not only Prox1-expressing taste bud cell but also perigemmal cell lineages.* Cell and tissue research, 2015. **359**(3): p. 743-753.

40. Okubo, T., L.H. Pevny, and B.L. Hogan, *Sox2 is required for development of taste bud sensory cells.* Genes & development, 2006. **20**(19): p. 2654-2659.

41. Hall, J.M., M.L. Bell, and T.E. Finger, *Disruption of sonic hedgehog signaling alters growth and patterning of lingual taste papillae.* Developmental biology, 2003. **255**(2): p. 263-277.

42. Liu, H.-X., et al., *Sonic hedgehog exerts distinct, stage-specific effects on tongue and taste papilla development.* Developmental biology, 2004. **276**(2): p. 280-300.

43. Eaton, S.L., et al., *Total protein analysis as a reliable loading control for quantitative fluorescent Western blotting.* PloS one, 2013. **8**(8): p. e72457.

44. Yu, W., et al., *Taste buds are not derived from neural crest in mouse, chicken, and zebrafish.* Developmental biology, 2021. **471**: p. 76-88.

45. Zhang, G.-H., et al., *Developmental change of α-gustducin expression in the mouse fungiform papilla.* Anatomy and embryology, 2006. **211**(6): p. 625-630.

46. Hendricks, S.J., P.C. Brunjes, and D.L. Hill, *Taste bud cell dynamics during normal and sodium-restricted development.* Journal of Comparative Neurology, 2004. **472**(2): p. 173-182.

47. Hosley, M.A. and B. Oakley, *Postnatal development of the vallate papilla and taste buds in rats.* The Anatomical Record, 1987. **218**(2): p. 216-222.

48. Murray, R., *The ultrastructure of taste buds.* The ultrastructure of sensory organs, 1973: p. 1-81.

49. Delay, R.J., S.D. Roper, and J.C. Kinnamon, *Ultrastructure of mouse vallate taste buds: II. Cell types and cell lineage.* Journal of Comparative Neurology, 1986. **253**(2): p. 242-252.

50. FINGER, T.E., *Cell biology of taste epithelium.* The neurobiology of taste and smell, 2000.

51. El-Sharaby, A., et al., *Development and maturation of taste buds of the palatal epithelium of the rat: histological and immunohistochemical study.* The Anatomical Record: An Official Publication of the American Association of Anatomists, 2001. **263**(3): p. 260-268.

52. El-Sharaby, A., K. Ueda, and S. Wakisaka, *Differentiation of the lingual and palatal gustatory epithelium of the rat as revealed by immunohistochemistry of α-gustducin.* Archives of histology and cytology, 2001. **64**(4): p. 401-409.

53. Ma, H., et al., *Qualitative and quantitative differences between taste buds of the rat and mouse.* BMC neuroscience, 2007. **8**(1): p. 1-13.

54. Ohtubo, Y. and K. Yoshii, *Quantitative analysis of taste bud cell numbers in fungiform and soft palate taste buds of mice.* Brain research, 2011. **1367**: p. 13-21.

55. Vandenbeuch, A., et al., *Role of the ectonucleotidase NTPDase2 in taste bud function.* Proceedings of the National Academy of Sciences, 2013. **110**(36): p. 14789-14794.

56. Thirumangalathu, S. and L.A. Barlow, *β-Catenin signaling regulates temporally discrete phases of anterior taste bud development.* Development, 2015. **142**(24): p. 4309-4317.

57. Kitagawa, M., et al., *Molecular genetic identification of a candidate receptor gene for sweet taste.* Biochemical and biophysical research communications, 2001. **283**(1): p. 236-242.

58. Montmayeur, J.-P., et al., *A candidate taste receptor gene near a sweet taste locus.* Nature neuroscience, 2001. **4**(5): p. 492-498.

59. Max, M., et al., *Tas1r3, encoding a new candidate taste receptor, is allelic to the sweet responsiveness locus Sac.* Nature genetics, 2001. **28**(1): p. 58-63.

60. Nelson, G., et al., *Mammalian sweet taste receptors.* Cell, 2001. **106**(3): p. 381-390.

61. Bachmanov, A.A., et al., *Positional cloning of the mouse saccharin preference (Sac) locus.* Chemical senses, 2001. **26**(7): p. 925-933.

62. Chandrashekar, J., et al., *The receptors and cells for mammalian taste.* Nature, 2006. **444**(7117): p. 288-294.

63. Miyoshi, M.A., K. Abe, and Y. Emori, *IP3 receptor type 3 and PLCβ2 are co-expressed with taste receptors T1R and T2R in rat taste bud cells.* Chemical senses, 2001. **26**(3): p. 259-265.

64. Ota, M.S., et al., *Combined in silico and in vivo analyses reveal role of Hes1 in taste cell differentiation.* PLoS Genet, 2009. **5**(4): p. e1000443.

65. Boughter Jr, J.D., et al., *Differential expression of α-gustducin in taste bud populations of the rat and hamster.* Journal of Neuroscience, 1997. **17**(8): p. 2852-2858.

66. Yang, R., et al., *Ultrastructural localization of gustducin immunoreactivity in microvilli of type II taste cells in the rat.* Journal of Comparative Neurology, 2000. **425**(1): p. 139-151.

67. Pérez, C.A., et al., *A transient receptor potential channel expressed in taste receptor cells.* Nature neuroscience, 2002. **5**(11): p. 1169-1176.

68. Zhang, Z., et al., *The transduction channel TRPM5 is gated by intracellular calcium in taste cells.* Journal of Neuroscience, 2007. **27**(21): p. 5777-5786.

69. Huang, T., L. Ma, and R.F. Krimm, *Postnatal reduction of BDNF regulates the developmental remodeling of taste bud innervation.* Developmental biology, 2015. **405**(2): p. 225-236.

70. Roper, S.D. and N. Chaudhari, *Taste buds: cells, signals and synapses.* Nature Reviews Neuroscience, 2017. **18**(8): p. 485-497.

71. Murray, R.G., *Cellular relations in mouse circumvallate taste buds.* Microscopy research and technique, 1993. **26**(3): p. 209-224.

72. Murray, R.G., A. Murray, and S. Fujimoto, *Fine structure of gustatory cells in rabbit taste buds.* Journal of ultrastructure research, 1969. **27**(5-6): p. 444-461.

73. LopezJimenez, N.D., et al., *Two members of the TRPP family of ion channels, Pkd1l3 and Pkd2l1, are co-expressed in a subset of taste receptor cells.* Journal of neurochemistry, 2006. **98**(1): p. 68-77.

74. Huang, A.L., et al., *The cells and logic for mammalian sour taste detection.* Nature, 2006. **442**(7105): p. 934-938.

75. Ishimaru, Y., et al., *Transient receptor potential family members PKD1L3 and PKD2L1 form a candidate sour taste receptor.* Proceedings of the National Academy of Sciences, 2006. **103**(33): p. 12569-12574.

76. Horio, N., et al., *Sour taste responses in mice lacking PKD channels.* PloS one, 2011. **6**(5): p. e20007.

77. Lewandowski, B.C., et al., *Amiloride-insensitive salt taste is mediated by two populations of type III taste cells with distinct transduction mechanisms.* Journal of Neuroscience, 2016. **36**(6): p. 1942-1953.

78. Tomchik, S.M., et al., *Breadth of tuning and taste coding in mammalian taste buds.* Journal of Neuroscience, 2007. **27**(40): p. 10840-10848.

79. Murray, R., *The mammalian taste bud type III cell: a critical analysis.* Journal of ultrastructure and molecular structure research, 1986. **95**(1-3): p. 175-188.

80. Yang, R., et al., *Taste cells with synapses in rat circumvallate papillae display SNAP-25-like immunoreactivity.* Journal of Comparative Neurology, 2000. **424**(2): p. 205-215.

81. Yang, R., C.L. Stoick, and J.C. Kinnamon, *Synaptobrevin-2-like immunoreactivity is associated with vesicles at synapses in rat circumvallate taste buds.* Journal of Comparative Neurology, 2004. **471**(1): p. 59-71.

82. Clapp, T.R., et al., *Mouse taste cells with G protein-coupled taste receptors lack voltage-gated calcium channels and SNAP-25.* BMC biology, 2006. **4**(1): p. 1-9.

83. Lossow, K., et al., *Genetic labeling of Car4-expressing cells reveals subpopulations of type III taste cells.* Chemical senses, 2017. **42**(9): p. 747-758.

84. DeFazio, R.A., et al., *Separate populations of receptor cells and presynaptic cells in mouse taste buds.* Journal of Neuroscience, 2006. **26**(15): p. 3971-3980.

85. Nelson, G.M. and T.E. Finger, *Immunolocalization of different forms of neural cell adhesion molecule (NCAM) in rat taste buds.* Journal of Comparative Neurology, 1993. **336**(4): p. 507-516.

86. Kataoka, S., et al., *The candidate sour taste receptor, PKD2L1, is expressed by type III taste cells in the mouse.* Chemical senses, 2008. **33**(3): p. 243-254.

87. Huang, Y.-J., et al., *The role of pannexin 1 hemichannels in ATP release and cell–cell communication in mouse taste buds.* Proceedings of the National Academy of Sciences, 2007. **104**(15): p. 6436-6441.

88. Huang, Y.-J., et al., *Mouse taste buds use serotonin as a neurotransmitter.* Journal of Neuroscience, 2005. **25**(4): p. 843-847.

89. Miura, H., et al., *A strong nerve dependence of sonic hedgehog expression in basal cells in mouse taste bud and an autonomous transcriptional control of genes in differentiated taste cells.* Chemical senses, 2004. **29**(9): p. 823-831.

90. Miura, H., et al., *Temporal changes in NCAM immunoreactivity during taste cell differentiation and cell lineage relationships in taste buds.* Chemical senses, 2005. **30**(4): p. 367-375.

91. Miura, H., et al., *Shh and Ptc are associated with taste bud maintenance in the adult mouse.* Mechanisms of development, 2001. **106**(1-2): p. 143-145.

92. Miura, H., et al., *Co-expression pattern of Shh with Prox1 and that of Nkx2. 2 with Mash1 in mouse taste bud.* Gene expression patterns, 2003. **3**(4): p. 427-430.

93. Kusakabe, Y., et al., *The neural differentiation gene Mash-1 has a distinct pattern of expression from the taste reception-related genes gustducin and T1R2 in the taste buds.* Chemical senses, 2002. **27**(5): p. 445-451.

94. Miura, H., Y. Kusakabe, and S. Harada, *Cell lineage and differentiation in taste buds.* Archives of histology and cytology, 2006. **69**(4): p. 209-225.

95. Farbman, A., *Renewal of taste bud cells in rat circumvallate papillae.* Cell Proliferation, 1980. **13**(4): p. 349-357.

96. Olivieri-Sangiacomo, C., *Ultrastructural aspects of the basal zone in the taste bud.* Experientia, 1972. **28**(7): p. 825-826.

97. Johnson, J.E., S.J. Birren, and D.J. Anderson, *Two rat homologues of Drosophila achaete-scute specifically expressed in neuronal precursors.* Nature, 1990. **346**(6287): p. 858-861.

98. Guillemot, F., et al., *Mammalian achaete-scute homolog 1 is required for the early development of olfactory and autonomic neurons.* Cell, 1993. **75**(3): p. 463-476.

99. Tomita, K., et al., *Mash1 promotes neuronal differentiation in the retina.* Genes to Cells, 1996. **1**(8): p. 765-774.

100. Seta, Y., et al., *The bHLH transcription factors, Hes6 and Mash1, are expressed in distinct subsets of cells within adult mouse taste buds.* Archives of histology and cytology, 2006. **69**(3): p. 189-198.

101. Takagi, H., et al., *Mash1-expressing cells could differentiate to type III cells in adult mouse taste buds.* Anatomical science international, 2018. **93**(4): p. 422-429.

102. Lee, J., et al., *Gli1 is a target of Sonic hedgehog that induces ventral neural tube development.* Development, 1997. **124**(13): p. 2537-2552.

103. Shi, Y., et al., *Gli1 identifies osteogenic progenitors for bone formation and fracture repair.* Nature Communications, 2017. **8**(1): p. 1-12.

104. Liu, H.X., et al., *Multiple Shh signaling centers participate in fungiform papilla and taste bud formation and maintenance.* Developmental biology, 2013. **382**(1): p. 82-97.

105. Brewer, S., et al., *Wnt1-Cre-mediated deletion of AP-2α causes multiple neural crest-related defects.* Developmental biology, 2004. **267**(1): p. 135-152.

106. Chai, Y., et al., *Fate of the mammalian cranial neural crest during tooth and mandibular morphogenesis.* Development, 2000. **127**(8): p. 1671-1679.

107. Ito, Y., et al., *Conditional inactivation of Tgfbr2 in cranial neural crest causes cleft palate and calvaria defects.* Development, 2003. **130**(21): p. 5269-5280.

108. Jiang, X., et al., *Tissue origins and interactions in the mammalian skull vault.* Developmental biology, 2002. **241**(1): p. 106-116.

109. Katayama, K.-i., et al., *Loss of RhoA in neural progenitor cells causes the disruption of adherens junctions and hyperproliferation.* Proceedings of the National Academy of Sciences, 2011. **108**(18): p. 7607-7612.

110. Merrill, A.E., et al., *Cell mixing at a neural crest-mesoderm boundary and deficient ephrin-Eph signaling in the pathogenesis of craniosynostosis.* Human molecular genetics, 2006. **15**(8): p. 1319-1328.

111. Tallquist, M.D. and P. Soriano, *Cell autonomous requirement for PDGFRα in populations of cranial and cardiac neural crest cells.* Development, 2003. **130**(3): p. 507-518.

112. Yoshida, T., et al., *Cell lineage in mammalian craniofacial mesenchyme.* Mechanisms of development, 2008. **125**(9-10): p. 797-808.

113. Chen, G., et al., *S pecific and spatial labeling of P0‐Cre versus Wnt1‐Cre in cranial neural crest in early mouse embryos.* genesis, 2017. **55**(6): p. e23034.

114. Yamauchi, Y., et al., *A novel transgenic technique that allows specific marking of the neural crest cell lineage in mice.* Developmental biology, 1999. **212**(1): p. 191-203.

115. Kawakami, M., et al., *Novel migrating mouse neural crest cell assay system utilizing P0-Cre/EGFP fluorescent time-lapse imaging.* BMC Developmental Biology, 2011. **11**(1): p. 1-17.

116. Cornett, B., et al., *Wntless is required for peripheral lung differentiation and pulmonary vascular development.* Developmental biology, 2013. **379**(1): p. 38-52.

117. Geske, M.J., et al., *Fgf9 signaling regulates small intestinal elongation and mesenchymal development.* Development, 2008. **135**(17): p. 2959-2968.

118. Lavine, K.J., et al., *Hedgehog signaling to distinct cell types differentially regulates coronary artery and vein development.* Development, 2008. **135**(18): p. 3161-3171.

119. Lin, C., et al., *Tissue-specific requirements of β-catenin in external genitalia development.* Development, 2008. **135**(16): p. 2815-2825.

120. Yin, Y., et al., *An FGF–WNT gene regulatory network controls lung mesenchyme development.* Developmental biology, 2008. **319**(2): p. 426-436.

121. Yu, K., et al., *Conditional inactivation of FGF receptor 2 reveals an essential role for FGF signaling in the regulation of osteoblast function and bone growth.* Development, 2003. **130**(13): p. 3063-3074.

122. Li, L., P. Cserjesi, and E.N. Olson, *Dermo-1: a novel twist-related bHLH protein expressed in the developing dermis.* Developmental biology, 1995. **172**(1): p. 280-292.

123. O'Rahilly, R. and F. Müller, *The development of the neural crest in the human.* Journal of anatomy, 2007. **211**(3): p. 335-351.

124. Debbache, J., V. Parfejevs, and L. Sommer, *Cre‐driver lines used for genetic fate mapping of neural crest cells in the mouse: An overview.* genesis, 2018. **56**(6-7): p. e23105.

125. Lewis, A.E., et al., *The widely used Wnt1-Cre transgene causes developmental phenotypes by ectopic activation of Wnt signaling.* Developmental biology, 2013. **379**(2): p. 229-234.

126. Robinson-Bennett, B. and A. Han, *Role of Immunohistochemistry in Elucidating Lung Cancer Metastatic to the Ovary from Primary Ovarian Carcinoma*, in *Handbook of Immunohistochemistry and in Situ Hybridization of Human Carcinomas*. 2006, Elsevier. p. 537-545.

127. Troeger, J.S., et al., *Deactivation of hepatic stellate cells during liver fibrosis resolution in mice.* Gastroenterology, 2012. **143**(4): p. 1073-1083. e22.

128. Southard-Smith, E.M., L. Kos, and W.J. Pavan, *Sox10 mutation disrupts neural crest development in Dom Hirschsprung mouse model.* Nature genetics, 1998. **18**(1): p. 60-64.

129. Kuhlbrodt, K., et al., *Sox10, a novel transcriptional modulator in glial cells.* Journal of Neuroscience, 1998. **18**(1): p. 237-250.

130. Bremer, M., et al., *Sox10 is required for Schwann‐cell homeostasis and myelin maintenance in the adult peripheral nerve.* Glia, 2011. **59**(7): p. 1022-1032.

131. Shakhova, O., et al., *Sox10 promotes the formation and maintenance of giant congenital naevi and melanoma.* Nature cell biology, 2012. **14**(8): p. 882-890.

132. Chen, Z., et al., *FGF signaling activates a Sox9-Sox10 pathway for the formation and branching morphogenesis of mouse ocular glands.* Development, 2014. **141**(13): p. 2691-2701.

133. Athwal, H.K., et al., *Sox10 regulates plasticity of epithelial progenitors toward secretory units of exocrine glands.* Stem cell reports, 2019. **12**(2): p. 366-380.

134. Lombaert, I.M., et al., *Combined KIT and FGFR2b signaling regulates epithelial progenitor expansion during organogenesis.* Stem cell reports, 2013. **1**(6): p. 604-619.

135. Piludu, M., et al., *Salivary histatins in human deep posterior lingual glands (of von Ebner).* Archives of oral biology, 2006. **51**(11): p. 967-973.

136. Riva, A., M.S. Lantini, and F.T. Riva, *Normal human salivary glands*, in *Ultrastructure of the extraparietal glands of the digestive tract*. 1990, Springer. p. 53-74.

137. Kist, R., et al., *The formation of endoderm-derived taste sensory organs requires a Pax9-dependent expansion of embryonic taste bud progenitor cells.* PLoS Genet, 2014. **10**(10): p. e1004709.

138. Rothova, M., et al., *Lineage tracing of the endoderm during oral development.* Developmental Dynamics, 2012. **241**(7): p. 1183-1191.

139. Sbarbati, A., C. Crescimanno, and F. Osculati, *The anatomy and functional role of the circumvallate papilla/von Ebner gland complex.* Medical hypotheses, 1999. **53**(1): p. 40-44.

140. Zalewski, A.A., *The neural induction of taste buds in the salivary ducts of the lingual gland of von Ebner.* Experimental neurology, 1976. **52**(3): p. 565-580.

141. Hirota, M., et al., *Expression of cyclin-dependent kinase inhibitors in taste buds of mouse and hamster.* Tissue and Cell, 2001. **33**(1): p. 25-32.

142. Beidler, L.M. and R.L. Smallman, *Renewal of cells within taste buds.* The Journal of cell biology, 1965. **27**(2): p. 263-272.

143. Cohn, Z.J., et al., *Lipopolysaccharide-induced inflammation attenuates taste progenitor cell proliferation and shortens the life span of taste bud cells.* BMC neuroscience, 2010. **11**(1): p. 72.

144. Nguyen, H.M. and L.A. Barlow, *Differential expression of a BMP4 reporter allele in anterior fungiform versus posterior circumvallate taste buds of mice.* BMC neuroscience, 2010. **11**(1): p. 129.

145. Southard-Smith, E.M., L. Kos, and W.J. Pavan, *Sox10 mutation disrupts neural crest development in Dom Hirschsprung mouse model.* Nature genetics, 1998. **18**(1): p. 60.

146. Shakhova, O., et al., *Sox10 promotes the formation and maintenance of giant congenital naevi and melanoma.* Nature cell biology, 2012. **14**(8): p. 882.

147. Hari, L., et al., *Temporal control of neural crest lineage generation by Wnt/β-catenin signaling.* Development, 2012. **139**(12): p. 2107-2117.

148. Matsuoka, T., et al., *Neural crest origins of the neck and shoulder.* Nature, 2005. **436**(7049): p. 347.

149. Mbiene, J.P. and J.D. Roberts, *Distribution of keratin 8‐containing cell clusters in mouse embryonic tongue: evidence for a prepattern for taste bud development.* Journal of Comparative Neurology, 2003. **457**(2): p. 111-122.

150. Rakowiecki, S. and D.J. Epstein, *Divergent roles for Wnt/β-catenin signaling in epithelial maintenance and breakdown during semicircular canal formation.* Development, 2013. **140**(8): p. 1730-1739.

151. Krimm, R.F. and D.L. Hill, *Quantitative Relationships between Taste Bud Development and Gustatory Ganglion Cells a.* Annals of the New York Academy of Sciences, 1998. **855**(1): p. 70-75.

152. Harada, S. and N. Kanemaru, *Developmental changes of the taste sensation depending on the maturation of the taste bud and its distribution in mammals.* Chemical senses, 2005. **30**(suppl_1): p. i56-i57.

153. Iwatsuki, K., et al., *Wnt signaling interacts with Shh to regulate taste papilla development.* Proceedings of the National Academy of Sciences, 2007. **104**(7): p. 2253-2258.

154. Le Douarin, N.M. and M.-A. Teillet, *The migration of neural crest cells to the wall of the digestive tract in avian embryo.* Development, 1973. **30**(1): p. 31-48.

155. Burns, A.J. and N.M. Le Douarin, *The sacral neural crest contributes neurons and glia to the post-umbilical gut: spatiotemporal analysis of the development of the enteric nervous system.* Development, 1998. **125**(21): p. 4335-4347.

156. Hagedorn, L., U. Suter, and L. Sommer, *P0 and PMP22 mark a multipotent neural crest-derived cell type that displays community effects in response to TGF-beta family factors.* Development, 1999. **126**(17): p. 3781-3794.

157. Bixby, S., et al., *Cell-intrinsic differences between stem cells from different regions of the peripheral nervous system regulate the generation of neural diversity.* Neuron, 2002. **35**(4): p. 643-656.

158. Nagoshi, N., et al., *Ontogeny and multipotency of neural crest-derived stem cells in mouse bone marrow, dorsal root ganglia, and whisker pad.* Cell stem cell, 2008. **2**(4): p. 392-403.

159. Touraine, R.L., et al., *Neurological phenotype in Waardenburg syndrome type 4 correlates with novel SOX10 truncating mutations and expression in developing brain.* The American Journal of Human Genetics, 2000. **66**(5): p. 1496-1503.

160. Cheng, Y.-C., et al., *Chick sox10, a transcription factor expressed in both early neural crest cells and central nervous system.* Developmental Brain Research, 2000. **121**(2): p. 233-241.

161. Inoue, K., Y. Tanabe, and J.R. Lupski, *Myelin deficiencies in both the central and the peripheral nervous systems associated with a SOX10 mutation.* Annals of Neurology: Official Journal of the American Neurological Association and the Child Neurology Society, 1999. **46**(3): p. 313-318.

162. Stolt, C.C., et al., *Terminal differentiation of myelin-forming oligodendrocytes depends on the transcription factor Sox10.* Genes & development, 2002. **16**(2): p. 165-170.

163. Knapp, L., et al., *Keratins as markers of differentiated taste cells of the rat.* Differentiation, 1995. **58**(5): p. 341-349.

164. Herrmann, H., et al., *Intermediate filaments: from cell architecture to nanomechanics.* Nature reviews Molecular cell biology, 2007. **8**(7): p. 562.

165. Chang, L. and R.D. Goldman, *Intermediate filaments mediate cytoskeletal crosstalk.* Nature reviews Molecular cell biology, 2004. **5**(8): p. 601.

166. Traub, P., *Intermediate filaments: a review*. 2012: Springer Science & Business Media.

167. Lodish, H., et al., *Molecular cell biology 4th edition.* National Center for Biotechnology Information, Bookshelf, 2000.

168. TAKEDA, M., N. OBARA, and Y. SUZUKI, *Intermediate filaments in mouse taste bud cells.* Archives of histology and cytology, 1988. **51**(1): p. 99-108.

169. Barlow, L.A. and O.D. Klein, *Developing and regenerating a sense of taste*, in *Current topics in developmental biology*. 2015, Elsevier. p. 401-419.

170. Vega-Lopez, G.A., S. Cerrizuela, and M.J. Aybar, *Trunk neural crest cells: formation, migration and beyond.* International Journal of Developmental Biology, 2017. **61**(1-2): p. 5-15.

171. Morrison, S.J., et al., *Prospective identification, isolation by flow cytometry, and in vivo self-renewal of multipotent mammalian neural crest stem cells.* Cell, 1999. **96**(5): p. 737-749.

172. Douarin, N.L., et al., *Glial cell lineages in the neural crest.* Glia, 1991. **4**(2): p. 175-184.

173. Sommer, L., *Specification of Neural Crest-and Placode-Derived Neurons.* Patterning and Cell Type Specification in the Developing CNS and PNS: Comprehensive Developmental Neuroscience, 2013. **1**: p. 385.

174. Weston, J.A., *A radioautographic analysis of the migration and localization of trunk neural crest cells in the chick.* Developmental biology, 1963. **6**(3): p. 279-310.

175. Le Douarin, N.M. and M.-A.M. Teillet, *Experimental analysis of the migration and differentiation of neuroblasts of the autonomic nervous system and of neurectodermal mesenchymal derivatives, using a biological cell marking technique.* Developmental biology, 1974. **41**(1): p. 162-184.

176. Schweizer, G., C. Ayer-Le Lièvre, and N.M. Le Douarin, *Restrictions of developmental capacities in the dorsal root ganglia during the course of development.* Cell differentiation, 1983. **13**(3): p. 191-200.

177. Ladher, R.K., P. O'Neill, and J. Begbie, *From shared lineage to distinct functions: the development of the inner ear and epibranchial placodes.* Development, 2010. **137**(11): p. 1777-1785.

178. Begbie, J., et al., *Induction of the epibranchial placodes.* Development, 1999. **126**(5): p. 895-902.

179. Webb, J.F. and D.M. Noden, *Ectodermal placodes contributions to the development of the vertebrate head.* American Zoologist, 1993. **33**(4): p. 434-447.

180. Baker, C.V. and M. Bronner-Fraser, *Vertebrate cranial placodes I. Embryonic induction.* Developmental biology, 2001. **232**(1): p. 1-61.

181. Schlosser, G., *Evolutionary origins of vertebrate placodes: insights from developmental studies and from comparisons with other deuterostomes.* Journal of Experimental Zoology Part B: Molecular and Developmental Evolution, 2005. **304**(4): p. 347-399.

182. Streit, A., *Early development of the cranial sensory nervous system: from a common field to individual placodes.* Developmental biology, 2004. **276**(1): p. 1-15.

183. Barlow, L.A. and R.G. Northcutt, *Embryonic origin of amphibian taste buds.* Developmental biology, 1995. **169**(1): p. 273-285.

184. Yu, W., et al., *SOX10-Cre-Labeled Cells Under the Tongue Epithelium Serve as Progenitors for Taste Bud Cells That Are Mainly Type III and Keratin 8-Low.* Stem Cells and Development, 2020.

185. Boggs, K., et al., *Contribution of underlying connective tissue cells to taste buds in mouse tongue and soft palate.* PloS one, 2016. **11**(1).

186. Wang, S.-K., Y. Komatsu, and Y. Mishina, *Potential contribution of neural crest cells to dental enamel formation.* Biochemical and biophysical research communications, 2011. **415**(1): p. 114-119.

187. Suzuki, J., et al., *Neural crest-derived horizontal basal cells as tissue stem cells in the adult olfactory epithelium.* Neuroscience Research, 2013. **75**(2): p. 112-120.

188. Katoh, H., et al., *The dual origin of the peripheral olfactory system: placode and neural crest.* Molecular brain, 2011. **4**(1): p. 1-16.

189. McKenzie, I.A., et al., *Motor skill learning requires active central myelination.* science, 2014. **346**(6207): p. 318-322.

190. Madisen, L., et al., *A robust and high-throughput Cre reporting and characterization system for the whole mouse brain.* Nature neuroscience, 2010. **13**(1): p. 133.

191. Chapman, S.C., et al., *Ubiquitous GFP expression in transgenic chickens using a lentiviral vector.* Development, 2005. **132**(5): p. 935-940.

192. Rodrigues, F.S., et al., *A novel transgenic line using the Cre–lox system to allow permanent lineage-labeling of the zebrafish neural crest.* Genesis, 2012. **50**(10): p. 750-757.

193. Wada, N., et al., *Hedgehog signaling is required for cranial neural crest morphogenesis and chondrogenesis at the midline in the zebrafish skull.* Development, 2005. **132**(17): p. 3977-3988.

194. Carney, T.J., et al., *A direct role for Sox10 in specification of neural crest-derived sensory neurons.* Development, 2006. **133**(23): p. 4619-4630.

195. Boniface, E.J., et al., *FlEx-based transgenic reporter lines for visualization of Cre and Flp activity in live zebrafish.* genesis, 2009. **47**(7): p. 484-491.

196. Fish, J.L., et al., *Multiple developmental mechanisms regulate species-specific jaw size.* Development, 2014. **141**(3): p. 674-684.

197. Nichols, D.H., *Ultrastructure of neural crest formation in the midbrain/rostral hindbrain and preotic hindbrain regions of the mouse embryo.* American journal of anatomy, 1987. **179**(2): p. 143-154.

198. Theveneau, E. and R. Mayor, *Neural crest delamination and migration: from epithelium-to-mesenchyme transition to collective cell migration.* Developmental biology, 2012. **366**(1): p. 34-54.

199. Kaufman, M.H., *Atlas of mouse development*. 1992: Academic press.

200. Giovannone, D., et al., *Chicken trunk neural crest migration visualized with HNK1.* Acta histochemica, 2015. **117**(3): p. 255-266.

201. Raible, D.W., et al., *Segregation and early dispersal of neural crest cells in the embryonic zebrafish.* Developmental dynamics, 1992. **195**(1): p. 29-42.

202. Schilling, T.F. and C.B. Kimmel, *Segment and cell type lineage restrictions during pharyngeal arch development in the zebrafish embryo.* Development, 1994. **120**(3): p. 483-494.

203. Kague, E., et al., *Skeletogenic fate of zebrafish cranial and trunk neural crest.* PloS one, 2012. **7**(11).

204. Raible, D.W. and J.S. Eisen, *Restriction of neural crest cell fate in the trunk of the embryonic zebrafish.* Development, 1994. **120**(3): p. 495-503.

205. Lee, R.T.H., et al., *An exclusively mesodermal origin of fin mesenchyme demonstrates that zebrafish trunk neural crest does not generate ectomesenchyme.* Development, 2013. **140**(14): p. 2923-2932.

206. Lee, R.T.H., J.P. Thiery, and T.J. Carney, *Dermal fin rays and scales derive from mesoderm, not neural crest.* Current Biology, 2013. **23**(9): p. R336-R337.

207. Landacre, F., *The fate of the neural crest in the head of the urodeles.* Journal of Comparative Neurology, 1921. **33**(1): p. 1-43.

208. Mongera, A., et al., *Genetic lineage labeling in zebrafish uncovers novel neural crest contributions to the head, including gill pillar cells.* Development, 2013. **140**(4): p. 916-925.

209. Huang, X. and J.-P. Saint-Jeannet, *Induction of the neural crest and the opportunities of life on the edge.* Developmental biology, 2004. **275**(1): p. 1-11.

210. Johnston, M., *Isotretinoin embryopathy in a mouse model: Cranial neural crest involvement.* Teratology, 1985. **31**: p. 26A.

211. Prochazkova, M., et al., *FGF signaling refines Wnt gradients to regulate the patterning of taste papillae.* Development, 2017. **144**(12): p. 2212-2221.

212. Beites, C.L., et al., *Follistatin modulates a BMP autoregulatory loop to control the size and patterning of sensory domains in the developing tongue.* Development, 2009. **136**(13): p. 2187-2197.

213. Castillo-Azofeifa, D., et al., *Sonic hedgehog from both nerves and epithelium is a key trophic factor for taste bud maintenance.* Development, 2017. **144**(17): p. 3054-3065.

214. Hirrlinger, P.G., et al., *Temporal control of gene recombination in astrocytes by transgenic expression of the tamoxifen‐inducible DNA recombinase variant CreERT2.* Glia, 2006. **54**(1): p. 11-20.

215. Witt, M., et al., *Fingerprinting taste buds: intermediate filaments and their implication for taste bud formation.* Philosophical Transactions of the Royal Society of London. Series B: Biological Sciences, 2000. **355**(1401): p. 1233-1237.

216. Le Douarin, N., *A biological cell labeling technique and its use in experimental embryology.* Developmental biology, 1973. **30**(1): p. 217-222.

217. Douarin, L., *Developmental Relationships between the Neural Crest and the Polypeptide-Hormone-Secreting Cells.* The Neural Crest. Cambridge, 1982: p. 91-107.

218. Le Lièvre, C.S. and N. Le Douarin, *Mesenchymal derivatives of the neural crest: analysis of chimaeric quail and chick embryos.* Development, 1975. **34**(1): p. 125-154.

219. Noden, D.M., *The role of the neural crest in patterning of avian cranial skeletal, connective, and muscle tissues.* Developmental biology, 1983. **96**(1): p. 144-165.

220. Dutton, J.R., et al., *An evolutionarily conserved intronic region controls the spatiotemporal expression of the transcription factor Sox10.* BMC developmental biology, 2008. **8**(1): p. 105.

221. Kwak, J., et al., *Live image profiling of neural crest lineages in zebrafish transgenic lines.* Molecules and cells, 2013. **35**(3): p. 255-260.

222. Kague, E., et al., *Skeletogenic fate of zebrafish cranial and trunk neural crest.* PloS one, 2012. **7**(11): p. e47394.

223. Dutton, K.A., et al., *Zebrafish colourless encodes sox10 and specifies non-ectomesenchymal neural crest fates.* Development, 2001. **128**(21): p. 4113-4125.

224. Hol, E.M. and Y. Capetanaki, *Type III intermediate filaments desmin, glial fibrillary acidic protein (GFAP), vimentin, and peripherin.* Cold Spring Harbor perspectives in biology, 2017. **9**(12): p. a021642.

225. Gonzalez‐Martinez, T., et al., *S‐100 proteins in the human peripheral nervous system.* Microscopy research and technique, 2003. **60**(6): p. 633-638.

226. Jessen, K.R. and R. Mirsky, *The success and failure of the Schwann cell response to nerve injury.* Frontiers in cellular neuroscience, 2019. **13**: p. 33.

227. Maro, G.S., et al., *Neural crest boundary cap cells constitute a source of neuronal and glial cells of the PNS.* Nature neuroscience, 2004. **7**(9): p. 930-938.

228. Grada, A. and K. Weinbrecht, *Next-generation sequencing: methodology and application.* The Journal of investigative dermatology, 2013. **133**(8): p. e11.

229. Whitley, S.K., W.T. Horne, and J.K. Kolls, *Research techniques made simple: methodology and clinical applications of RNA sequencing.* Journal of Investigative Dermatology, 2016. **136**(8): p. e77-e82.

230. Schaum, N., et al., *Single-cell transcriptomics of 20 mouse organs creates a Tabula Muris: The Tabula Muris Consortium.* Nature, 2018. **562**(7727): p. 367.

231. Sukumaran, S.K., et al., *Whole transcriptome profiling of taste bud cells.* Scientific reports, 2017. **7**(1): p. 1-15.

232. Ren, W., et al., *Transcriptome analyses of taste organoids reveal multiple pathways involved in taste cell generation.* Scientific reports, 2017. **7**(1): p. 1-13.

233. Venkatesan, N., K. Boggs, and H.-X. Liu, *Taste bud labeling in whole tongue epithelial sheet in adult mice.* Tissue Engineering Part C: Methods, 2016. **22**(4): p. 332-337.

234. Nguyen-Ngoc, K.-V., et al., *3D culture assays of murine mammary branching morphogenesis and epithelial invasion*, in *Tissue Morphogenesis*. 2015, Springer. p. 135-162.